UNITED STATES AIR FORCE

AIR UNIVERSITY

AIR FORCE INSTITUTE OF TECHNOLOGY

Wright-Patterson Air Force Base, Ohio

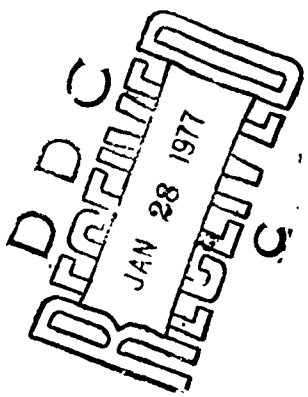

STABILITY AND CONTROL CHARACTERISTICS OF THE WINGLET CONFIGURED KC-135A

THESIS

GAE/MC/76D-5 Kent R. Crenshaw
Captain USAF

GAE/MC/76D-5

STABILITY AND CONTROL CHARACTERISTICS OF THE WINGLET CONFIGURED KC-135A

Master's
THESIS

Presented to the Faculty of the School of Engineering
of the Air Force Institute of Technology
Air University
in Partial Fulfillment of the
Requirements for the Degree of
Master of Science

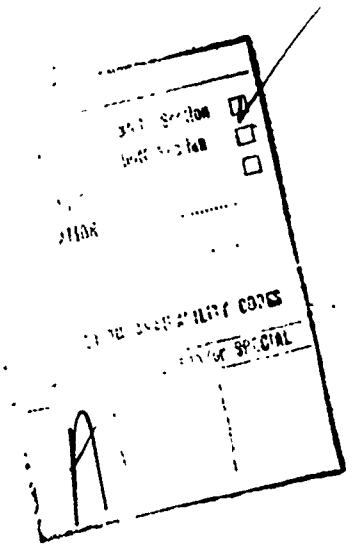

by
Kent R. Crenshaw
Captain USAF

Graduate Aeronautical Engineering

293 p.

December 1976

Preface

This paper represents nearly eight months of study and data gathering and over two thousand dollars of computer time. Much of the effort behind the results to follow consists of several trial and error attempts in using the FLEXSTAB computer system. In this respect, I am extremely grateful to Capt. George C. Perley and Mr. Robert C. Schwanz of the Control Criteria Branch, Air Force Flight Dynamics Laboratory, for their conscientious assistance and support in using FLEXSTAB. Without their help, I doubt that this paper would have been completed in the time allowed.

Dr. D. W. Breuer, my thesis advisor, provided invaluable assistance in analyzing and interpreting much of the theoretical data from FLEXSTAB and other sources. Also his suggestions as to style, organization and content were much appreciated.

Special thanks also go to Capt. Edwin H. Jessup and Capt. John A. Wright, fellow students, for the use of their dynamic time history program, STATVAR. It is well written and proved to be an excellent analytical tool.

Lastly, I want to thank my wife for her steadfast patience and understanding during the final preparation of this report.

Kent R. Crenshaw

Contents

Contents

List of Figures

List of Figures

List of Tables

List of Tables

List of Symbols

NOTE: The symbols used in this report are standard and defined in detail in reference 6. Only nonstandard or uncommon symbols are shown below.

Symbol	Definition
$\bar{C}_{L\hat{u}} = C_{L\hat{u}} + 2C_{L_1}$ $\bar{C}_{D\hat{u}} = C_{D\hat{u}} + 2C_{D_1}$ $\bar{C}_{M\hat{u}} = C_{M\hat{u}} + 2C_{M_1}$	FLEXSTAB speed stability derivatives
d_T	Moment arm of thrustline
N.P.	Neutral point
N.W.	No winglets
q	Perturbed pitch rate
$\bar{q}$	Dynamic pressure
T2	Time to double amplitude
T 1/2	Time to half amplitude
T_R	Characteristic rolling mode time
T_s	Characteristic spiral mode time
$\hat{u} = \frac{u}{U_1}$	Nondimensional velocity
V_ℓ	Velocity of the c.g.
V_T	True airspeed (fps)
W.W.	With winglets
$n_V = \frac{\bar{q}_V}{\bar{q}}$	Dynamic pressure ratio of the vertical tail
$\delta_e = \delta_s$	Used interchangeably as horizontal stabilizer deflection

List of Symbols

Symbol	Definition
Subscript 1	Steady state value
Subscript B	Body
Subscript FRL	Fuselage reference line
Subscript w	Wing

Abstract

Using the Boeing FLEXSTAB digital computer system, rigid and elastic models of the winglet configured KC-135A are made. With a rigid analysis, the winglets reduce total drag from 2 to almost 8% with improvements both laterally and longitudinally in static stability. Dynamically, the rigid winglet model is more stable laterally but slightly more oscillatory longitudinally. The lateral dutch roll mode damping ratio increased with winglets from 3 to 12% with only a 3% increase in frequency. The effect of shortening the vertical stabilizer on the rigid winglet model reveals less stable values for C_{y_β}, C_{n_β} and C_{n_r} and somewhat less lateral dynamic stability than the baseline model. For the elastic winglet model, the drag reductions noted are only 1.3% due to the "washout" effect at the wing tip. Elastic static stability is still improved both laterally and longitudinally with winglets; and dynamically, the winglets improve lateral stability with very little effect longitudinally. With aeroelastic effects, the overall benefit derived from winglet application to the model is less. However, no significant detrimental effects due to winglets are found.

STABILITY AND CONTROL CHARACTERISTICS OF THE WINGLET CONFIGURED KC-135A

I. Introduction

Background

In view of the recent fuel crisis, there has been considerable renewed interest in ways to improve the aerodynamic efficiency of large aircraft. Research in this area is critical when it is realized that energy use for commercial aviation alone has tripled in the past ten years. Even though fuel allocations for the most part have disappeared, fuel prices remain high, comprising, for example, as much as 40% of the direct operating costs of the commercial airplane (Ref 1:19). Also there is no promise that fuel allocations, and their crippling effect on aviation, will not reappear in the future. For these reasons, research and development efforts are currently being concentrated on ways to improve the energy efficiency of existing and future aircraft designs.

One aerodynamic concept being studied is the use of winglets, which are small, nearly vertical, aerodynamic surfaces mounted at the wing tips. This idea has been reviewed extensively by Dr. Richard T. Whitcomb at the NASA Langley Research Center as an effective method of increasing aerodynamic efficiency. Winglets were found to cause a net reduction in induced drag by lessening the downwash

intensity of the wing tip vortices. NASA calculations and wind tunnel tests have shown potential for a 4 to 6% fuel savings by current jet transports modified with winglets (Ref 1:26).

A design study of winglets for the KC-135A and the C-141 aircraft, conducted by the Boeing Commercial Airplane Company for the Air Force, showed a 15.5% reduction in induced drag for the KC-135A. Boeing also discovered that winglets were more effective than wing tip extensions by 15.7% in reducing induced drag (Ref 2:iii). This result was also verified by NASA Langley research.

In the NASA research program, a study was made using a tailless full-span wind tunnel model of a representative jet transport aircraft. Analysis of the model was made both with and without winglets. Their conclusions were that winglets were stabilizing both laterally and longitudinally. NASA also concluded that increases in the directional stability of a winglet-configured aircraft presented the possibility of reducing the vertical tail surface, thereby resulting in a further decrease in drag (Ref 3:7).

The U.S. Air Force, in close association with the Boeing Company, is now giving serious attention to the actual application of winglets to an existing line aircraft. The airplane selected to be retrofitted and flight tested for this purpose is the Boeing KC-135A. The

winglet to be used is the one designed specifically for this aircraft by the Boeing Company. The proposed winglet application is shown in Fig. 1.

In view of the approaching application phase of winglets to the KC-135A, considerable work must be done in analyzing and predicting the stability and control characteristics of the aircraft in its winglet configuration. The beneficial effect of induced drag reduction must be compared carefully with any detrimental side effects that may be discovered. Stability and control, aeroelastic effects, and handling qualities predictions for both longitudinal and lateral aircraft motion are necessary before the comprehensive flight testing phase begins.

Research Objectives

The primary objectives of this report are to:

1. construct a valid rigid and elastic mathematical model of the Boeing KC-135A aircraft both with and without winglets,

2. analyze the incremental effect of winglets on aircraft static and dynamic stability and control,

3. investigate the aeroelastic effects of winglets, and

4. evaluate the overall beneficial versus detrimental effect of winglets.

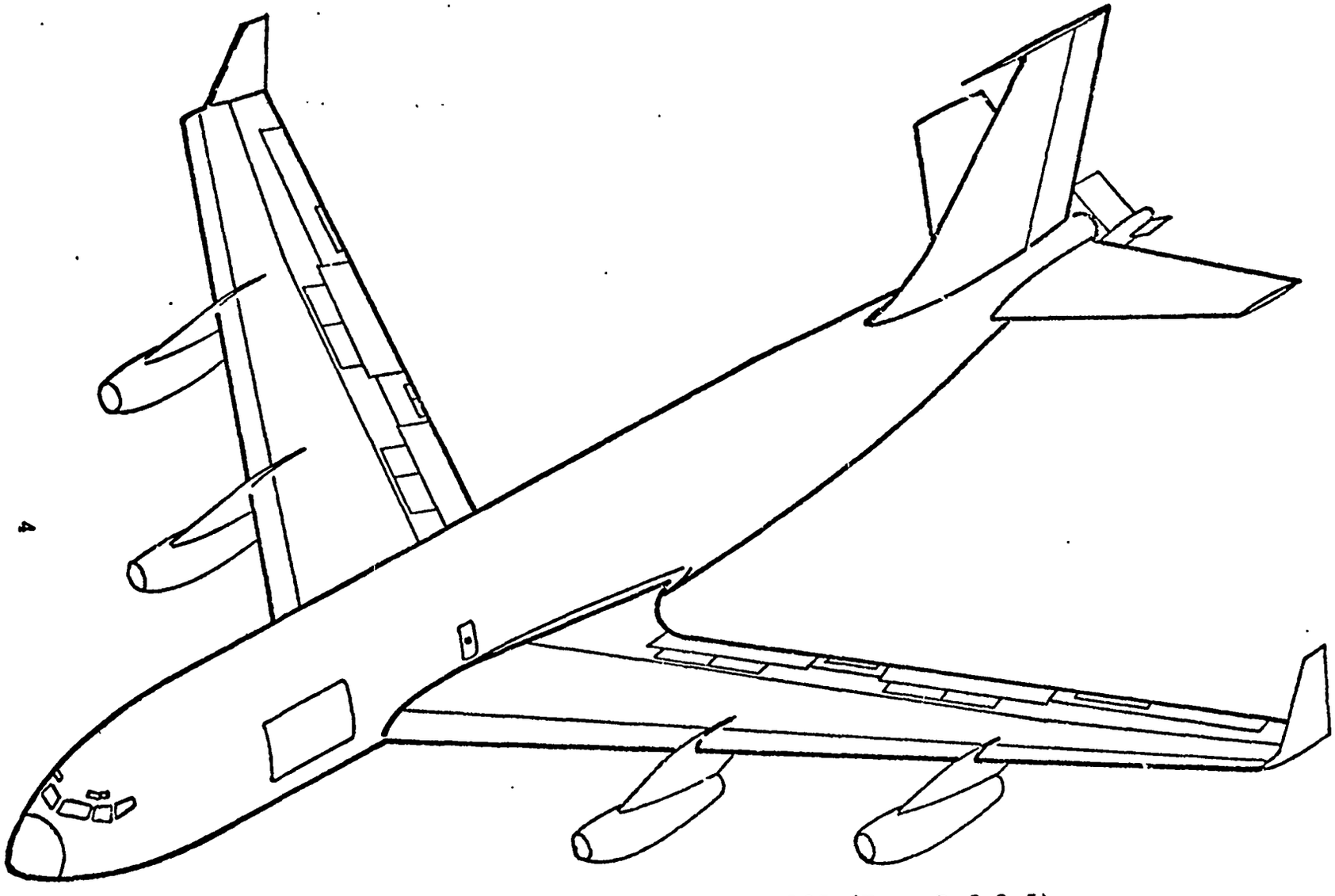

Fig 1. Proposed Winglet Application to KC-135 (From Ref 2:5)

Scope

Static and dynamic stability and control predictions, using two rigid KC-135A models, one with and one without winglets, are accomplished for five different flight conditions. These are specified in Table 1. The three cruise flight conditions, one heavyweight climb condition and the approach configuration with 30 degrees of flaps are representative of this aircraft's operational mission profile and are chosen for this reason.

As an additional part of the rigid stability and control study, the upper quarter of the aircraft's vertical stabilizer on the winglet model is removed for flight condition 2A. This is done to investigate the effect on the lateral-directional stability of the winglet configured model.

Aeroelastic effects prove to be important factors with the addition of the winglet to the wing tip. However, due to time considerations and limited availability of structural data on the KC-135A, the aeroelastic analysis is essentially confined to one basic aircraft weight and center of gravity location. Nevertheless, aeroelastic effects on static and dynamic stability are observed for three different altitudes and dynamic pressures as shown in Table 2.

With only a few exceptions, all of these case studies of the KC-135A stability and control are conducted

Table 1
Rigid Model Flight Conditions

Flight Condition	Cruise 1	Cruise 2	Cruise 2A	Climb 3	Approach 4
Altitude (feet)	28,500.	45,600.	28,500.	S.L.	S.L.
Mach Number	.77	.77	.77	.422	.211
Gross Weight	284,000.	130,000.	130,000.	297,000.	130,000.
c.g. in % $\bar{c}$	.242	.321	.321	.247	.321
Flaps (degs)	0	0	0	0	30°
γ (degs)	0	0	0	4.01°	-2.5°

Table 2
Elastic Model Cruise Parameters

Flight Condition	Cruise 1	Cruise 2	Cruise 3
Altitude (feet)	30,000.	45,000.	10,000.
Mach Number	.77	.77	.422
$\bar{q}$ (psf)	261.67	128.59	181.45
Gross Weight	268,000 lbs		
Center of Gravity	.23 $\bar{c}$		

using two models--one with and one without winglets. This allows the overall incremental effect of the winglets on the aircraft to be observed.

Analytical Tools

The analytical tools that are applied in satisfying the objectives of this report consist of three digital computer routines--FLEXSTAB, CALMAT and STATVAR.

FLEXSTAB is the primary analytical device that is used in this report. It is a program system which actually consists of fourteen separate programs of varying complexity (Ref 4:3-11), not all of which are used in this study. FLEXSTAB has the capability to evaluate static and dynamic stability, trim state, inertial and aerodynamic loading, and elastic deformations of aircraft flight configurations at both supersonic and subsonic speeds. All of these features of the system are used in this report; however, only for subsonic and near transonic flight regimes. More specific information about FLEXSTAB is contained in Appendix D.

CALMAT is an individual computer program written for this report to calculate the aircraft stability derivatives and control matrices for insertion into the state variable time histories program. CALMAT also uses subroutines to calculate the eigenvalues and eigenvectors of the stability derivatives matrix as explained in Appendix B.

STATVAR is the state variable time histories program used to analyze the aircraft dynamic modes and responses

to controller inputs. Details concerning this program are given in Appendix C.

Where needed, these digital computer programs are executed using a Control Data Corporation (CDC) 6600 computer with both off line and on line access to a CalComp plotter.

Assumptions

The overall assumptions made in this report are the direct result of the analytical tools used and the approach to mathematically modeling the aircraft.

FLEXSTAB uses linear theories to perform all of its critical calculations. Therefore, consistent linear aerodynamic, structural and dynamic analytical methods are used. The linear aerodynamic method incorporated is that introduced by Woodward (Ref 5). This method has been extended in FLEXSTAB to include subsonic flow, low-frequency unsteady aerodynamics, and arbitrary wing-body-nacelle-tail arrangements. Also viscous flow effects are neglected as with all linear aerodynamic potential flow programs.

The structural portion of FLEXSTAB used in this study consists of a structural elastic axis program that uses beam theory to predict structural deformations due to aerodynamic loads (Ref 4:1). The aircraft fuselage, and aerodynamic surfaces are divided up into elastic axis segments which are assumed to have constant stiffness properties.

Both CALMAT and STATVAR, employed in the dynamic analysis, use the uncoupled linearized aircraft perturbation

equations of motion, with the inherent assumption that disturbances to the aircraft steady state flight condition are small. This method is commonly used in most stability and control problems and yields good results when compared to more exact methods. These equations are developed and discussed in detail in Appendix A.

An implicit assumption in STATVAR exists in that the program uses a numerical integration technique to predict the aircraft response to control inputs. The assumption is that the value of the control input over a sufficiently small time interval is constant.

Due to time considerations, much of this analysis is conducted using a rigid airplane model. The rigid assumption in this case is not very good; however, a constant awareness of its limitations in analyzing stability and control data does alleviate some of the problems it causes.

The models used in this analysis have no under wing mounted engine nacelles as does the actual aircraft. Again, this is a time and also a computer cost consideration in the modeling process. The incremental effects of the winglets are of primary concern, and the magnitude of the interrelated effects between the winglets and the engines is assumed to be negligible. A ficticious engine, however, is modeled using the fuselage as a nacelle in such a way that the thrust vector, located at the aircraft tail, acts along the fuselage reference line.

Since the principal aerodynamic interactions are between the wing and the winglet, thickness effects of the vertical and horizontal tail are ignored. The thickness of the winglets and the wing are modeled using airfoil definitions from two Boeing documents (Ref 2 and Ref 7).

In order to evaluate the aeroelastic effects of the winglets, the structural model used is a modified model taken from a FLEXSTAB case study of the Boeing 707-320B. Again, this was done primarily due to the lack of pertinent structural information on the KC-135A. The 707-320B and the KC-135A are geometrically similar with the exceptions of a longer fuselage and slightly higher aspect ratio wing in the case of the 707-320B. The tail sections and fuselage contours of both aircraft are identical. Therefore, the assumption is that the elastic properties of the two aircraft are nearly the same. However, by shortening the fuselage and wing of the 707 structural model to make it compatible with the geometry of the KC-135A, the result is a stiffer aircraft. Also, on the winglet configured elastic model, the winglet is maintained rigid.

Approach Procedure

The first step in beginning this evaluation was to obtain as much geometric, static and dynamic data on the Boeing KC-135A and the Boeing winglet as possible. This information was found in a Boeing document on -135 Series

aircraft (Ref 7) and in a Boeing report on winglet design and analysis (Ref 2).

Having the necessary information on the aircraft and the winglet, mathematical models of the KC-135A with and without winglets were made using the appropriate programs in FLEXSTAB.

The programs required in the modeling process are the Geometry Definition (GD), Aerodynamic Influence Coefficient (AIC), Internal Structural Influence Coefficient (ISIC), Elastic Axis Plot (EAPLOT), and Stability Derivatives and Static Stability (SDSS) program.

Using a scaled representative drawing of the KC-135A, the GD program is used to calculate a geometric description of the aircraft. This data is required for use in almost all of the subsequently used FLEXSTAB programs. The AIC program uses the data from the GD model to calculate the theoretical aerodynamic definition. This is done by using aerodynamic influence coefficients that satisfy the compressible potential flow equations. The ISIC program calculates mass distributions, stiffness and flexibility of the modified 707-320B structural model. Having the inertial, structural, aerodynamic and geometric properties of the model defined, the SDSS program predicts the rigid and aeroelastic stability and control characteristics needed to complete much of this analysis.

After completion of the basic modeling process, the model without winglets is validated with the actual aircraft

by comparing aerodynamic data and dynamics obtained from flight tests (Ref 7).

Using the rigid models, which allow more ease in changing gross weights and center of gravity locations, the five flight conditions of Table 1 are compared with and without winglets.

Aeroelastic effects are compared separately using structural models. Elastic to rigid ratios for C_{L_α}, C_{m_α}, C_{m_q}, $C_{m_{\delta_s}}$, $C_{m_{\dot{\alpha}}}$, C_{n_β}, C_{y_β}, C_{ℓ_β}, C_{ℓ_p}, and C_{n_r} are calculated for three values of dynamic pressure; 128.59, 181.69 and 261.67 psf and are faired over a pressure range from 0 to 300 psf. Deflections of the wing due to the winglet and the resulting effects on stability and control are observed for these same dynamic pressures.

The next section contains a detailed discussion of the FLEXSTAB modeling process and a validation of the model against existing flight test data.

II. Validation of FLEXSTAB Computer Model

Introduction

This section attempts to validate the FLEXSTAB geometry and structural models in order to represent them as reasonable mathematical approximations of the actual aircraft. Comparisons between the FLEXSTAB model and flight test data are made for the stability and control derivatives and the longitudinal and lateral dynamic modes.

Airplane and Winglet Geometry Definition

From the aircraft dimensions shown in reference 7, the KC-135A geometry is modeled using the Geometry Definition (GD) program of FLEXSTAB. This program produces the three-dimensional baseline model shown in Fig. 2. The fuselage slender body and thin body aerodynamic surfaces such as the wing and tail occupy the same relative locations as those defined by the actual aircraft (Ref 4:31).

The panelling scheme that is used on the model in Fig. 2. follows the summary of guidelines given in the FLEXSTAB user's manual (Ref 4:47-48).

The interference body, also shown with the model, is extended one-half of the root chord in front of the wing leading edge. Its purpose is to account for the upwash effect ahead of the wing attachment at the fuselage (Ref 4:39).

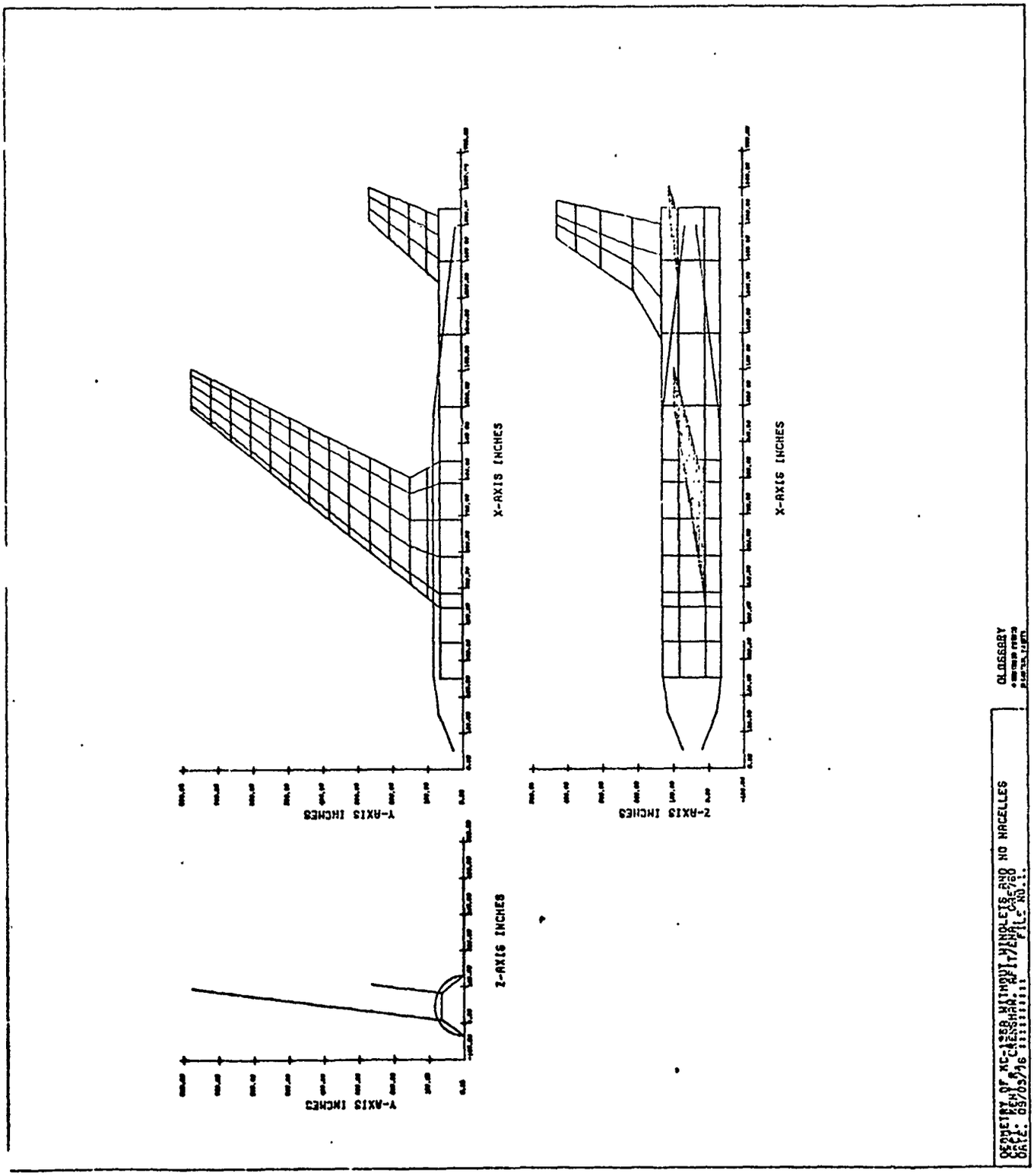

Fig. 2. Baseline Geometry Model

Dihedral angles on the wing and the horizontal tail are 7° as shown on the plot. What is not shown, however, are the fuselage camber definition, the wing incidence angle and the wing thickness definition. These are input into the GD program and are included by FLEXSTAB where necessary in all program calculations.

Airfoil definitions are input into the GD program at five spanwise locations in order to define the wing thickness. Tail thicknesses are not defined on the model.

The winglet is modeled from geometry and airfoil definitions of the Boeing KC-135 winglet design of reference 2. Airfoils are defined at three spanwise locations from root to tip. The winglet twist distribution shown with the dimensions in Fig. 3 is also input. The dihedral angle, with reference to the horizontal plane, is 70°. Fig. 4 shows the winglet configured geometry model of the KC-135 used throughout this report. A FLEXSTAB plot of only the winglet is shown in Fig. 5.

In order to model the 30° of flaps needed for flight condition 4 in the rigid analysis, the camber of the airfoils at the respective flap locations along the wing is modified. This is done as shown in Fig. 6. Realize that this differs from the actual aircraft flap geometry, however, in that the result is a slotted flap arrangement. The actual aircraft uses fowler flaps. The differences that result because of this are believed to be negligible.

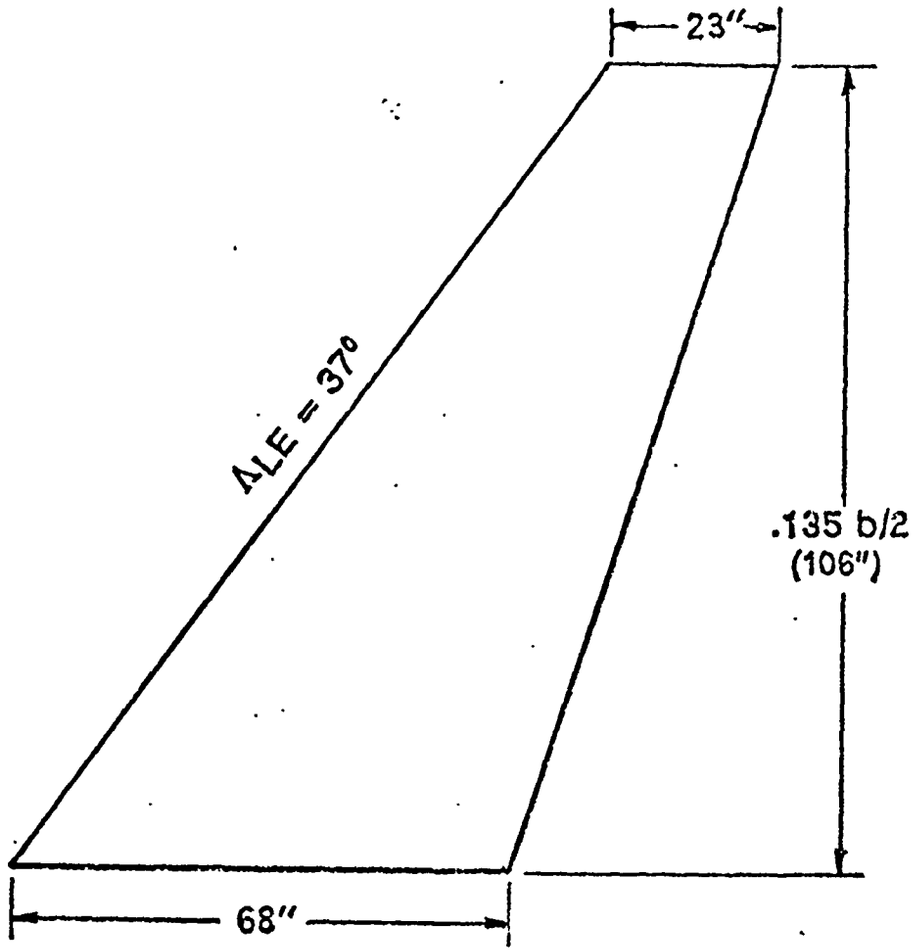

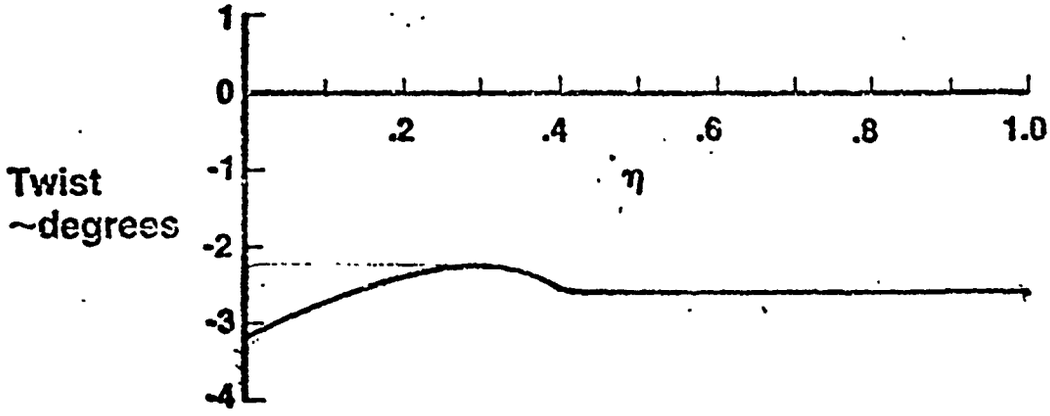

Fig. 3. Boeing Winglet Dimensions and Twist Distribution (From Ref 2:12&196)

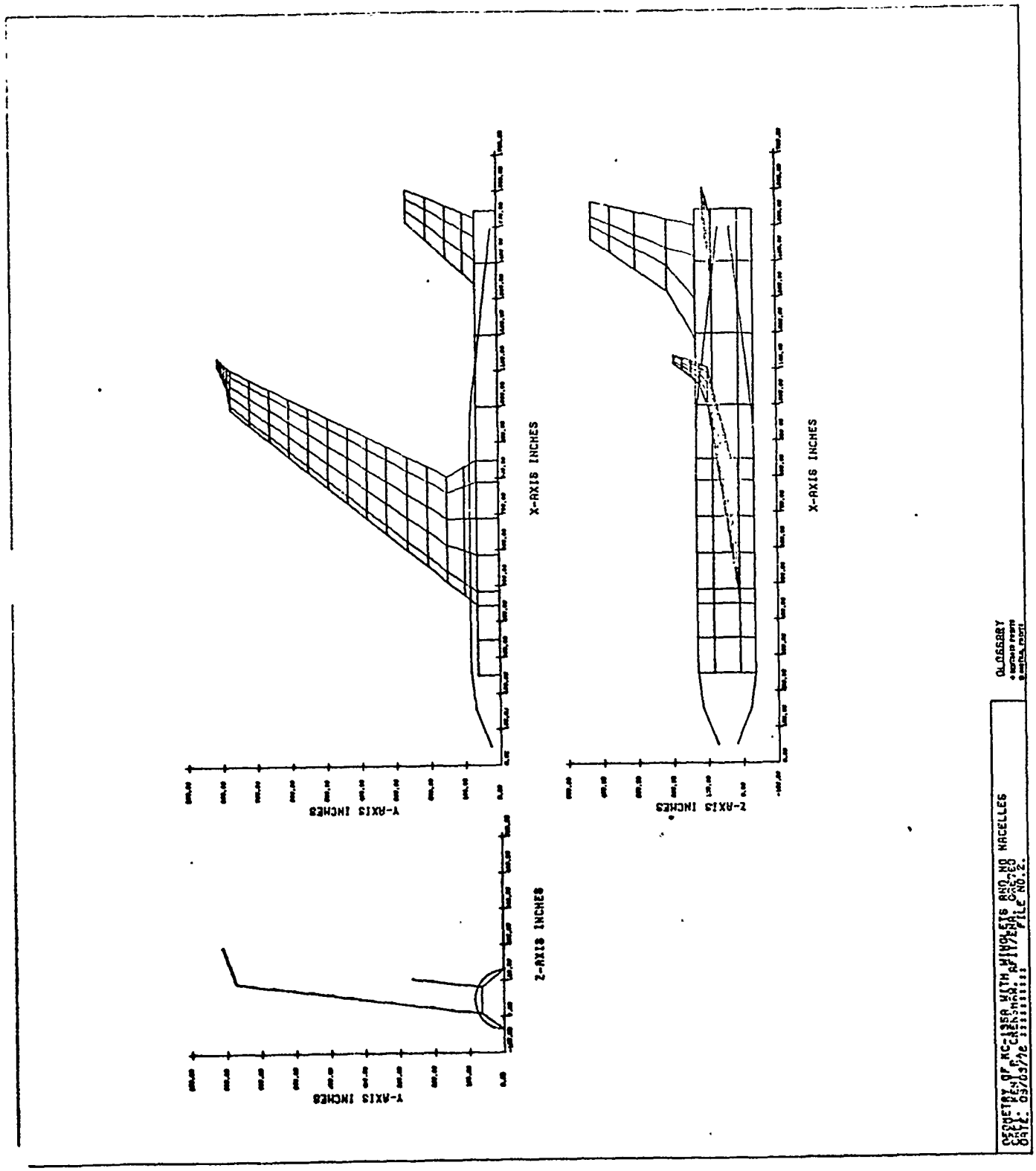

Fig. 4. Winglet Configured Geometry Model

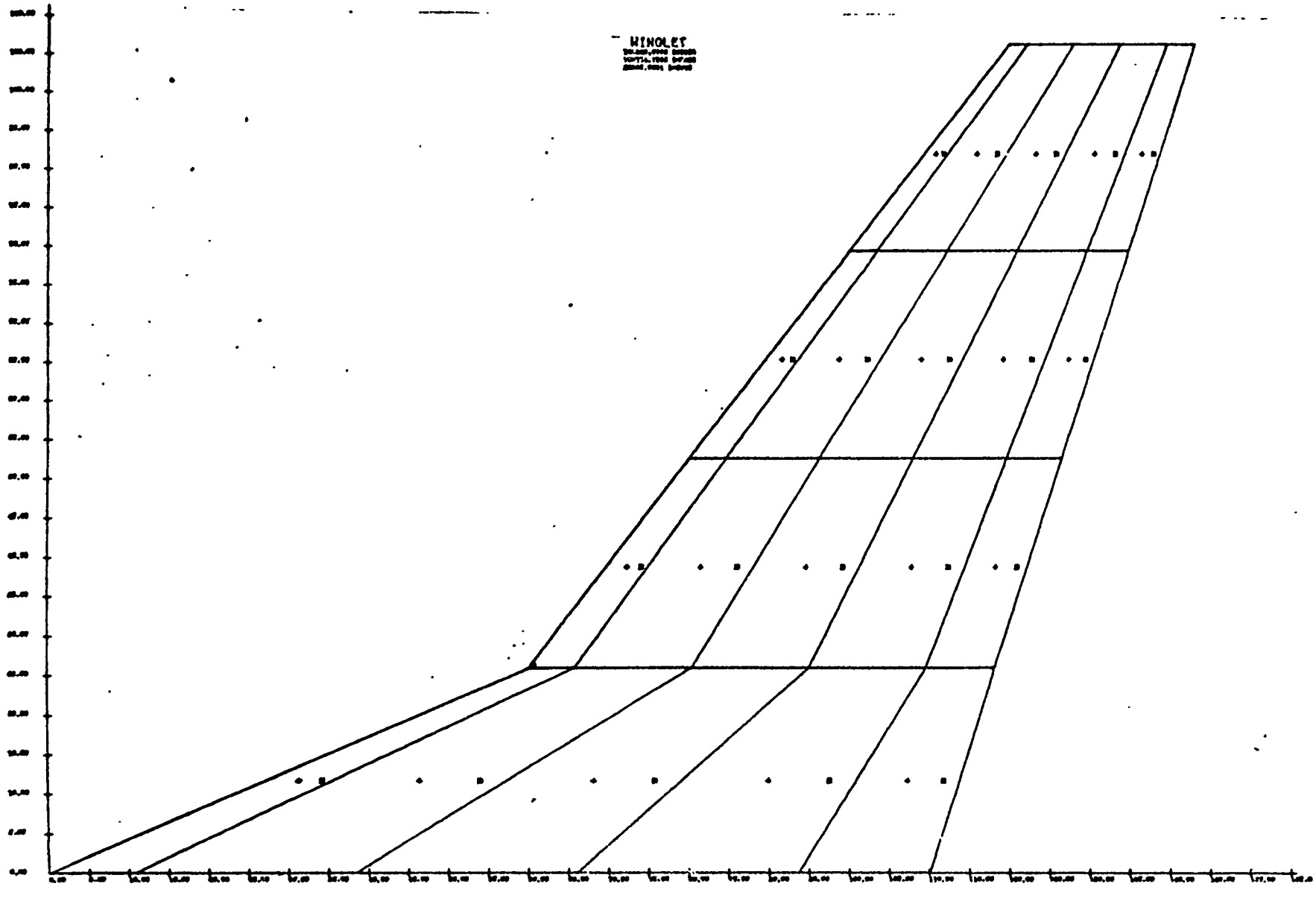

Fig. 5. FLEXSTAB Winglet Geometry

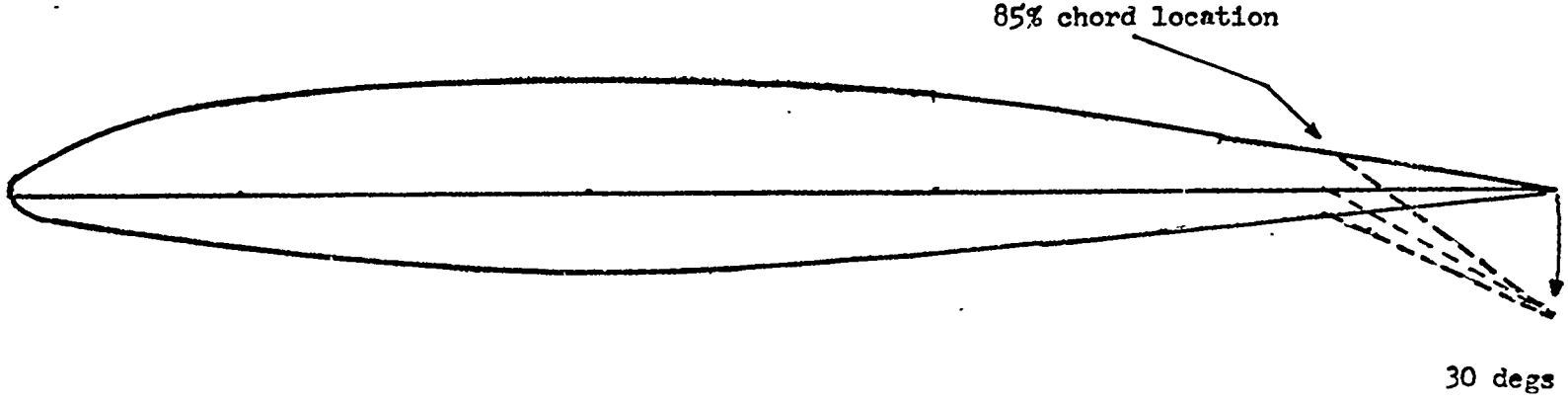

Fig.6 . Sample Wing 'irfoil Showing Camber Changes made for 30 Degrees of Flaps

The aircraft control surfaces are modeled in the Stability Derivatives and Static Stability (SDSS) program of FLEXSTAB by defining hingelines and designating representative panels. Fig. 7 shows the essential control surfaces for the model. The entire horizontal stabilizer defines the elevator in order to observe more realistically the trim conditions that result for the various flight conditions. The rudder is defined with the same geometric dimensions as the actual aircraft; but like the vertical tail, it has no thickness. The inboard aileron, designated by only one panel, is also shown. As far as aileron control is concerned, the KC-135 uses spoilers as well. However, for the steady state equilibrium flight conditions studied here, the inboard aileron is believed to be all that is necessary. The spoilers cannot be modeled using the linearized potential flow equations of FLEXSTAB.

Airplane and Winglet Structural Definition

The aircraft structural definition used in this report is a modified version of the Boeing 707-320B structural model provided by the Control Criteria Branch of the Air Force Flight Dynamics Laboratory.

The 707 model is a comprehensive structural representation of this aircraft. However, it differs in wing and fuselage geometry from the KC-135A. Also, the -135 geometry model, as defined here, has no underwing engine mounted

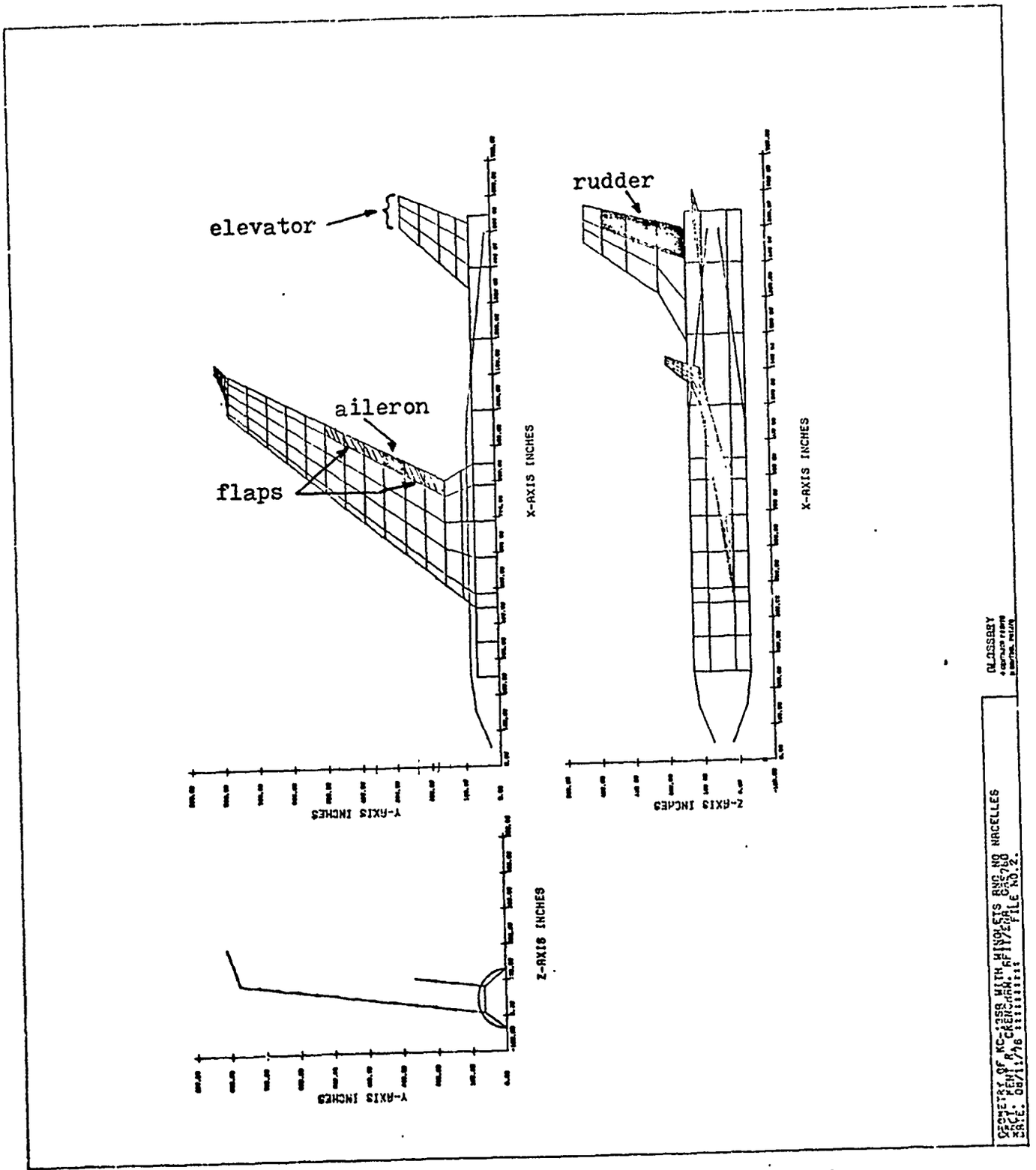

Fig. 7. Winglet Configured Geometry Model Showing Control Surface Definitions

nacelles. The 707 structural model is modified by making changes in fuselage, wing and engine configurations.

Fuselage modifications to the 707 model amount to shortening the fuselage structure by 16.83′. This is done just ahead of the wing root and just aft of the root trailing edge. The structural integrity defined along the wing root and at the tail is not affected by this change. Also, the shortening is accomplished by combining fuselage elastic axis segments with nearly the same elastic properties. When masses are involved, these are lumped together and positioned in the middle of the shortened interval. This same procedure is used on sections in front and aft of the wing. The center of gravity location of the model remains nearly unaffected. However, the result is a stiffer fuselage than the 707 model, which, for the shorter KC-135, is a reasonable approximation.

The wing is longer spanwise on the 707 model by 5′ over the KC-135. The structural elastic axis along the entire wing is therefore compressed 5′ to make it conform in the same proportion to the -135 wing. In addition, this is necessary in order to align the stronger wing structure with the KC-135 chord segments where engines are normally mounted. Even though the -135 geometry model has no wing-mounted engines, there is still a requirement to model the engine support structure along the wing.

The engines on the 707 model create a different problem, however. With modifying the entire structural model, there

is still a need to represent the engine structural weight effect on the wing. This is done first by numerically calculating the combined center of gravity locations for each engine and strut. Two rigid "dumbbells" of appropriate length with total engine and strut masses are then placed at the required elastic axis points on the wing. The result is shown in Fig. 8. Realize that FLEXSTAB does not require that the aircraft structural definition fall entirely within the boundaries of the geometry model. Consequently the engine center of gravity locations may be positioned where required, which for the KC-135 model is in front of the wing leading edge.

The final result of these modifications on the 707-320B structural model is shown in Fig. 8. Figures 9 and 10 show the model's representative fuselage and wing stiffness properties.

In adding the winglet to the structural model, the elastic axis of the wing is extended, with the same outboard stiffness, to the wing tip. Three elastic segments of nearly rigid stiffness are then added along the winglet, ending at the nominal winglet center of gravity location defined in reference 2. Here the 190 pound mass of the winglet is added. Note that the exact elastic axis of the winglet is not modeled here. As a result, the axis used is given rigid properties. Nonetheless, the winglet weight effect on the elastic characteristics of the wing is

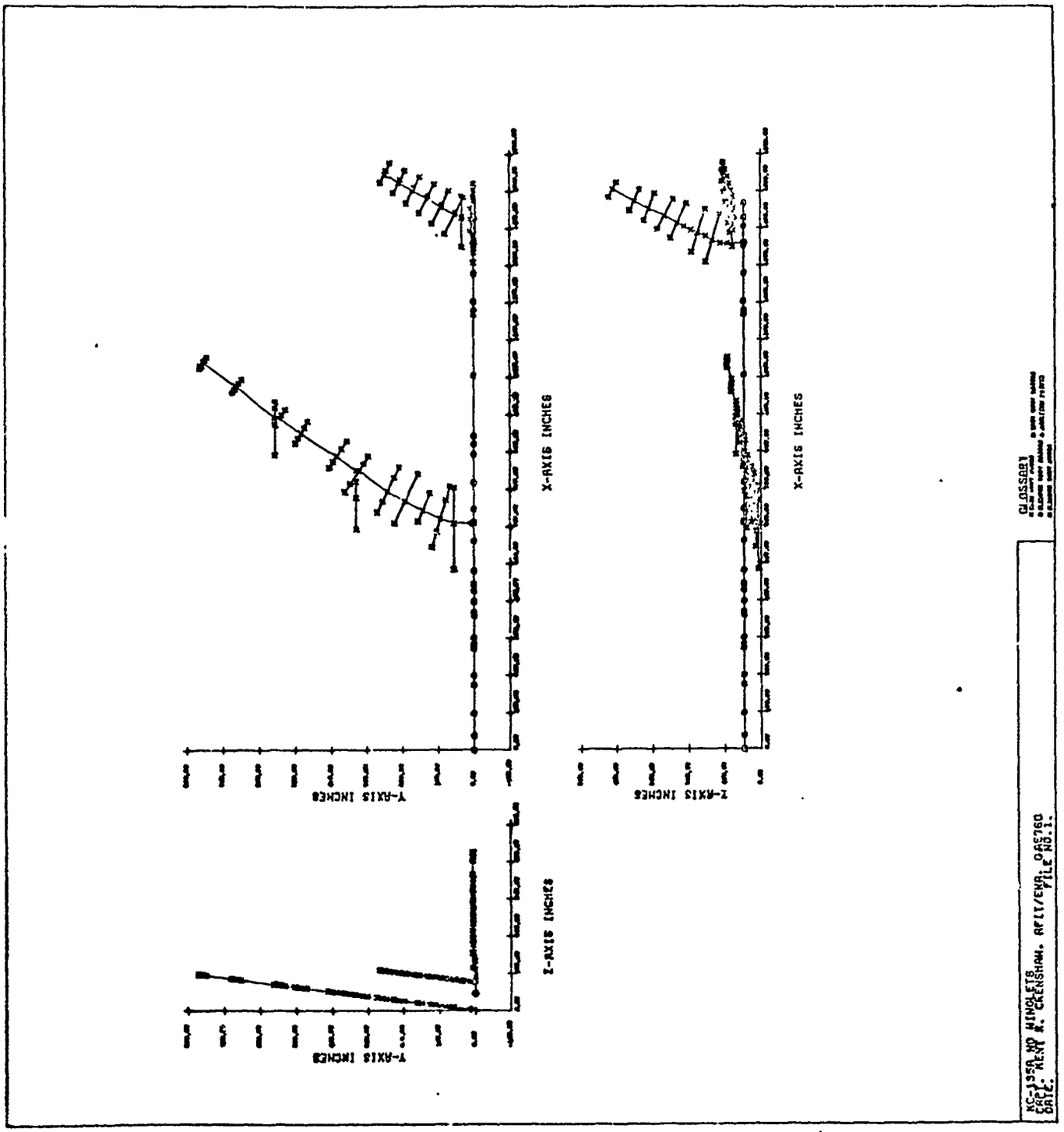

Fig. 8. Baseline Structural Model

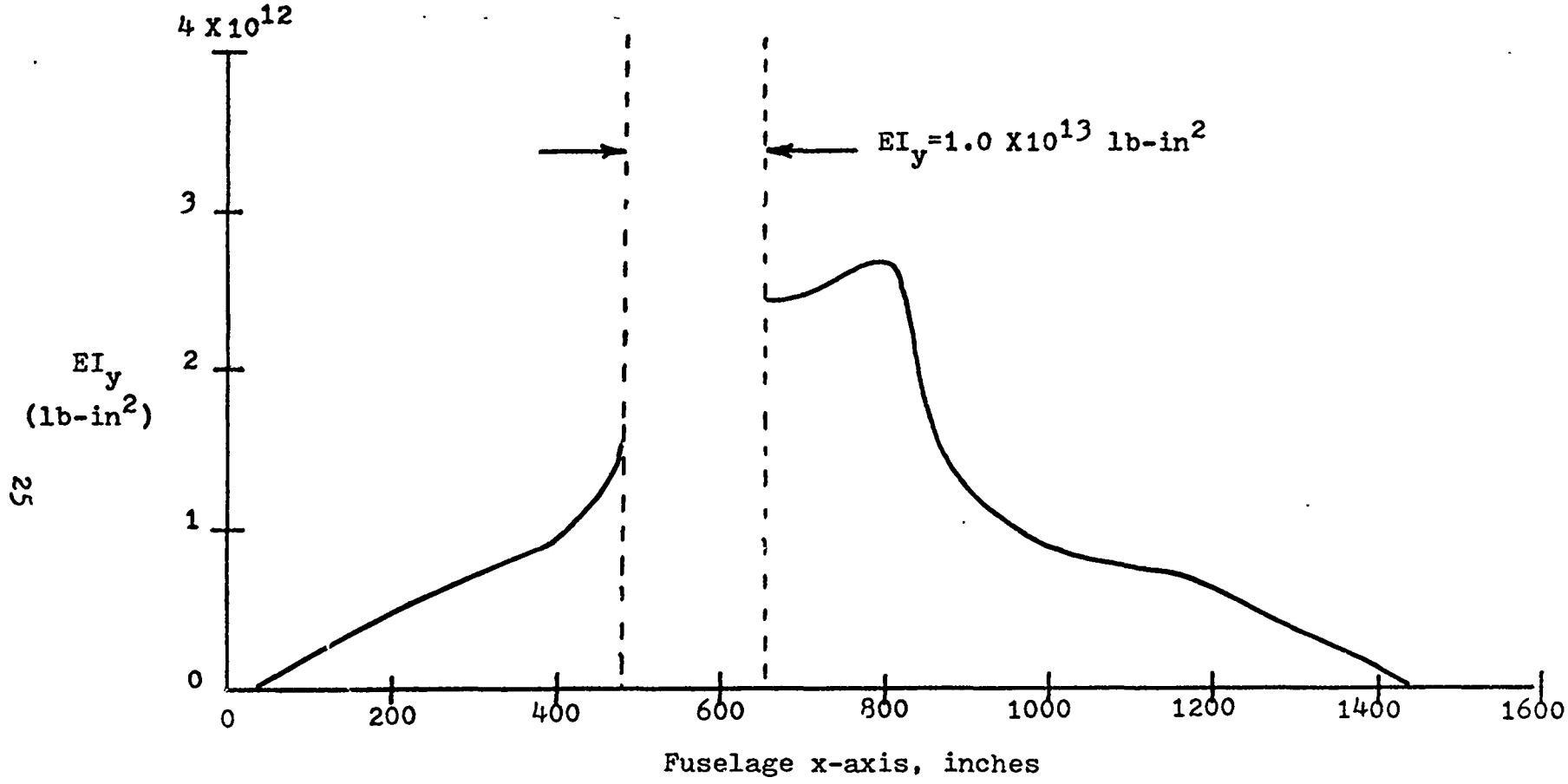

Fig. 9. Fuselage Model Stiffness Distribution

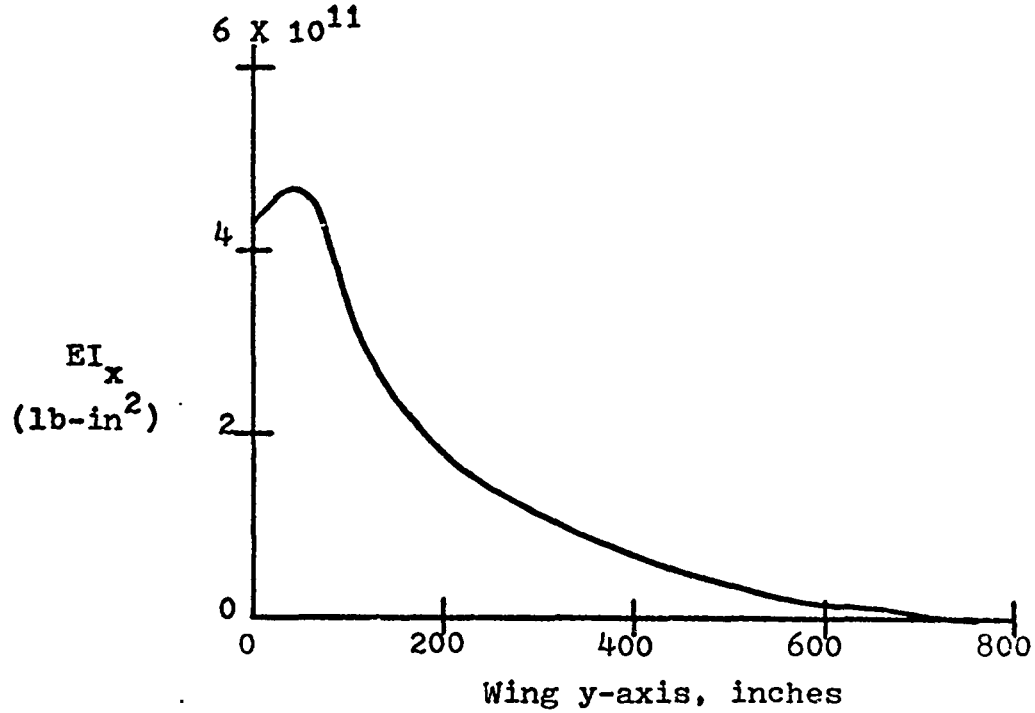

Fig. 10. Wing Model Stiffness Distribution

achieved. Fig. 11 shows the structural definition with winglets added.

For details on FLEXSTAB internal structural modeling, see reference 2.

Model Comparisons With Flight Test Data

Rigid. Having a physical model of the KC-135 aircraft without winglets, its rigid flight characteristics are compared in Table 3 to flight test data from reference 7. Note that this flight test data is semi-elastic since the longitudinal derivatives include elastic effects while the lateral derivatives do not.

In studying Table 3, realize also that Mach number, altitude, flight path angle, center of gravity location, gross weight and mass moments of inertia for the rigid model are not calculated by FLEXSTAB but are input by the user in defining a given flight condition. All of the other model values shown are calculated by the program.

Trim conditions, even with the model's fictitious fuselage reference line engine, compare fairly well. Trim angles of attack and thrust required show the least differences in flight condition 1. Nevertheless, the other flight conditions also show good correlation with the flight test trim values.

Looking at the longitudinal data for the flight conditions shown, only significant stability and control derivatives are compared. The best correlation here in seen in C_{L_α}. C_{m_α} and C_{m_q}, however, are also close in magnitude.

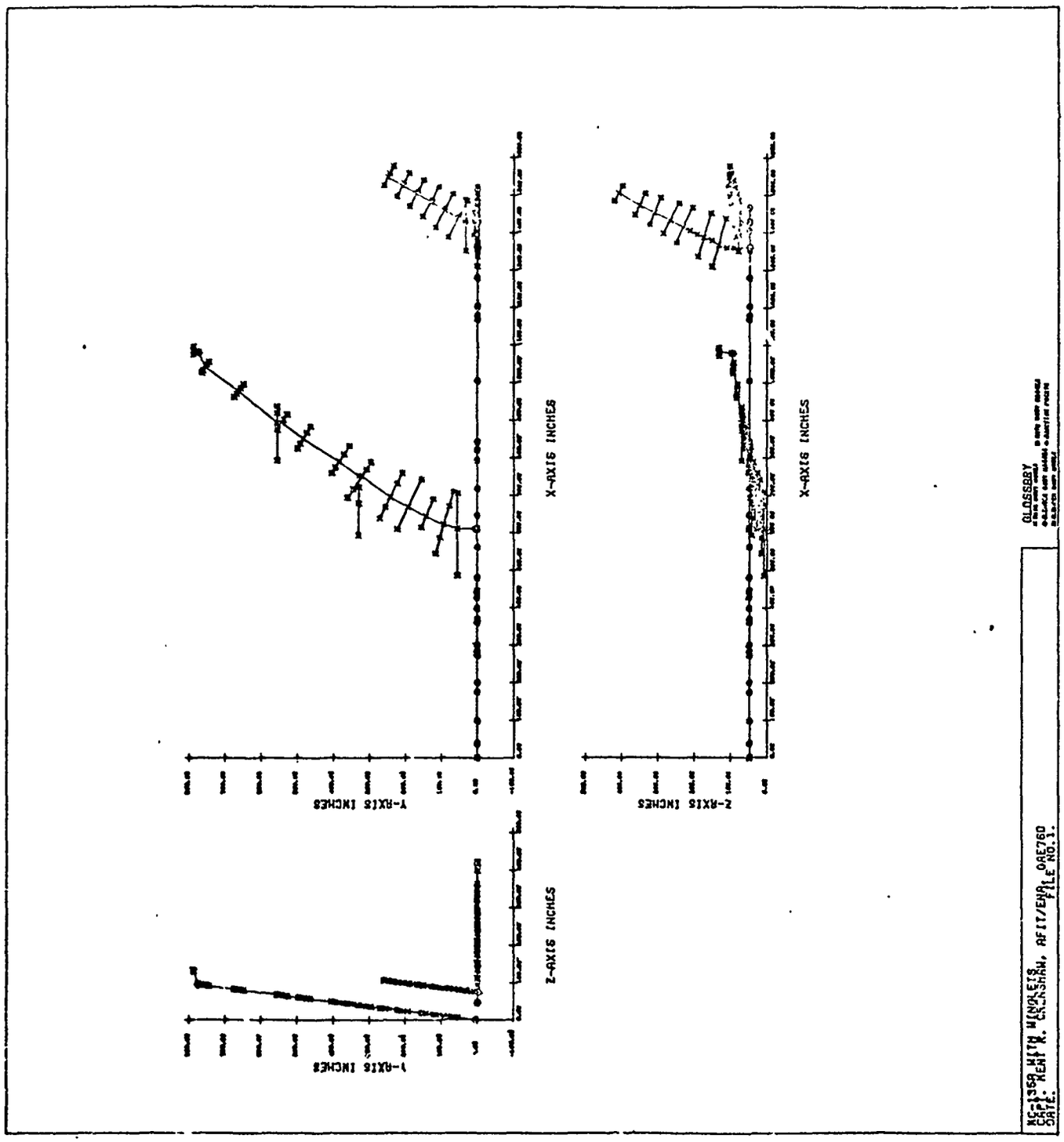

Fig. 11. Winglet Configured Structural Model

Table 3
Validation of FLEXSTAB Rigid Computer Model
With Flight Test Data

Flight Condition (rigid model)	1 (cruise)		3 (climb)		4 (flaps 30°)	
	Common Flight Parameters					
Mach Number	.77		.422		.211	
Altitude, (ft)	28,500		S.L.		S.L.	
γ (degs)	0		4.01		-2.5	
c.g.$\bar{c}$	.242		.247		.321	
$I_{xx} \times 10^6$ (sl-ft^2)	2.93		3.17		2.05	
$I_{yy} \times 10^6$ (sl-ft^2)	4.66		4.72		2.46	
$I_{zz} \times 10^6$ (sl-ft^2)	7.48		7.7		4.36	
$I_{xz} \times 10^6$ (sl-ft^2)	0		0		0	
Aircraft Weight	284,000		297,000		130,000	
	Longitudinal Data					
	*F.T.	FLEX	*F.T.	FLEX	*F.T.	FLEX
θ_{Btrim} (deg)	2.40	2.52	7.00	7.07	-.10	.07
T_1 (lbs)	16,352	16,323	38,800	45,910	9,000	13,080
C_{L_α} (1/deg)	.0825	.0986	.0715	.0837	.0781	.0791
C_{m_α} (1/deg)	-.015	-.0212	-.012	-.0173	-.0175	-.0106
C_{m_q} (1/rad)	-14.65	-18.27	-13.35	-15.636	-14.05	-14.252
C_{L_1}	.426	.416	.463	.460	.811	.804
C_{D_1}	.024	.024	.025	.039	.091	.117
$C_{m_{\dot{\alpha}}}$ (1/rad)	-6.57	-10.22	-5.47	-6.79	-5.52	-6.23

*Flight Test Values (Ref 7:6.52)

	Lateral Data					
C_{y_β} (1/deg)	-.0133	-.0116	-.0122	-.0105	-.0134	-.0102
C_{ℓ_β} (1/deg)	-.0035	-.0025	-.0031	-.0022	-.0040	-.0022
C_{n_β} (1/deg)	.0028	.0034	.0024	.0029	.0023	.0026
C_{ℓ_p} (1/rad)	-.3450	-.4969	-.3150	-.4428	-.3850	-.4277
C_{n_r} (1/rad)	-.1940	-.2926	-.1720	-.2648	-.1860	-.2580
$C_{y_{\delta R}}$ (1/deg)	.0046	.0076	.0041	.0064	.0040	.0061
$C_{\ell_{\delta R}}$ (1/deg)	.0006	.0007	.0005	.0006	.0005	.0005
$C_{n_{\delta R}}$ (1/deg)	-.0002	-.0036	-.0002	-.0030	-.0002	-.0028

*(From Ref 7:7.4)

Laterally in Table 3 more flight test derivatives are available, and since they are also rigid, closer comparisons with the FLEXSTAB values are expected. Note that in general all the flight test values shown are reasonably close in magnitude to the FLEXSTAB derivatives with the exception of $C_{n_{\delta_R}}$.

Table 4 shows the longitudinal and lateral dynamic modes comparison. Longitudinally, the phugoid and short period modes are fairly compatible with the flight test data shown. Only flight condition 3 shows a significant discrepancy where FLEXSTAB calculates a phugoid damping ratio that is less than half of that for the actual airplane. This dynamic mode, however, does not play a significant role in this report.

Laterally, the model dynamics do not compare as closely. Dutch roll damping is consistently higher for the model, and as a result, the times to half amplitude shown are lower. Also, for all flight conditions, the model has an unstable spiral mode whereas the flight test data indicates a stable spiral throughout. The rolling mode shows the best correlation as Table 4 indicates.

Elastic. Table 5 shows the model's mass moments of inertia and center of gravity locations compared with both the KC-135A aircraft values and those of the 707-320B structural model. I_{zz} compares very well with the same value for the actual KC-135. I_{xx} and I_{yy} do not correlate as well, however.

Table 4
Dynamic Modes Comparison

Flight Condition (rigid model)	1 (cruise)		3 (climb)		4 (flaps 30°)	
Short Period	*F.T.	FLEX	*F.T.	FLEX	*F.T.	FLEX
ω_n (rad/sec)	1.67	1.99	1.54	1.81	1.39	1.17
period (sec)	4.07	3.49	4.93	4.17	6.12	9.24
$\zeta_{s.p.}$	.386	.418	.558	.556	.676	.814
T 1/2 (sec)	1.07	.835	.805	.687	.733	.726
Phugoid						
ω_n (rad/sec)	.0571	.065	.086	.094	.157	.151
period (sec)	109.7	96.59	72.8	67.13	39.5	41.66
ζ_p	.0339	.0240	.028	.011	.055	.080
T 1/2 (sec)	355.0	439.2	285.0	663.96	79.0	57.08
Dutch Roll						
ω_n (rad/sec)	1.43	1.57	1.31	1.39	.95	.92
period (sec)	4.4	4.03	4.81	4.59	6.6	6.98
$\zeta_{D.R.}$	.056	.129	.063	.184	.069	.198
T 1/2 (sec)	8.6	3.41	8.4	2.71	10.5	3.82
Spiral						
T 1/2 (sec)	84.6	unstable	60.8	unstable	44.8	unstable
Roll						
T 1/2 (sec)	.700	.558	.510	.434	.520	.545

*(From Ref 7:6.55 & 7.43)

Table 5
Mass Moments of Inertia Comparison

	*KC-135A Aircraft	KC-135A Model	Boeing 707-320B
G.W. (lbs)	268,500	268,500	268,500
c.g. $\bar{c}$	.25$\bar{c}$	.23$\bar{c}$	.25$\bar{c}$
$I_{xx} \times 10^6$ (sl-ft^2)	2.90	3.694	4.928
$I_{yy} \times 10^6$ (sl-ft^2)	4.60	3.716	4.966
$I_{zz} \times 10^6$ (sl-ft^2)	7.35	7.256	9.746
$I_{xz} \times 10^6$ (sl-ft^2)	-	.252	.245

*(From Ref 7:1.4-1.5)

Table 6 shows the elastic model comparison with the actual aircraft. This is done for elastic cruise condition 1 only. No significant improvement is seen here over the rigid model comparison. $C_{n_{\delta_R}}$ again shows the greatest discrepancy.

Dynamic modes for the elastic model are not compared because the stability derivatives show the same relative correlation as the rigid model.

Conclusion

Since the primary objective of this report is to investigate the incremental effect of the winglet on the Boeing KC-135A, the correlation shown in this section between the FLEXSTAB model and the actual aircraft is adequate.

The detailed analysis of the winglet effect on the model in the following sections should do well in predicting the trends in aircraft stability and control that will come out of future flight tests.

Table 6
Elastic Model Comparison With
Actual Aircraft

Cruise Condition 1	Common Flight Parameters	
Mach Number	.77	
Altitude (feet)	30,000	
Aircraft Weight	268,500	
	Longitudinal Data	
	F.T.	FLEXSTAB
$\theta_{B_{trim}}$ (deg)	2.4	2.6
T_1 (lbs)	19,536.39	19,502.00
C_{L_α} (1/deg)	.0825	.0964
C_{m_α} (1/deg)	-.0150	-.0201
C_{m_q} (1/rad)	-14.65	-17.1325
C_{L_1}	.421	.421
C_{D_1}	.031	.031
$C_{m_{\dot{\alpha}}}$ (1/rad)	-6.57	-9.1353
	Lateral	
	F.T.	FLEXSTAB
C_{y_β} (1/deg)	-.0133	-.0137
C_{ℓ_β} (1/deg)	-.0034	-.0024
C_{n_β} (1/deg)	.0024	.0044
C_{ℓ_p} (1/rad)	-.3600	-.4275
C_{n_r} (1/rad)	-.1940	-.3524
$C_{y_{\delta_R}}$ (1/deg)	.0052	.0052
$C_{\ell_{\delta_R}}$ (1/deg)	.0005	.0004
$C_{n_{\delta_R}}$ (1/deg)	-.0002	-.0025

III. Rigid Model Analysis of the Incremental Effect of Winglets

Introduction

The rigid analysis to follow contains a detailed evaluation of the winglet effect on drag and on static and dynamic stability and control. A brief study of the effect of reducing the vertical tail on the winglet model is also made.

Because aeroelastic effects are significant, decisive conclusions from the results of this section alone cannot be made. A rigid study is useful, however, in that it reveals trends in stability and control, trim states, and dynamic behavior with the addition of winglets.

Winglet Effect on Drag Coefficient and Lift Over Drag, L/D

The primary objectives of the Boeing winglet design are to develop drag coefficient reductions and subsequent improvements in lift over drag ratios. Referring to Table 7, these objectives are satisfied for each of the flight conditions tested.

Notice that flight condition 2A showed the greatest improvement in L/D and largest total per cent decrease in drag. The 5.58% increase noted in L/D, and the 5.02% reduction in drag for flight condition 1 compare well with the Boeing wind tunnel results shown in Table 8.

Table 7
Winglet Effect on Drag and L/D

Flight Condition (rigid airplane)	1	2	2A	3	4 (Flaps 30°)
Mach Number M	.77	.77	.77	.422	.211
Altitude (feet) h	28,500	45,600	28,500	S.L.	S.L.
Lift Coefficient C_{L_1}	.416	.427	.191	.460	.804
% Total Drag Reduction	5.02	5.26	7.89	4.09	2.32
% Increase in Lift/Drag, L/D	5.58	5.61	8.58	4.34	2.47

Table 8
Boeing Wind Tunnel Model Results
and FLEXSTAB Flight Condition
1

	Boeing	F. C. 1
Mach Number M	.77	.77
Altitude (feet) h	30,000	28,500
Lift Coefficient C_{L_1}	.426	.416
% Total Drag Reduction	7.0	5.02
% Increase in Lift/Drag, L/D	8.4	5.58

Static Steady State Stability

Definitions. As used in this report, static stability is defined as the tendency of an aircraft to develop moments or forces which oppose an instantaneous perturbation of a motion variable from a steady-state flight condition. Steady state motion is defined as motion for which speed and rotational velocity remain constant with time in a body-fixed coordinate system (Ref 6:5.1).

Static Stability Criteria. The winglet effect on static stability will be evaluated using the significant static stability criteria shown in Table 9. Also, mention of handling qualities considerations will be made where appropriate.

Longitudinal Static Stability. The longitudinal static stability derivatives discussed here, and shown in Table 9, are C_{L_α}, and C_{m_α}. In addition, the winglet effect on the aircraft aerodynamic center location and the resulting effect on static margin is studied.

From Table 10, it can be seen that a positive winglet effect on C_{L_α} is consistently noted. The implication is that, with winglets, the aircraft reaches a required lift coefficient at a smaller angle of attack than without winglets. This is shown graphically in Figure 12.

Of great interest to static stability is the position of the aerodynamic center in its relation to the aircraft center of gravity. As shown in Table 10, the winglet effect moved this point aft in all cases from 7 to 8%.

Table 9
Static Stability Criteria for Selected
Longitudinal and Lateral Derivatives

Perturbation Variable Units	Opposing Force or Moment Coefficient
w (fps)	$C_{L_\alpha} > 0$
$\alpha = \frac{w}{u_1}$ (degs)	$C_{m_\alpha} < 0$
$\beta = \frac{v}{u_1}$ (degs)	$C_{n_\beta} > 0$

Table 10
Winglet Effect on C_{L_α}, $\bar{x}_{ac}$, C_{m_α}, and
Stabilizer Trim, δ_s

Flight Condition (rigid airplane)	1	2	2A	3	4 (Flaps 30°)
% Increase in C_{L_α}	3.14	3.14	3.14	2.87	2.78
% Aft Shift in $\bar{x}_{ac}$	8.19	8.3	7.98	7.23	7.08
% Increase in Static Margin	17.43	28.13	27.69	15.85	24.03
% Negative Increase in C_{m_α}	21.23	31.58	31.01	19.08	27.36
% Negative Increase in δ_{strim}	28.5	38.5	51.81	19.62	46.41

KC-135A FLEXSTAB Model Flight Condition 1

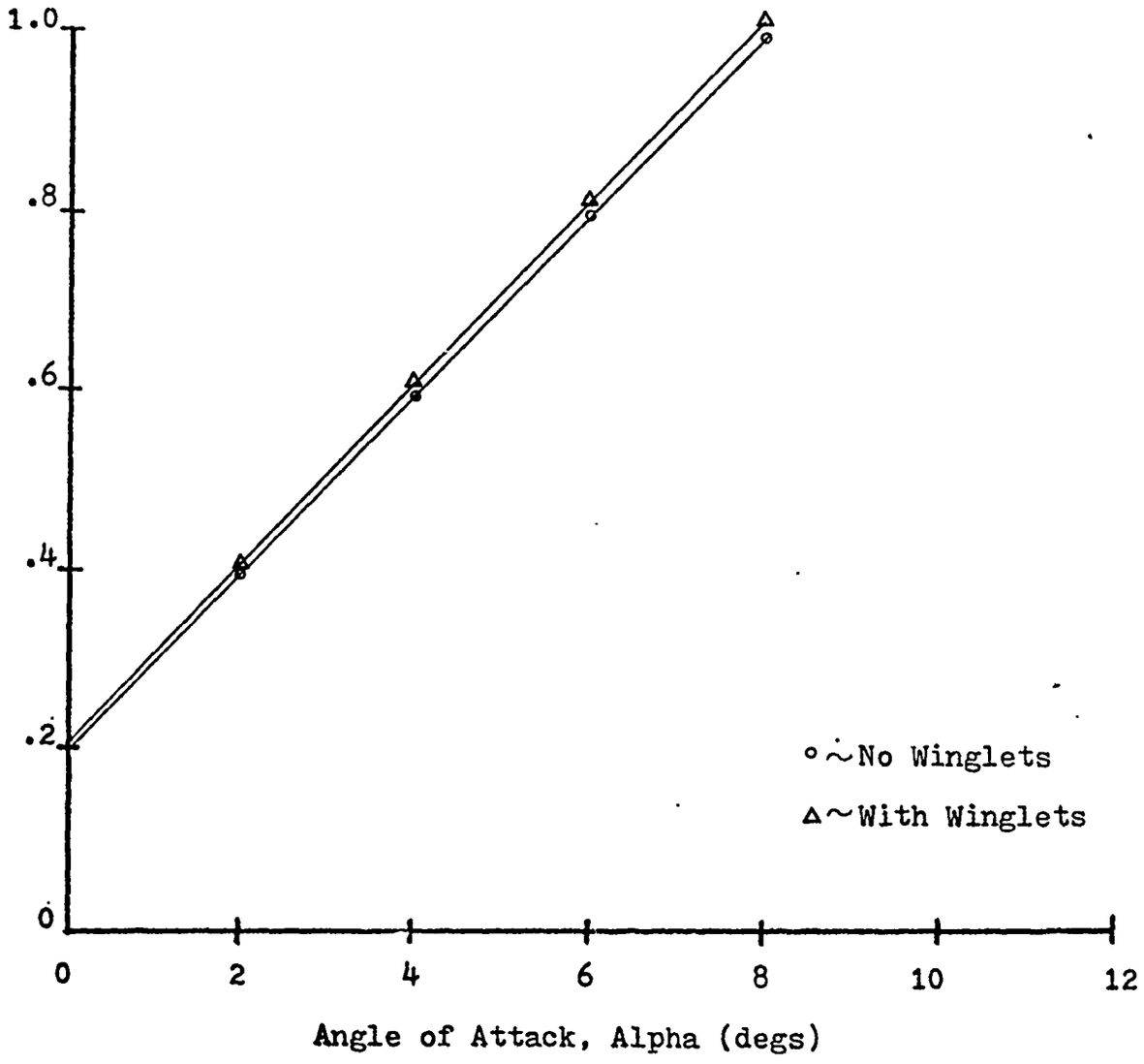

Fig. 12. Winglet Effect on Lift vs. Angle of Attack

Since the winglet increases the effective angle of attack of the outboard wing, this essentially moves the center of lift distribution for the total wing aft. This has a stabilizing effect in increasing the aircraft static margin and pitch stiffness, C_{m_α}:

$$C_{m_\alpha} = C_{L_\alpha}(\bar{x}_{cg} - \bar{x}_{ac})$$

where $(\bar{x}_{ac} - \bar{x}_{cg})$ is defined as the static margin. Table 10 shows that C_{m_α} increases negatively from 19 to 31%.

The stabilizing changes in C_{m_α} and C_{L_α} noted thus far with the winglet model are significant. However, when viewed in another way they reveal a slight trim penalty. Referring to Figure 13 for a $.242\bar{c}$ center of gravity location, the winglet model shows a smaller range of useful trim lift coefficients and angles of attack for a given range of horizontal stabilizer settings. Note also that because of the more negative nose down pitching moment due to angle of attack, a more negative stabilizer setting is required for trim with winglets. This trend is consistent and can also be seen in Table 10.

Lateral Static Stability. The significant lateral static stability derivative analyzed here, and indicated in Table 9, is C_{n_β}, which defines the yaw stiffness of the aircraft. However, the winglet effect on C_{y_β}, C_{ℓ_β}, C_{ℓ_p} and C_{n_r} along with C_{n_β} is also shown.

As indicated in Table 11, the winglets cause a positive increment in yawing moment due to sideslip, C_{n_β}. Note that

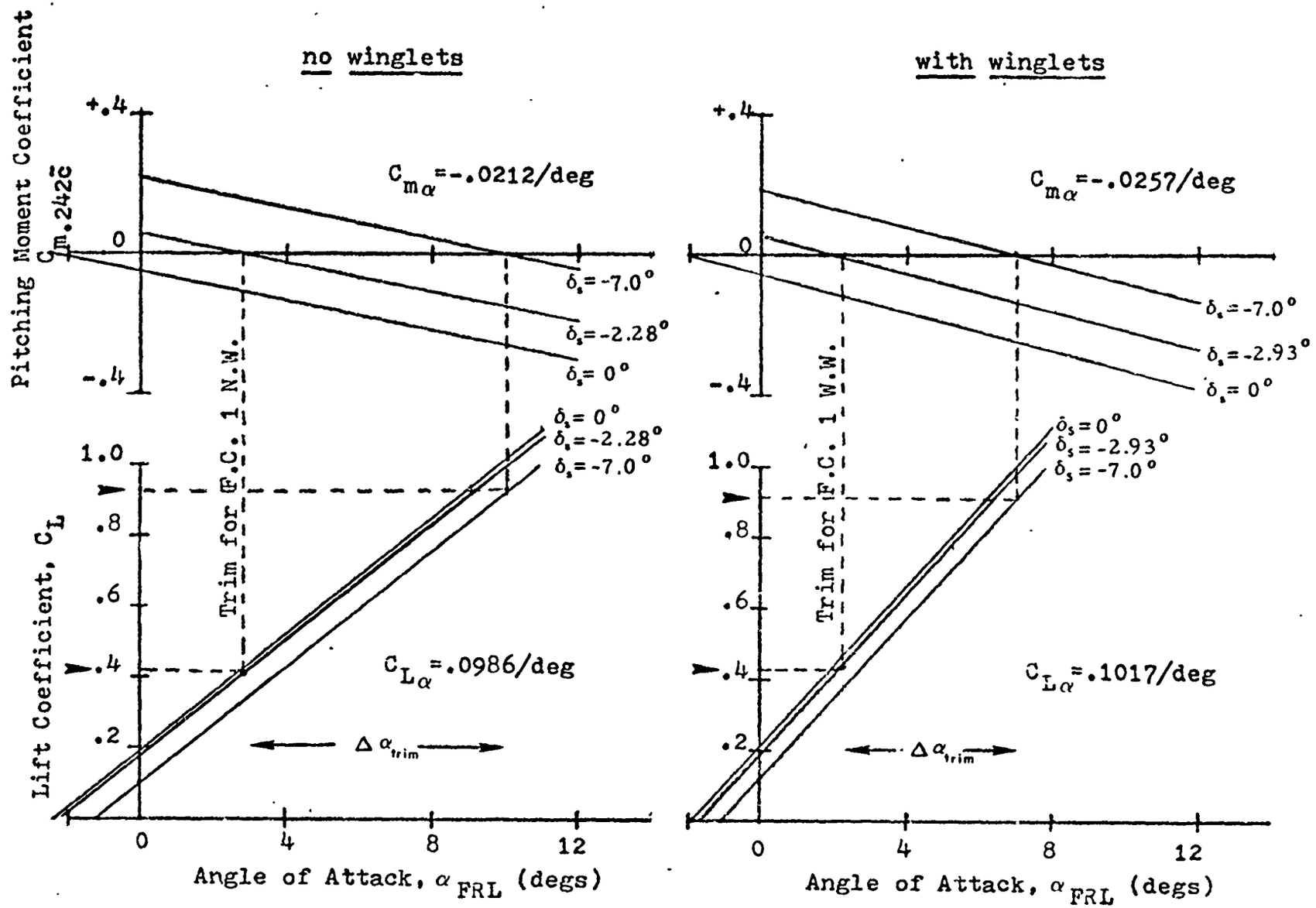

Fig. 13. Winglet Effect on $C_{L_{trim}}$ and α_{trim} for c.g. = .242$\bar{c}$

Table 11
Winglet Effect on Lateral Stability Derivatives

Flight Condition (rigid model)	1	2	2A	3	4 (Flaps 30°)
% Negative Increase in C_{y_β}	14.66	14.66	14.66	14.29	13.73
% Positive Increase in C_{n_β}	5.88	6.25	6.25	6.90	3.85
% Negative Increase in C_{ℓ_β}	28.0	28.0	30.77	31.82	22.73
% Negative Increase in C_{ℓ_p}	12.5	12.38	12.53	11.38	11.06
% Negative Increase in C_{n_r}	8.03	7.92	6.50	6.57	5.74

NOTE: The negative side force components on the winglets act behind and above the aircraft center of gravity.

a positive C_{n_β} is a necessary condition in Military Airworthiness Requirements (Ref 6:5.11). In comparing the incremental change in this derivative due to winglets, it is small but stabilizing for all five flight conditions.

Observe in Table 11 that all the changes in the other lateral derivatives shown are also stabilizing.

Summary. In the longitudinal case, positive winglet effects were observed in C_{L_α} and C_{m_α}. The slight trim penalty caused by C_{L_α} and C_{m_α} was explained in Fig. 13.

Laterally, it was noted that the winglets have a positive stabilizing effect on lateral static stability.

Control Characteristics for Steady State Flight

The next area to be analyzed regards stability and control effects with winglets. The control aspect of stability encompasses two requirements:

1. sufficient control power, and
2. no extraordinary pilot effort (Ref 6:5.19).

Both of these are considered in the following analysis.

Longitudinal. Here, the slight trim penalty with winglets has already been discussed. As indicated in Table 10, the stabilizer trim setting required with winglets was more negative. Again, the reason for this is the more nose down pitching moment effect of the winglets.

Referring to Appendix E, Table I, the control derivatives $C_{m\delta_s}$, $C_{L\delta_s}$ and $C_{D\delta_s}$ are the same with or without winglets, which is not surprising. Apparently, the winglets are too far outboard from the tail to have any influence on the effectiveness of the horizontal stabilizer.

Another practical consideration for longitudinal stability and control is stick speed stability, or $\frac{\partial \delta e}{\partial Vp}$. Assuming an unpowered glide and a shallow glide angle, the uncoupled aircraft longitudinal equations become

$$mg = (C_{L_o} + C_{L_\alpha}\alpha + C_{L\delta_s}\delta_s)\bar{q}s \qquad \text{and} \qquad (1)$$

$$C_{m_1} = 0 = C_{m_o} + C_{m_\alpha}\alpha + C_{m\delta_s}\delta_s \qquad (2)$$

where equation (2) is the moment trim condition (Ref 6:5.21). Solving equations (1) and (2) for δ_s and α, the result for

δ_s can be differentiated with respect to C_L such that

$$\frac{\partial \delta_s}{\partial C_L} = \frac{-C_{m_\alpha}}{C_{L_\alpha} C_{m_{\delta_s}} - C_{m_\alpha} C_{L_{\delta_s}}} \tag{3}$$

(Ref 6:5.22)

Since $C_L = \frac{W}{\bar{q}s}$, $\frac{\partial C_L}{\partial V_p} = -\frac{4W}{\rho S V_p^3}$. From this relation stick speed stability becomes (assuming constant Mach number)

$$\left.\frac{\partial \delta_s}{\partial V_p}\right|_M = \left.\frac{\partial \delta_s}{\partial C_L}\right|_M \frac{\partial C_L}{\partial V_p} = \frac{4W}{\rho S V_p^3} \frac{C_{m_\alpha}}{C_{L_\alpha} C_{m_{\delta_s}} - C_{m_\alpha} C_{L_{\delta_s}}} \tag{4}$$

Since the winglet effect caused little or no change in $C_{m_{\delta_s}}$ or $C_{L_{\delta_s}}$, the changes in stick speed stability shown in Table 12 are due to changes in C_{m_α} and C_{L_α}. Looking at equation (4) in another way:

$$\left.\frac{\partial \delta_s}{\partial V_p}\right|_M = \frac{1}{\frac{C_{L_\alpha} C_{m_{\delta_s}}}{C_{m_\alpha}} - C_{L_{\delta_s}}} \tag{5}$$

where $\frac{C_{L_\alpha}}{C_{m_\alpha}} = \frac{1}{(\bar{x}_{cg} - \bar{x}_{ac})} \approx \frac{1}{S.M.}$.

Consequently, equation (5) can be written as a function of static margin and $C_{m_{\delta_s}}$ and $C_{L_{\delta_s}}$:

$$\left.\frac{\partial \delta_s}{\partial V_p}\right|_M = \frac{1}{\frac{-C_{m_{\delta_s}}}{S.M.} - C_{L_{\delta_s}}} \tag{6}$$

From Table 10, the winglet effect consistently increases the aircraft static margin, which results in decreasing the denominator of equation (6). Consequently, the stick speed

Table 12
Winglet Effect on Stick Speed Stability

Flight Condition (rigid airplane)	1	2	2A	3	4 (Flaps 30°)
% Increase in Stick Speed Stability, $\frac{\partial \delta e}{\partial Vp}$	14.29	23.08	20.59	15.48	25.41

stability increase of Table 12, due to the winglets, is verified. The implication of this increase, from a pilot's viewpoint, is that more positive elevator deflection is required to cause a change in speed from a given trim speed, V_{p1}. The effect of stabilizing increases in static margin on longitudinal control is evident.

Lateral. Looking at lateral-directional stability and control, the winglet had almost no effect on the rudder control derivatives $C_{y_{\delta R}}$, $C_{n_{\delta R}}$ and $C_{\ell_{\delta R}}$, as can be seen in Table I of Appendix E. However, some small changes were noted in the inboard aileron control effectiveness as shown in Table 13.

Of some concern here are the FLEXSTAB calculated derivatives of rolling moment due to aileron, $C_{\ell_{\delta A}}$. These values, for both models and all flight conditions, were negative. This is not compatible with flight test data in reference 7 nor is it reasonable physically. The explanation for this sign reversal is not understood and is

Table 13
Winglet Effect on Inboard Aileron Lateral
Control Effectiveness

Flight Condition (rigid model)	1	2	2A	3	4 (Flaps 30°)
% Decrease in $C_{y_{\delta A}}$ (less positive)	29.0	29.0	29.0	25.26	23.86
% Decrease in $C_{\ell_{\delta A}}$ (more negative)	2.75	2.76	2.78	2.08	1.98
% Increase in $C_{n_{\delta A}}$ (less negative)	3.23	2.46	3.78	2.11	1.02

difficult to analyze due to the complexity of the FLEXSTAB computer system. The aileron control derivatives $C_{n_{\delta A}}$ and $C_{y_{\delta A}}$, however, are acceptable.

Also important to lateral-directional stability and control is the capability to maintain straight and level flight with engines out. This is crucial to flying qualities requirements in that this must be accomplished at bank angles $\phi_1 \leq 5°$ for all speeds larger than $1.2V_{stall}$ (Ref 8:para 3.4.12).

Flight condition 4 provides a fairly realistic example for which engine out handling characteristics can be evaluated. In this approach configuration, the model has 30° of flaps and is at 130,000 pounds gross weight. Also for this condition

$$V = 140 \text{ knots} \quad \text{and}$$

$$V_{stall} = 107 \text{ knots} \qquad \text{(From Ref 9:6-2B)}$$

$$\therefore 1.2V_{stall} = 128.4 \text{ knots} < 140 \text{ knots}$$

The minimum control speed, with rudder boost on, is 116 knots for a standard day at sea level (Ref 10:1A9-14). Having satisfied the airspeed requirements for an engine out approach, it is assumed that the bank angle is also less than 5°. Using the simplified approach to the lateral control problem about the z axis only, the following equation results for zero sideslip rudder deflection:

$$\delta_R = \frac{-N_T}{C_{n_{\delta R}} \bar{q} S b} \qquad \text{(Ref 6:5.39)} \qquad (1)$$

Also assuming no pilot action at all

$$\beta_{max} = \frac{-N_T}{C_{n_\beta} \bar{q} S b} \qquad \text{(Ref 6:5.39)} \qquad (2)$$

Having β_{max}, an approximate way of determining the amount of lateral control needed to counteract any "sideslip induced" rolling moment is available:

$$\delta_A = \frac{-C\ell_\beta \beta_{max}}{C\ell_{\delta A}} \qquad \text{(Ref 6:5.39)} \qquad (3)$$

Note that equations (1), (2) and (3) come from the lateral-directional equations of motion (Ref 6:5.36). Using these

simplified relations, it is possible to determine the δ_R and δ_A required with and without winglets to counteract the yawing and rolling moments created after engine failure.

Instead of using the questionable $C_{\ell_{\delta_A}}$ FLEXSTAB derivative, a control wheel derivative, $C_{\ell_{\delta_W}}$, from reference 7 is used. This includes, in addition to the inboard aileron, the effect of the outboard ailerons and spoilers, on rolling moment.

Using the approach configuration of flight condition 4 and the engine out condition shown in Figure 14:

No Winglets	With Winglets
N_T = 150,747 ft-lbs	N_T = 145,814 ft-lbs
$C_{n_{\delta R}} = \frac{-.0028}{deg}$, $C_{n_\beta} = \frac{.0026}{deg}$	$C_{n_{\delta R}} = \frac{-.0028}{deg}$, $C_{n_\beta} = \frac{.0027}{deg}$
$C_{\ell_\beta} = \frac{-.0022}{deg}$, $*C_{\ell_{\delta_W}} = \frac{.00065}{deg}$	$C_{\ell_\beta} = \frac{-.0027}{deg}$, $*C_{\ell_{\delta_W}} = \frac{.00065}{deg}$

($\bar{q}$ = 66.04 psf, S = 2433 ft^2, b = 70.83 ft.)

*(From Ref 7 :7.4)

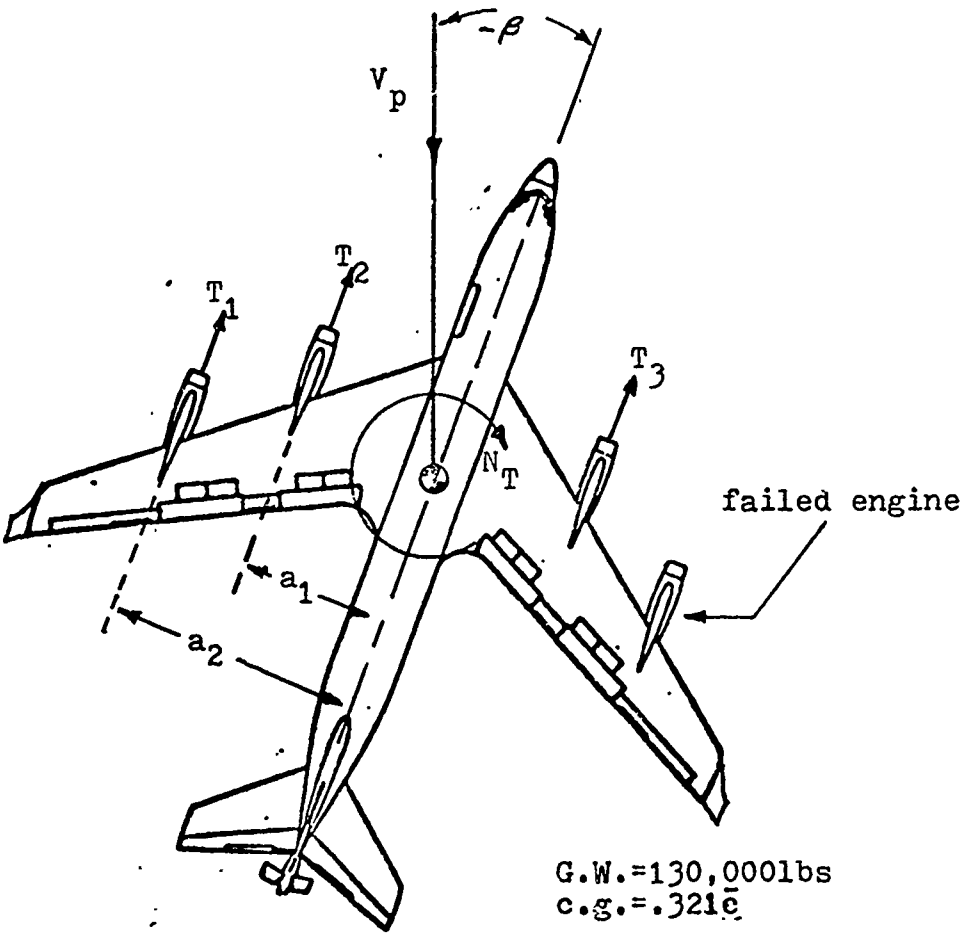

$T_1=T_2=T_3=3270$lbs no winglets (NW)
$T_1=T_2=T_3=3163$lbs with winglets (WW)
$a_1=27.2$feet $a_2=46.1$feet

$$N_T=a_2T_1+a_1T_2-a_1T_3=a_2T_1$$

$$N_{T_{NW}}=46.1(3270)=\underline{150,747\text{ft-lbs}}$$

$$N_{T_{WW}}=46.1(3163)=\underline{145,814\text{ft-lbs}}$$

FLIGHT CONDITION 4 Flaps 30 Degrees

Fig. 14. Yawing Moment for Outboard Engine Failure

Evaluating δ_R, β_{max} and δ_w for each model

No Winglets

$$\delta_R \approx \frac{-150,747}{(-.0028)(66.04)(2433)(130.83)}$$

$$\delta_R \approx \underline{2.56°} \quad \text{for } \beta = 0°$$

$$\beta_{max} \approx \frac{-150,747}{(.0026)(66.04)(2433)(130.83)}$$

$$\beta_{max} \approx \underline{-2.76°} \text{ , for } \delta_R = 0$$

$$\delta_w \approx \frac{-(-.0022)(-2.76)}{.00065}$$

$$\delta_w \approx \underline{-9.34°}$$

With Winglets

$$\delta_R \approx \frac{-145,814}{(-.0028)(66.04)(2433)(130.83)}$$

$$\delta_R \approx \underline{2.48°} \quad \text{for } \beta = 0°$$

$$\beta_{max} \approx \frac{-145,814}{(.0027)(66.04)(2433)(130.83)}$$

$$\beta_{max} \approx \underline{-2.57°} \text{ , for } \delta_R = 0$$

$$\delta_w \approx \frac{-(-.0027)(-2.57)}{.00065}$$

$$\delta_w \approx \underline{-10.68°}$$

δ_R and δ_w are, in both cases, within their respective mechanical limits. Note that even though the maximum sideslip and engine out yawing moment is less with winglets, the required control wheel deflection is slightly more. Also,

if $\delta_{R_{max}}$ is allowed to define the minimum directional control speed, it can be seen from the above calculations that this speed would be slightly less for the winglet model. This is considering the same amount of rudder deflection as that required by the baseline configuration.

Steady State Maneuvering Flight. Since all the flight conditions tested in this report are for symmetrical flight only, the maneuvering characteristics involve pull ups only.

Based on this, FLEXSTAB calculated the elevator per g derivative $\frac{\partial \delta e}{\partial n}$. This derivative is required to be less than zero by handling quality requirements in reference 8. It has the proper sign for both models over the entire range of flight conditions observed.

A small negative increment in elevator per g is consistently noted with the winglet model. Although this model is statically more stable, the implication here is that it is slightly less maneuverable longitudinally. This same result is also reflected in the increase in stick fixed maneuver margin defined as

$$\left(\bar{x}_{Ref} \middle| \frac{\partial \delta e}{\partial n} = 0 - \bar{x}_{cg} \right)$$

See Table 14 for changes in these parameters.

Summary. It was seen that the winglets created a requirement for a negative increment in horizontal stabilizer trim angles. The added nose down pitching moment tendency from the winglets is the primary cause of this effect and

Table 14
Winglet Effect on Longitudinal Control
Parameters Steady Pull-Up

Flight Condition (rigid airplane)	1	2	2A	3	4 (Flaps 30°)
% Aft Shift in Stick Fixed Maneuver Point, $\frac{\partial \delta e}{\partial n} = 0$	7.95	8.03	7.47	6.79	6.25
% Increase in Maneuver Margin	16.00	24.32	20.75	13.30	14.50
% Decrease in Longitudinal Control/G, $\frac{\partial \delta e}{\partial n}$	17.41	25.83	22.08	14.47	15.54

results in a slightly reduced C_L and α trim range for the aircraft. Also overall increases in stick speed stability were noted. Laterally, the winglets had no effect on rudder effectiveness and only a small effect on inboard aileron effectiveness. An engine out example revealed less yaw induced sideslip and rudder required but slightly more control wheel deflection with winglets. Maneuvering in a steady state pull up, the winglets were found to offer increases in maneuver margin along with increases in elevator required per g.

Dynamic Stability Analysis of Winglet Effect

Introduction. Dynamic stability, as defined in this report, is the tendency of the amplitudes of the perturbed

motion of an airplane to decrease to zero or to values corresponding to a new steady state, at some time after the disturbance has stopped (Ref 6:6.1). Using this definition, the effect of the winglets on the dynamic stability of the FLEXSTAB model is evaluated. Note again that the dynamic stability, studied in this report, uses linear small perturbation theory.

Because of time considerations, aircraft dynamic modes with and without winglets are compared in detail for Flight Condition 1 only. Also for this flight condition, sample model responses to longitudinal and lateral control inputs are looked at. Here, changes in the state variables are plotted versus time. However, in an attempt to evaluate the overall dynamic effect of the winglets for all of the flight conditions tested, tables showing the winglet effect on various dynamic mode parameters are provided.

General Effect of Winglets on Dynamics. By way of some general remarks, the winglets, when applied to the rigid model, provide no significant stabilizing effects on the longitudinal modes. As can be seen in Table 15, the decrease in short period damping ratio varies from over 6 to 11 per cent along with an 8 to almost 13% increase in undamped natural frequency. However, time to half amplitude did decrease very slightly.

The pitch damping derivative, C_{m_q}, is important to stability in that, along with C_{L_α}, it determines short period damping (Ref 6:5.16). For all the flight conditions

Table 15.
Winglet Effect on Short Period Dynamic Mode and C_{m_q}

Flight Condition (rigid model)	1	2	2A	3	4 (Flaps 30°)
% Increase in Undamped Natural Frequency, ω_n	9.05	12.75	11.81	8.29	8.55
% Decrease in Period, T	10.32	14.87	17.44	10.07	17.69
% Decrease in Time to Half Amplitude T 1/2	.24	.44	.47	.87	1.24
% Decrease in Damping Ratio $\zeta_{S.P.}$	8.37	11.59	10.13	6.65	6.63
% Change of Negative Increment in C_{m_q}	3.1	2.96	2.82	2.85	2.6

observed, the winglets resulted in a small stabilizing change in C_{m_q}, also shown in Table 15.

As far as the phugoid mode is concerned, almost no change is noticed due to the winglets. This long period dynamic mode is influenced primarily by changes in C_{D_u}, which, from Appendix E, Table I, is almost totally unaffected by adding winglets to the model.

Laterally, the winglets are consistently stabilizing to the dutch roll, spiral and rolling characteristic modes. Referring to Table 16, a 5 to almost 14% decrease in time to half amplitude and a 3 to 12% increase in damping ratio is observed for the dutch roll mode. In Table 17, an average

Table 16
Winglet Effect on Dutch Roll Dynamic Mode

Flight Condition (rigid model)	1	2	2A	3	4 (Flaps 30°)
% Increase in Undamped Natural Frequency, ω_n	3.18	3.01	2.59	2.88	2.40
% Decrease in Period, T	2.98	2.74	2.42	2.18	2.15
% Decrease in Time to Half Amplitude T 1/2	13.62	12.50	11.44	9.23	5.24
% Increase in Damping Ratio $\zeta_{D.R.}$	12.4	10.28	9.80	7.07	3.03

Table 17
Winglet Effect on Rolling Dynamic Mode

Flight Condition (rigid model)	1	2	2A	3	4 (Flaps 30°)
% Decrease in Time to Half Amplitude, T 1/2	9.86	9.77	10.43	10.14	10.28

10% decrease in the time to half amplitude is seen for the rolling mode. As for the stabilizing effect on the spiral mode, the reader is referred to Appendix E, Table I.

Flight Condition 1 Dynamics. Before analyzing the dynamics of flight condition 1, the flight parameters defining it are reproduced below:

Altitude = 28,500 feet

Mach = .77

Gross Weight = 284,000 pounds

c.g. in % $\bar{c}$ = .242

This cruise configuration has stability and control derivatives, from FLEXSTAB, tabulated in Table I of Appendix E.

Using the FLEXSTAB data for flight condition 1, CALMAT calculated longitudinal and lateral stability derivatives matrices, control matrices, and the necessary eigenvalues and eigenvectors, from which STATVAR time plots of the characteristic dynamic mode shapes were made.

Before going any further, it is necessary to point out that the eigenvalues calculated by CALMAT are somewhat different than those calculated by FLEXSTAB. Table 18 reflects these differences. The greatest variations between CALMAT and FLEXSTAB are in the real spiral roots and the real parts of the phugoid roots. A possible explanation for these differences is that CALMAT uses equations of motion that assume $C_{D_{\dot{\alpha}}}$, C_{D_q}, $C_{y_{\dot{\beta}}}$, $C_{\ell_{\dot{\beta}}}$ and $C_{n_{\dot{\beta}}}$ are zero. FLEXSTAB, on the other hand, includes these derivatives; and as listed in Appendix E, the computed FLEXSTAB values are not zero. Because these modes have small roots and are easily controlled, these differences are relatively unimportant. Note that the short period, dutch roll and rolling roots of CALMAT and FLEXSTAB compare quite well.

Table 18
Comparison of CALMAT and FLEXSTAB Eigenvalues

Flight Condition 1	No Winglets	With Winglets
	Short Period	Short Period
CALMAT	(-.8322 + 1.8051j)	(-.8333 + 2.0102j)
FLEXSTAB	(-.8297 ∓ 1.8029j)	(-.8321 ∓ 2.0080j)
	Phugoid	Phugoid
CALMAT	(-.0024 + .0649j)	(-.0022 + .0641j)
FLEXSTAB	(-.0016 ∓ .0650j)	(-.0015 ∓ .0642j)
	Dutch Roll	Dutch Roll
CALMAT	(-.2126 + 1.5574j)	(-.2464 + 1.6021j)
FLEXSTAB	(-.2030 ∓ 1.5590j)	(-.2350 ∓ 1.6050j)
	Spiral	Spiral
CALMAT	(+.0027)	(+.0009)
FLEXSTAB	(+.0044)	(+.0026)
	Roll	Roll
CALMAT	(-1.2514)	(-1.3815)
FLEXSTAB	(-1.2430)	(-1.3780)

As mentioned previously, the winglet effect longitudinally is confined to the short period mode of oscillation, with almost no effect observed on the phugoid mode. Figure 15 shows the winglet effect on the short period. It reveals that the winglets increase the relative amplitudes of the angle of attack α and pitch angle θ state variables, with only small changes noted in phase angle relationships. Looking at time history plots in Figures 16a and 16b from

No Winglets

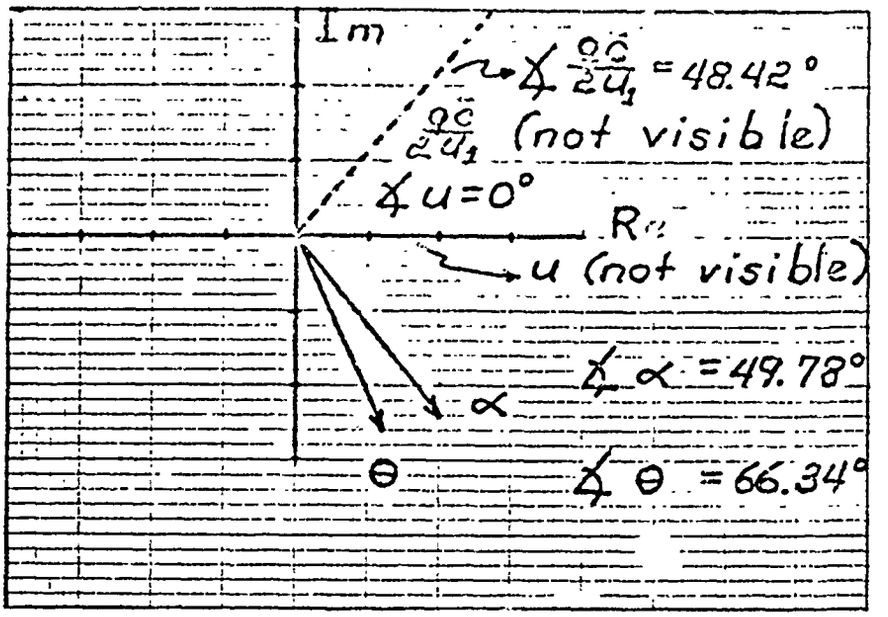

With Winglets

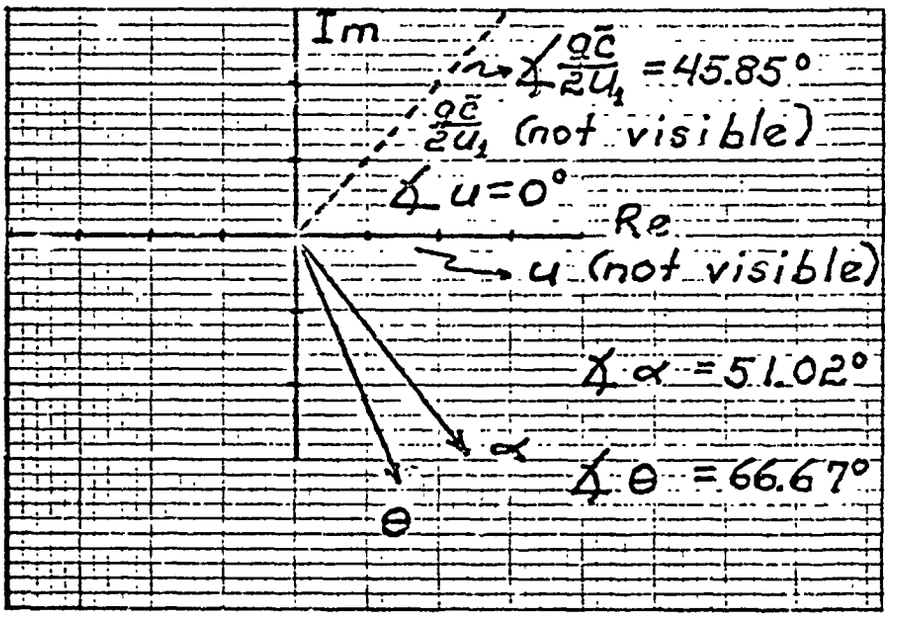

Fig. 15. Phase Angle and Magnitude Plots of Short Period With and Without Winglets

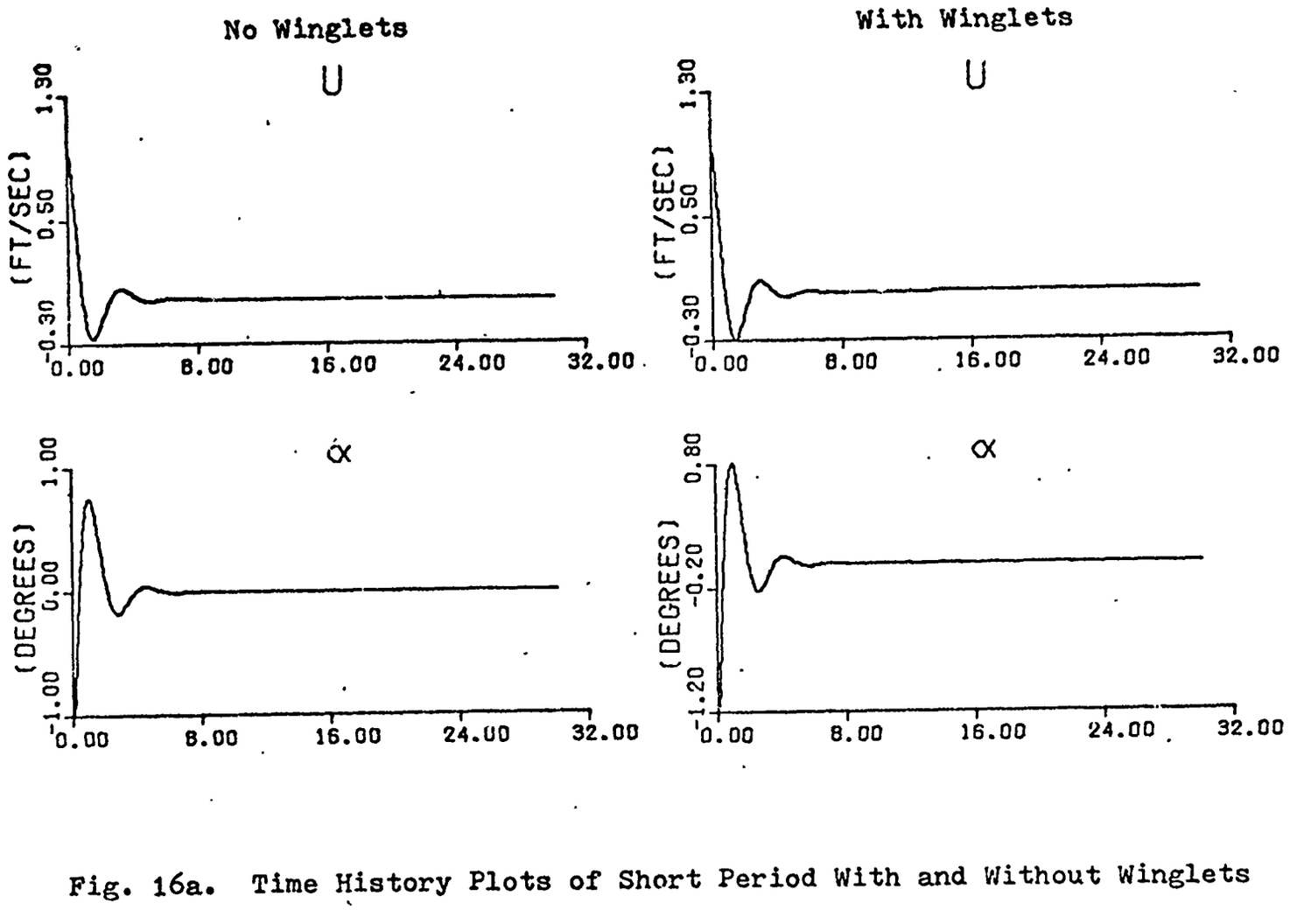

Fig. 16a. Time History Plots of Short Period With and Without Winglets

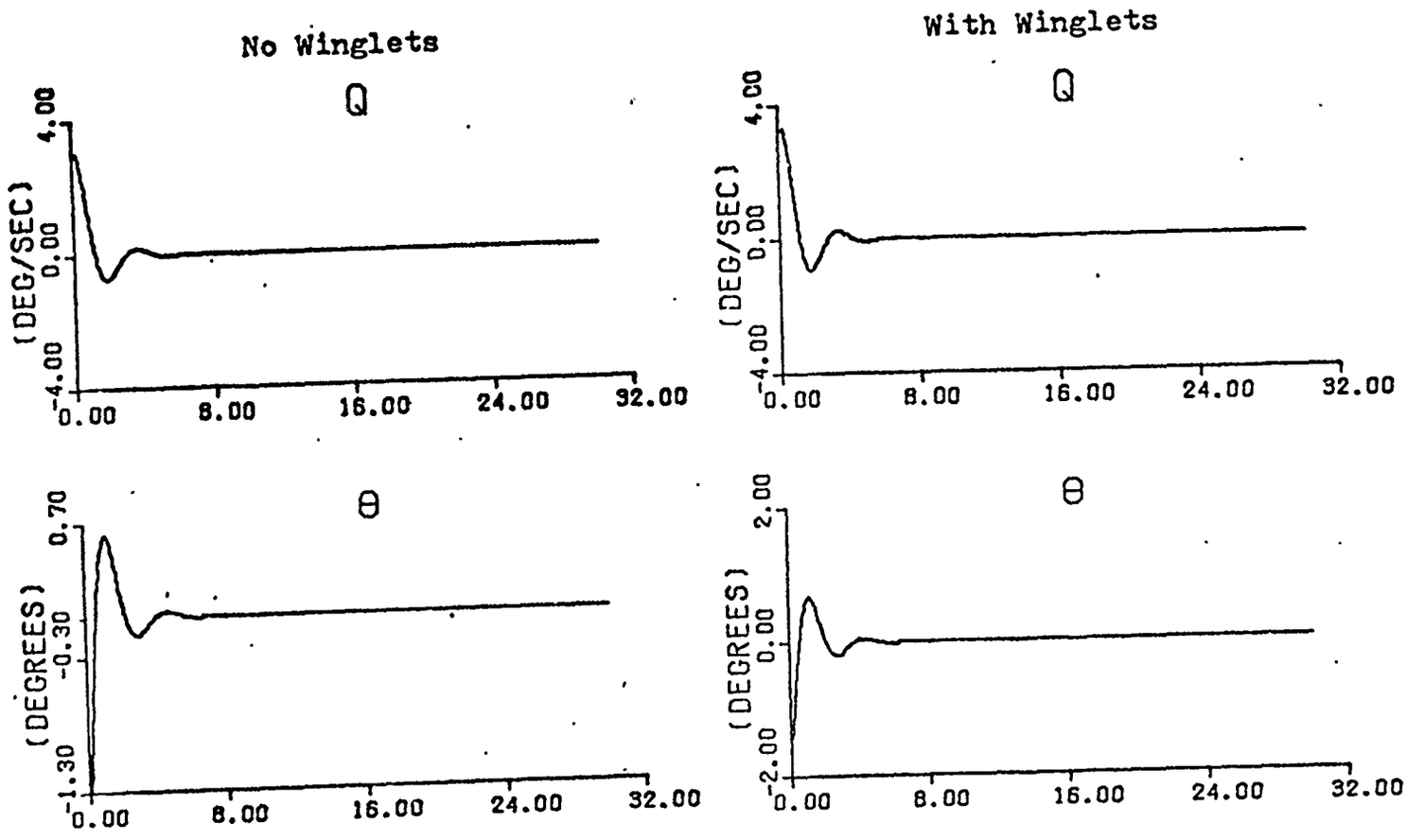

Fig. 16b. Time History Plots of Short Period With and Without Winglets (cont'd)

STATVAR, the amplitude differences in α and θ are also apparent. Almost no differences, however, in amplitudes or phase relations are seen in u and q. The overall conclusion is that the effect of the winglets on the short period mode is small. Table 19 shows the short period dynamic characteristics.

Laterally, the winglet effect on the dutch roll mode is the most important. The spiral and rolling modes are nonoscillatory and are usually well within the pilot's capability to control. Suffice it to say that the winglets are stabilizing to these modes as can be seen in Table 20. The derivative C_{n_r} usually has the most effect on spiral stability while C_{ℓ_p} primarily affects the rolling mode (Ref 6:6.77-6.85). The winglet effect on these derivatives is also shown in Table 20.

As previously noted, the winglet effect on the dutch roll lateral aircraft mode is stabilizing. For flight condition 1, the overall effect of the winglets on this dynamic mode is shown in Table 21. From this, it can be seen that the directional stability derivative C_{n_β}, which normally has a strong effect on dutch roll frequency and damping, changes little with winglets. Consequently, the dynamics shown in Table 21 are mostly affected by changes in C_{n_r} and C_{y_β} (Ref 8:134). These derivatives have a powerful effect particularly on dutch roll damping (Ref 6:6.77-6.85).

The dutch roll mode shapes for flight condition 1 are shown in Fig. 17. Here it can be seen that little change

Table 19
Winglet Effect on Short Period Dynamic Behavior

Flight Condition 1 (rigid model)	No Winglets	With Winglets
$\omega_{n_{s.p.}}$ (rad/sec)	1.99	2.17
$\zeta_{s.p.}$	.418	.383
$T_{s.p.}$	3.49	3.13
$T_{s.p.}1/2$ (sec)	.835	.833

Table 20
Winglet Effect on Spiral and Rolling Modes

Flight Condition 1 (rigid models)	No Winglets	With Winglets
Spiral Divergence T2 (secs)	156.35	263.42
Rolling Time to Half Amplitude	.558	.503
C_{ℓ_p} (1/rad)	-.4969	-.5590
C_{n_r} (1/rad)	-.2926	-.3161

in the state variable relationships results. The amplitudes of β and θ are reduced slightly along with small changes in r and p. Also phase angle relationships remain fairly constant with or without winglets. Figures 18a and 18b show the dutch roll state variable response versus time

No Winglets

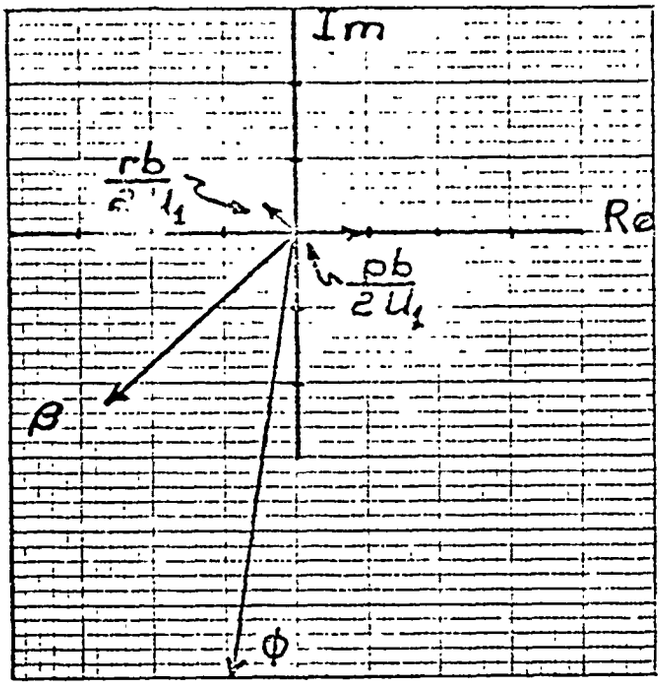

With Winglets

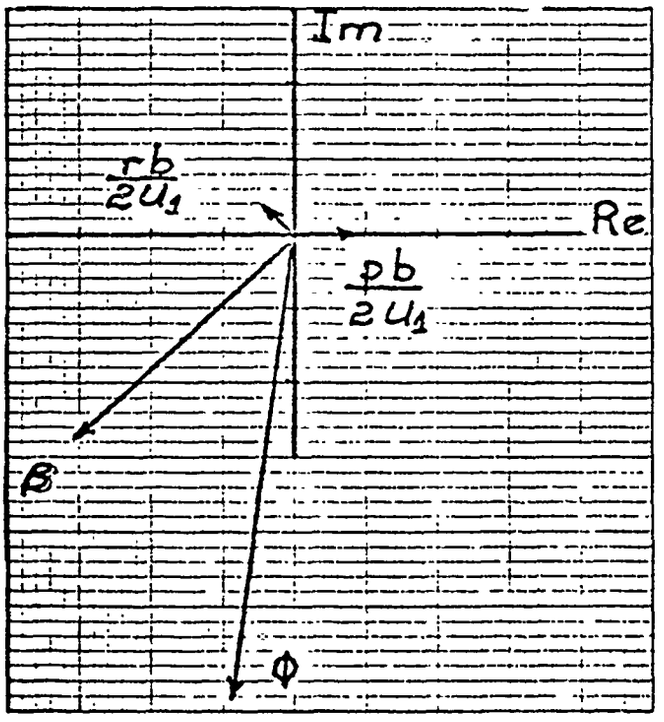

Fig. 17. Phase Angle and Magnitude Plots of Dutch Roll With and Without Winglets

Table 21
Winglet Effect on Dutch Roll Dynamic Behavior and Selected Lateral Derivatives

Flight Condition 1 (rigid model)	No Winglets	With Winglets
$\omega_{n_{D.R.}}$ (rad/sec)	1.57	1.62
$\zeta_{D.R.}$	.129	.145
$T_{D.R.}$ (sec)	4.03	3.91
$T_{D.R.}1/2$ (sec)	3.414	2.949
C_{n_r} (1/rad)	-.2926	-.3161
C_{y_β} (1/deg)	-.0116	-.0133
C_{n_β} (1/deg)	.0034	.0036

using the real parts of the eigenvectors shown in Fig. 17 as initial conditions. Here the amplitude differences are more easily seen. The greatest apparent winglet effect is in reducing the amplitude of β.

Figures 19 (a & b) and 20 (a & b) attempt to show the winglet effect on the longitudinal and lateral state variables for two control inputs--a 20° elevator impulse and a 10° rudder impulse.

In Fig. 19 (a & b), the model's response to a 20° elevator impulse shows only small differences in the changes of the state variables compared with and without winglets.*

*Note that, 20° of elevator here is actually 20° of stabilizer which exceeds the mechanical limits on the actual aircraft. The stabilizer was used for amplification purposes.

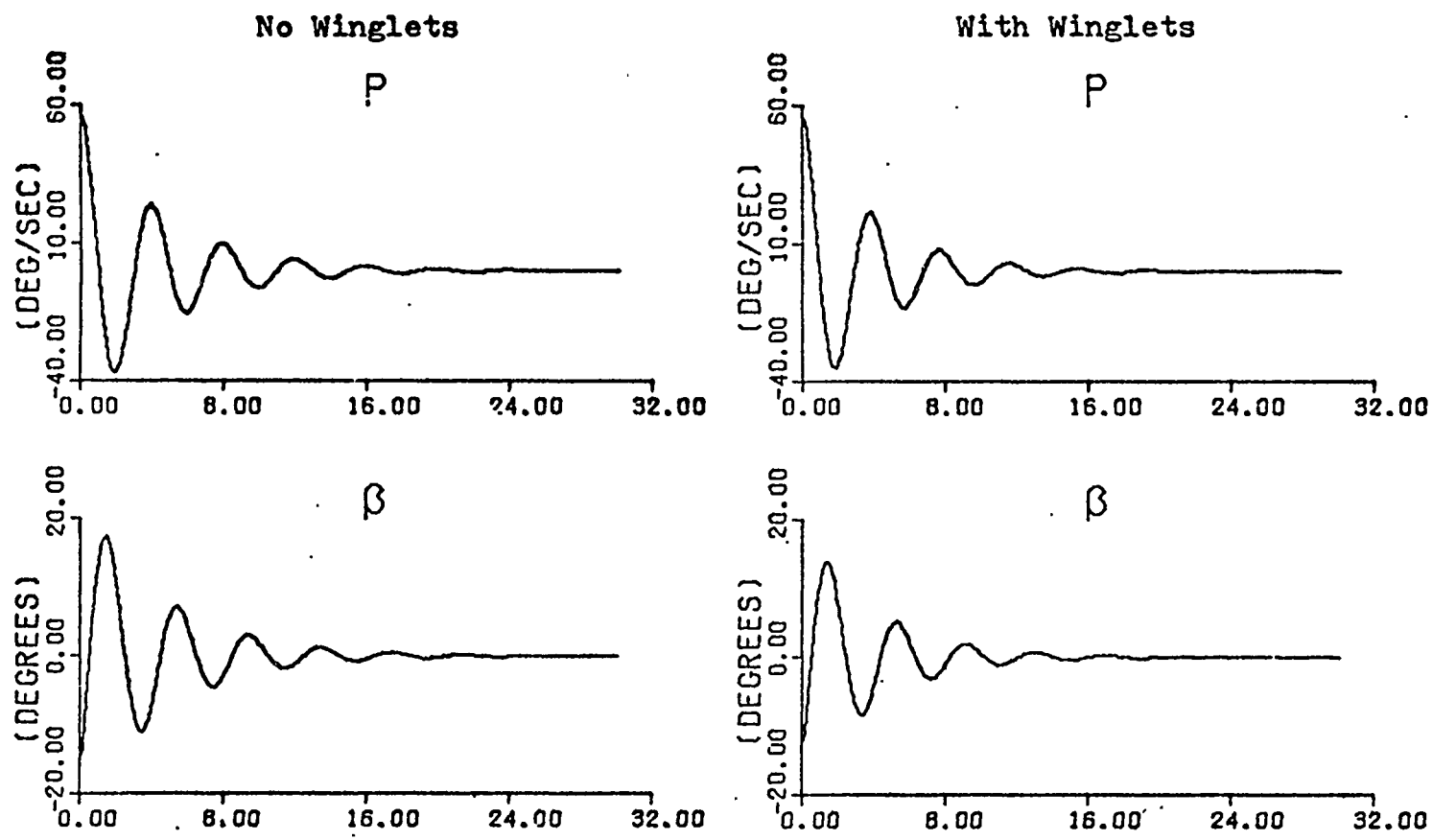

Fig. 18a. Time History Plots of Dutch Roll With and Without Winglets

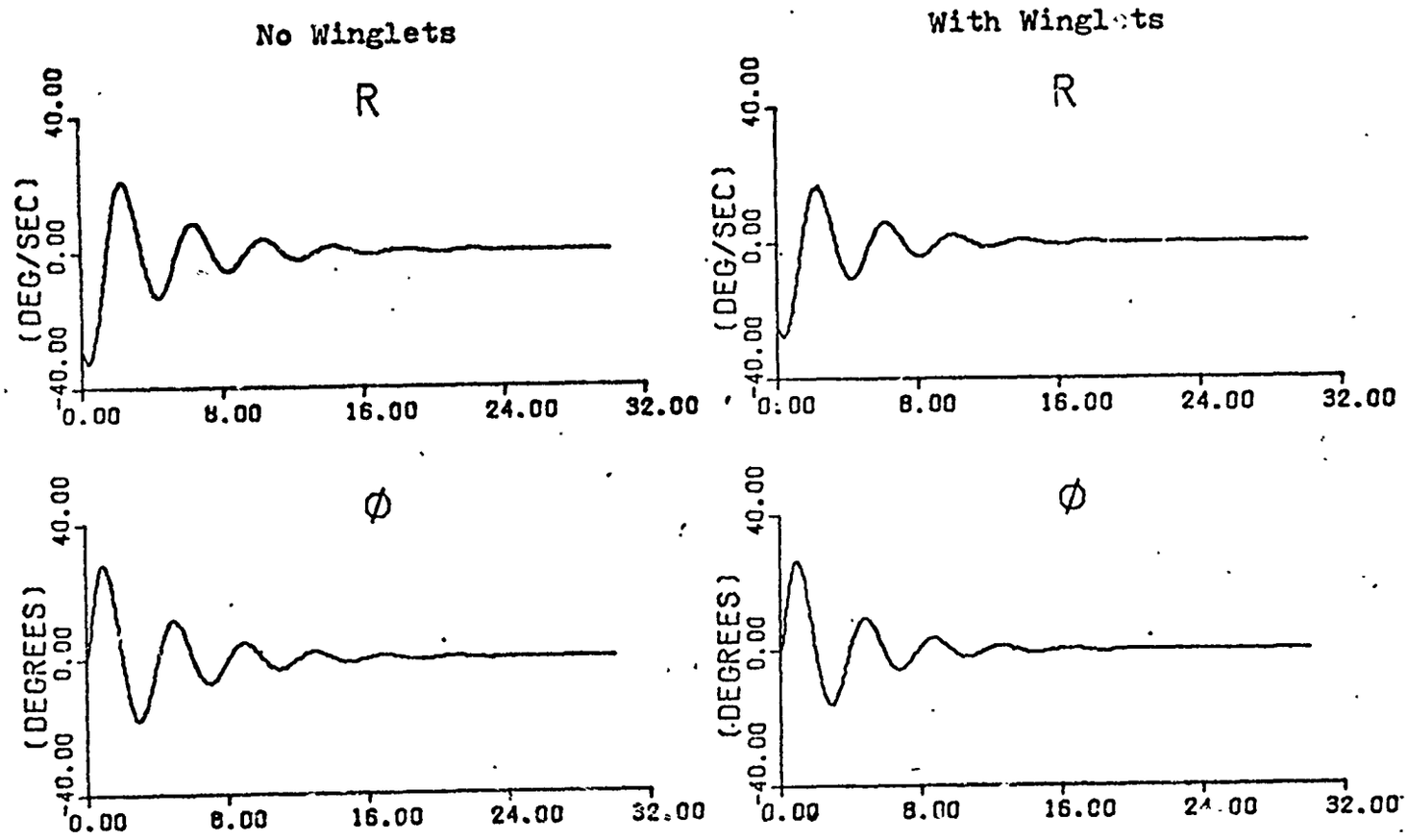

Fig. 18b. Time History Plots of Dutch Roll With and Without Winglets (cont'd)

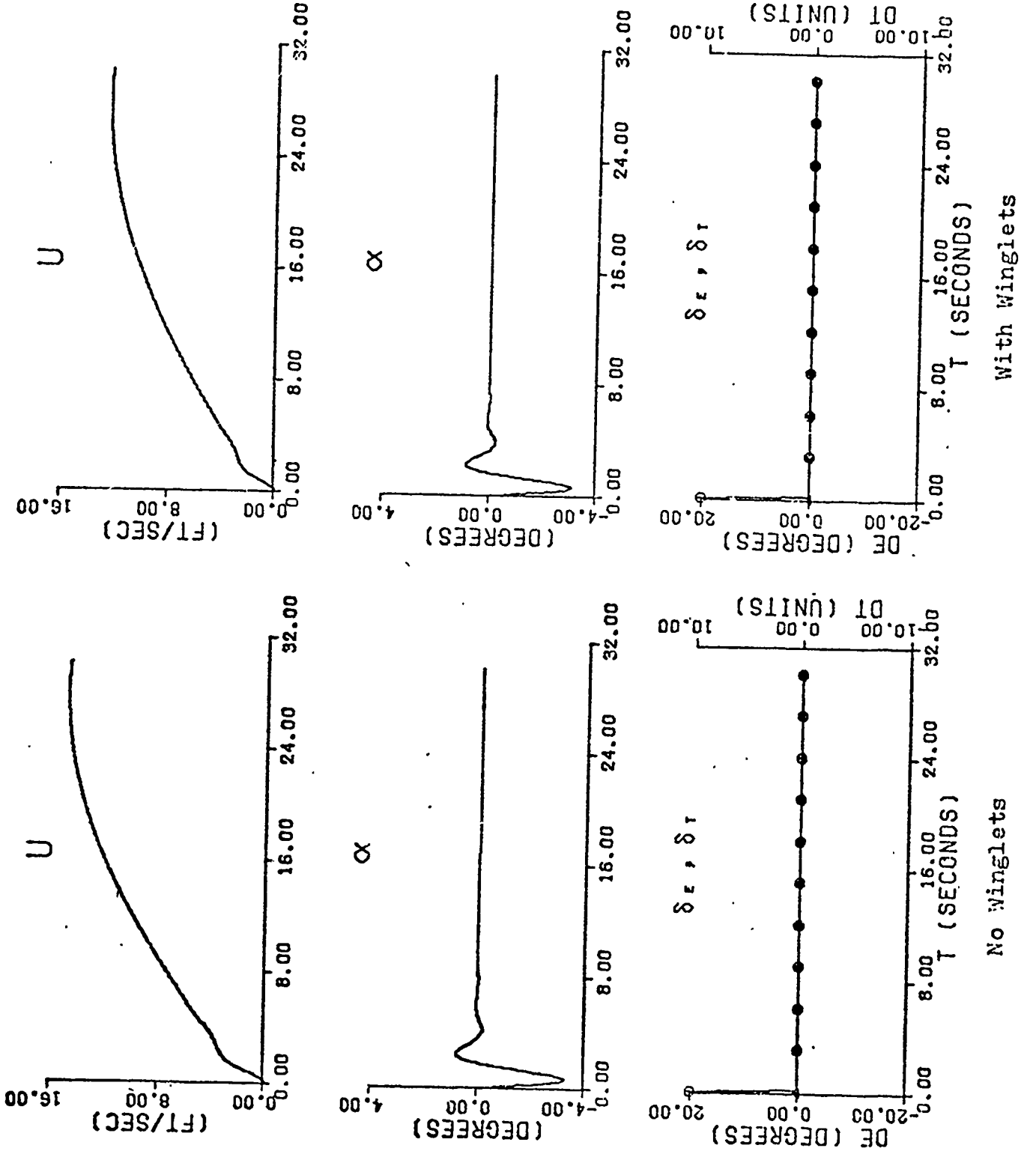

Fig. 19a. Comparison of Longitudinal Response to a 20° Elevator Impulse

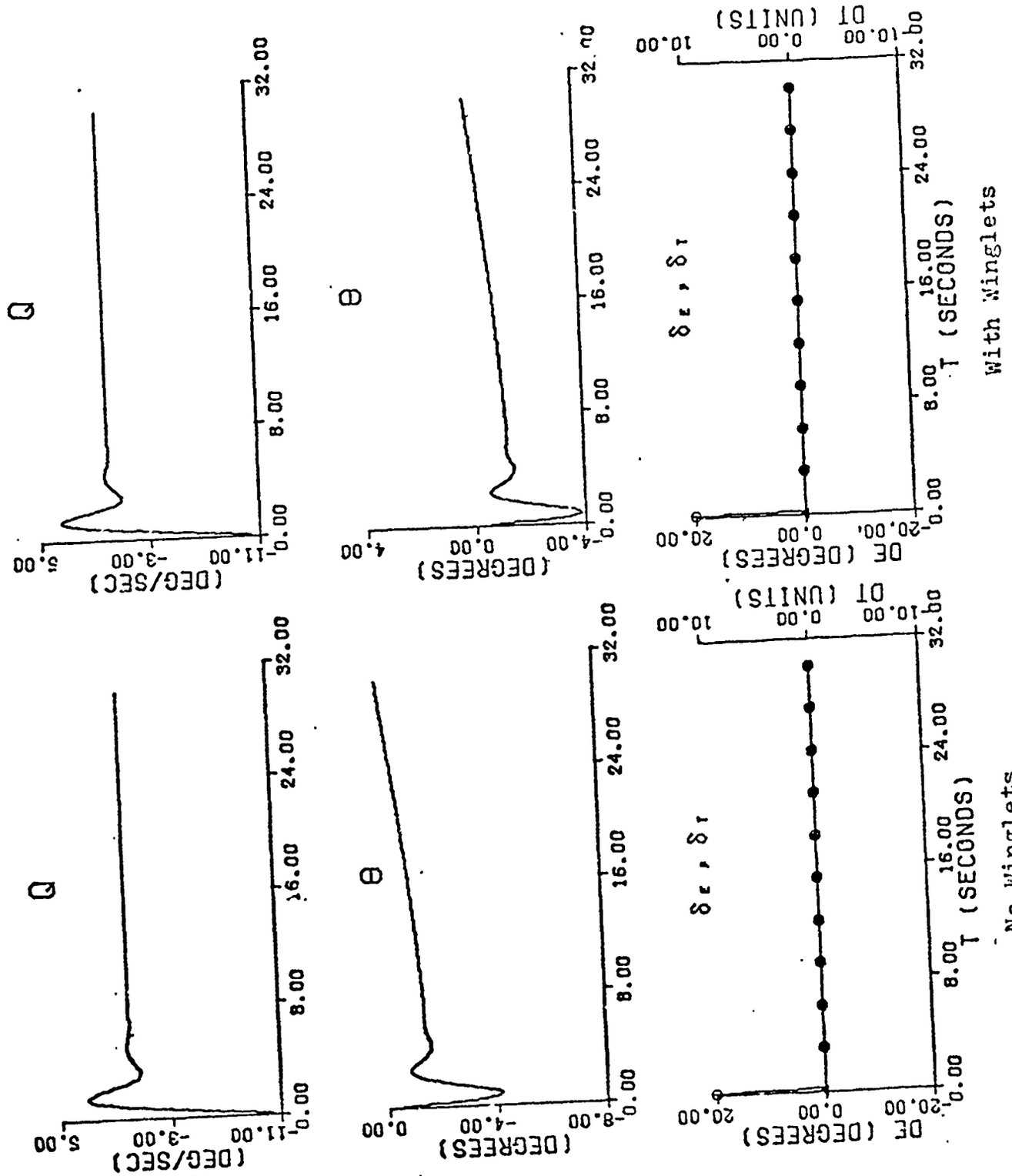

Fig. 19b. Comparison of Longitudinal Response to a 20° Elevator Impulse (cont'd)

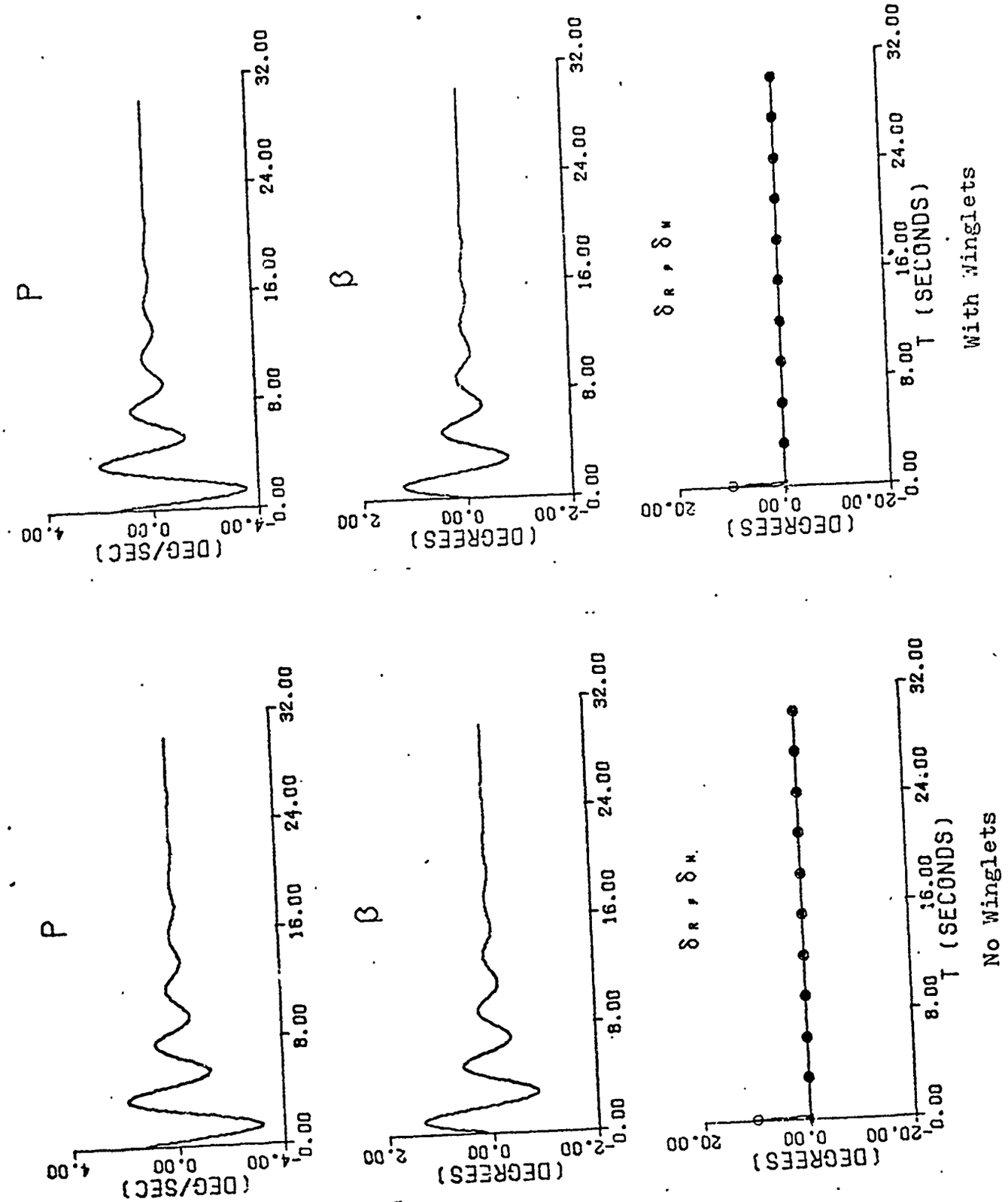

Fig. 20a. Comparison of Lateral Response to 10° Rudder Impulse.

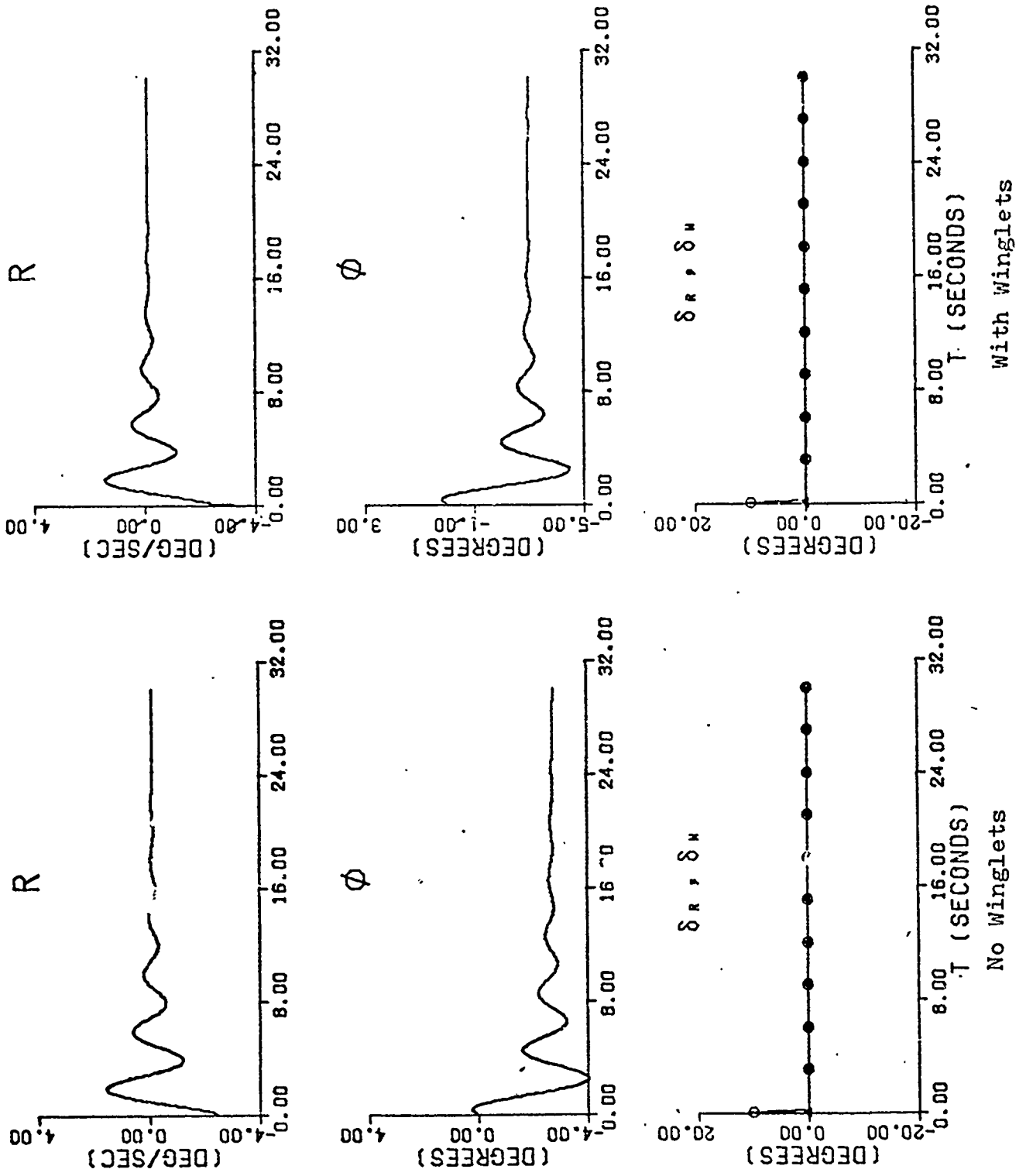

Fig. 20b. Comparison of Lateral Response to 10° Rudder Impulse (cont'd)

The most noticeable difference is in u. Its peak value is slightly greater without winglets. Also, to a lesser extent, the amplitudes of the other variables are less with winglets although this is difficult to see.

Laterally, for impulsive 10 degree rudder inputs, the winglets do not appear to affect the frequency or magnitudes of the state variables. This is shown in Fig. 20 (a & b).

Summary. The overall winglet effect on the longitudinal dynamic modes was felt primarily in the short period. Here decreases in damping ratios varied from over 6% to almost 12%. Laterally, the dutch roll mode was more stable with winglets. Damping ratios increased from 3 to 12%. Positive effects on the rolling and spiral modes were seen also. As far as the model responses to control inputs are concerned, only very small changes in the state variable responses were seen with winglets added to the model.

Analysis of the Effect of a Shorter Vertical Tail on the Winglet Model

Introduction. As it affects lateral-directional and dynamic stability and control, the purpose of this section is to investigate the possibility of reducing the vertical stabilizer on the winglet configured aircraft model as shown in Fig. 21. No reduction of the rudder control surface itself is involved.

Because the shortened vertical stabilizer has no thickness definition, FLEXSTAB, in its calculations, shows no effect on the longitudinal characteristics of the model.

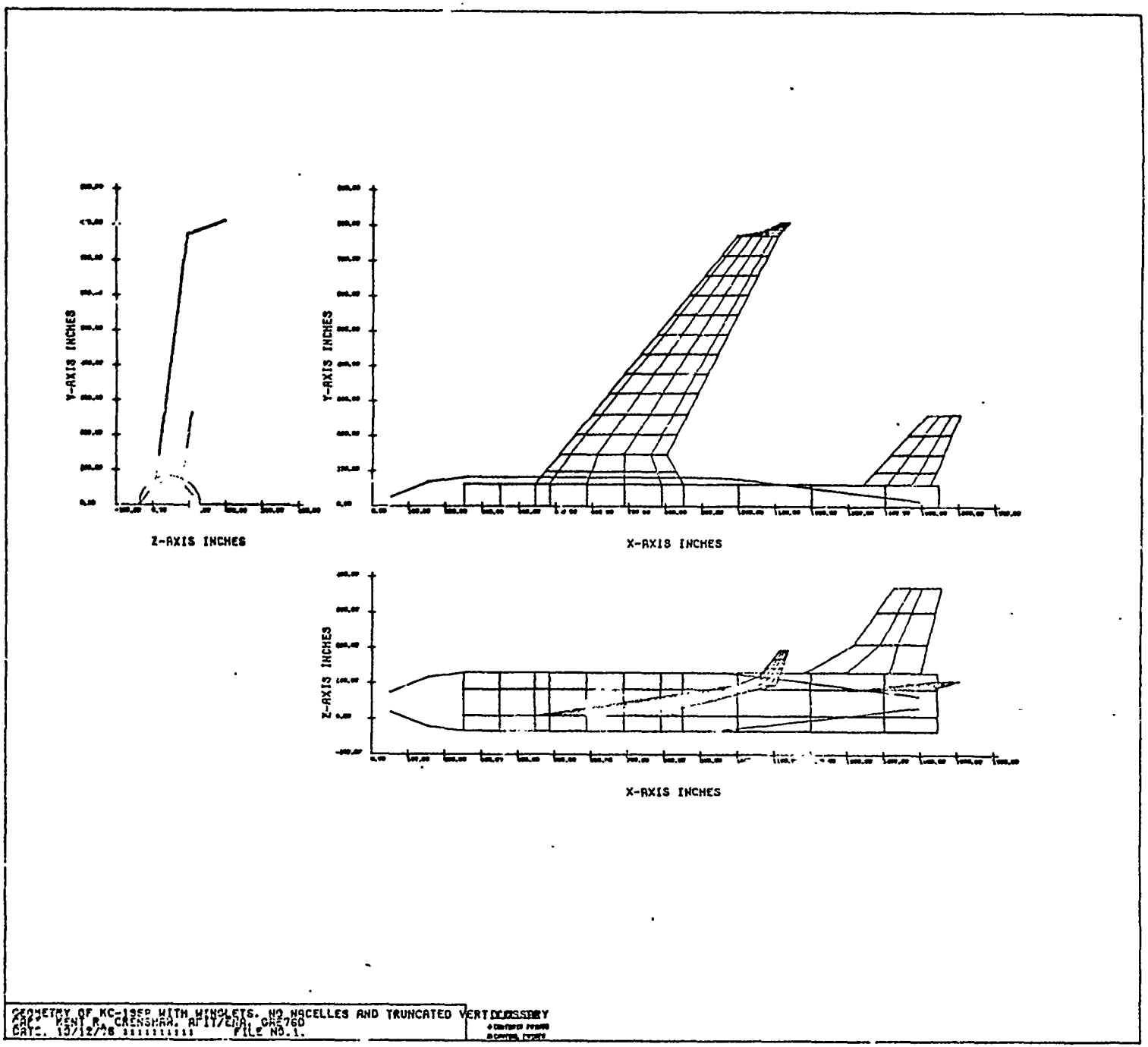

Fig. 21 Truncated Vertical Tail Model

Also, no observation of the additional drag reduction involved can be made. In reality, such a reduction would be small, and the primary interest here is in lateral stability and control. It has been proposed that the added lateral stability provided by the winglets could make the shortened vertical tail configuration of Fig. 21 feasible. The complete data calculated by FLEXSTAB for this model is shown in Table II of Appendix E.

In making this analysis, the lateral characteristics of the short tail configuration are compared with those of the full tail model with and without winglets. This is done only for flight condition 2A, defined as cruise equilibrium flight at 28,500 feet altitude, .77 Mach number and 130,000 pounds gross weight.

Lateral-Directional Stability. Here selected lateral stability derivatives are discussed. These are C_{y_β}, C_{n_β}, C_{ℓ_β}, C_{ℓ_p} and C_{n_r}.

From Table 22, it can be seen that the side force derivative, C_{y_β}, becomes less negative with the short tail winglet model. This is not surprising due to the strong effect the vertical tail surface has on this derivative. However, C_{y_β} with this configuration, is a less stable value than that calculated for the full tail model without winglets by 4.3%. Also, when compared to the full tail winglet model, this difference in C_{y_β} is 17.16%.

The yaw stiffness derivative, C_{n_β}, moves in a less stable direction by shortening the vertical tail. When

Table 22
Lateral Derivatives Comparison With
Short Tail Winglet Model

Flight Condition 2A (rigid models)	N.W. (full tail)	W.W. (full tail)	W.W. (short tail)
Cy_β (1/deg)	-.0116	-.0134	* -.0111
Cn_β (1/deg)	.0032	.0034	* .0024
$C\ell_\beta$ (1/deg)	-.0026	-.0034	-.0029
$C\ell_p$ (1/rad)	-.4959	-.5577	-.5533
Cn_r (1/rad)	-.2677	-.2851	* -.2237

*Note that these values are less stable than those for the no winglet model in the first column.

compared to the full tail winglet model, Cn_β is 29.41% less stable. Cn_β is a less stable value than that for the full tail model without winglets by 25%.

$C\ell_\beta$, or the dihedral effect derivative, becomes 14.71% less stable than the same value for the full tail winglet model shown in Table 22. Notice that here the winglets are able to create a compensating effect on this derivative to make it 11.54% more stable than the value calculated for the baseline model.

The destabilizing effect of reducing the vertical tail had the least effect on $C\ell_p$. Again, the winglets still have a strong compensating influence on this derivative by making it 11.57% more stable than the value shown for the no winglet model.

C_{n_r}, or the yaw damping derivative, is not as stable with the shorter tail when compared to either of the full tail models. Here again, the winglets fail to offer a compensating effect. C_{n_r} for the short tail winglet model is 16.44% less stable than the same value for the baseline configuration.

Lateral Control. Because of the 12% reduction of the vertical tail area, the result is a less effective aerodynamic surface. The value of S_v, the planform vertical tail area, is smaller. This effectively reduces the rudder control authority as Table 23 indicates. Note that

$$C_{y_{\delta_R}} = C_{L_{\delta_v}} \alpha_{\delta_R} n_v \frac{S_v}{S} ,$$

(Ref 6:4.44)

$$C_{\ell_{\delta_R}} = C_{L_{\alpha_v}} \alpha_{\delta_R} n_v \frac{S_v}{S} \frac{Z_{v_s}}{b}$$

(Ref 6:4.40)

and

$$C_{n_{\delta_R}} = -C_{L_{\alpha_v}} \alpha_{\delta_R} n_v \frac{S_v}{S} \frac{X_{v_s}}{b}$$

(Ref 6:4.79)

These equations show the linear dependence of $C_{y_{\delta_R}}$, $C_{\ell_{\delta_R}}$, and $C_{n_{\delta_R}}$ on S_v. For a given dynamic pressure, $n_v = \frac{\bar{q}_v}{\bar{q}}$; the rudder deflection required in controlling a yawing moment, rolling moment and side force is increased. Note that the percentages shown in Table 23 are independent of

Table 23
Short Tail Effect in Reducing Rudder Authority
for $C_{y_{\delta R}}$, $C_{n_{\delta R}}$ and $C_{\ell_{\delta R}}$

Flight Condition 2A (rigid models)	Compared to Full Tail Models With or Without Winglets
*% Decrease in $C_{y_{\delta R}}$ (less positive)	12%
% Decrease in $C_{\ell_{\delta R}}$ (less positive)	21.43%
*% Increase in $C_{n_{\delta R}}$ (less negative)	11.76%

*Note that these reductions in rudder effectiveness in side-force and yawing moment are comparable to the 12% reduction of the vertical tail.

winglets. It was noted earlier that the winglets themselves have almost no effect on rudder authority.

Dynamic Lateral-Directional Stability. Table 24 shows the comparison of the short tail model dynamics with both of the full tail model configurations. Here the effect of the shorter vertical tail is primarily on the dutch roll and spiral modes. No effect is noted on the rolling mode.

Looking at the dutch roll mode in Table 24, the short tail model has a longer time to half amplitude and a smaller undamped natural frequency than either of the other two full tail models. Damping ratio, however, falls between the value for the baseline model and the full tail winglet model. This value is 3.27% better than the baseline

Table ?4
Dynamic Modes Comparison With
Short Tail Winglet Model

Flight Condition 2A (rigid models)	N.W. (full tail)	W.W. (full tail)	W.W. (short tail)
Dutch Roll			
ω_n (rad/sec)	1.93	1.98	1.66
period (sec)	3.3	3.22	3.83
$\zeta_{D.R.}$	.153	.168	.158
T 1/2 (sec)	2.36	2.09	2.65
Spiral (FLEXSTAB)	(S=-.0034)	(S=-.0049)	(S=-.0064)
T 1/10 (sec)	675.68	470.42	358.3
T 1/2 (sec)	203.4	141.61	107.86
Spiral Approximation	(S=-.0604)	(S=-.109)	(S=-.1044)
T 1/10 (sec)	38.12	21.18	22.06
T 1/2 (sec)	11.48	6.36	6.64
Roll			
T 1/10 (sec)	1.242	1.113	1.113
T 1/10 (sec)	.374	.335	.335

configuration. When comparing the full tail and short tail winglet models, there is a 5.95% reduction in damping ratio caused by the shorter vertical tail. The overall net effect is a less stable dutch roll mode.

As far as the spiral mode is concerned, the FLEXSTAB values in Table 24 show a large increase in spiral stability for the short tail winglet model over both of the full tail configurations. This is an unexpected result, particularly after having noted the consistently less stable derivatives discussed for this model earlier. Using the spiral approximation shown in reference 6, page 6.54, a more reasonable trend is found in comparing the three models. Because this approximation ignores the angle of bank degree of freedom, the large differences in the magnitudes of the time characteristics compared to the FLEXSTAB values are somewhat expected. However, the important point of the comparison is that the spiral for the short tail winglet model is less stable than the full tail winglet model, which is a more intuitive result. Without a more detailed analysis, the contrast among the FLEXSTAB calculated spiral mode characteristics is not understood.

Summary. Reducing the vertical tail by 12% on the winglet model results in less stable values for Cy_β, Cn_β, $C\ell_\beta$, $C\ell_p$ and Cn_r. Cy_β, Cn_β, and Cn_r were noted to be less stable than those values calculated for the full tail baseline model.

As for lateral control effectiveness, the shorter tail, and hence smaller S_V, revealed reductions in rudder authority for $Cy_{\delta R}$, $C\ell_{\delta R}$ and $Cn_{\delta R}$. This was verified by equations from reference 6.

Dynamically, the dutch roll mode for the shortened vertical tail model was less stable than either of the two full tail models. Improvements in spiral stability, with the short tail winglet model, actually surpassed that of the full tail winglet model. This result was very surprising and is not understood. If one can accept the comparison made with the spiral approximation, the FLEXSTAB results seem questionable. Finally, the rolling mode remained unaffected by the change in the vertical tail.

IV. Elastic Model Analysis

Introduction

As mentioned earlier, aeroelastic effects, particularly with large aircraft such as the KC-135A, are significant. Furthermore, the weight of the winglet and its aerodynamic forces and moments create additional elastic deflections of the wing. These deflections yield somewhat different winglet effects than the rigid model analysis of the previous section.

Winglet Effect on Drag Coefficient and Lift Over Drag L/D

As with the rigid analysis, the winglet produces drag reductions and improvements in L/D ratios. However, using the elastic models, these improvements are much less as shown in Table 25. For all the cruise conditions observed, drag reductions due to winglets amount to only 1.3%. Consequently, L/D ratios are not greatly improved either. In reducing drag, the elastic winglet model is 4 to 6 per cent below the figures for the rigid model.

Winglet Elastic Effect at the Wing Tip

In order to place the following part of this section into a proper physical perspective, some discussion of the elastic winglet effect on the wing is ›ded.

Table 26 shows the "washout" angles and fuselage reference line angles of attack with and without winglets.

Table 25
Winglet Effect on Drag and Lift/Drag, L/D

Cruise Condition (static elastic models)	1	2	3
$\bar{q}$ (psf)	261.67	128.59	181.69
Mach Number, M	.77	.77	.422
Altitude (feet), h	30,000.	45,000.	10,000.
Airplane Lift Coefficient, C_{L_1}	.421	.849	.603
% Increase in L/D	1.45	1.39	1.54
% Decrease in Drag	1.31	1.29	1.29

Table 26
"Washout" Angles and Angles of Attack

Cruise Condition (static elastic models)	1 ($\bar{q}$=261.67psf)		2 ($\bar{q}$=128.57psf)		3 ($\bar{q}$=181.69psf)	
	N.W.	W.W.	N.W.	W.W.	N.W.	W.W.
"Washout" Angle at the Wing Tip (degs)	-3.1	-4.1	-2.9	-3.9	-2.9	-3.8
Angle of Attack of Fuselage (degs)	2.573	2.583	7.262	7.212	5.716	5.687

"Washout," as used here, means a negative rotation about the structural y-axis of the wing, i.e., leading edge down. Note that the model without winglets displays a fairly

constant -3° "washout" at the tip. The winglet model has a degree more "washout." This effect is due to three things:

1. a small spanwise shift in the pressure distribution outboard along the aft chord section of the wing,
2. an aft chordwise shift in pressure at the outboard wing, and
3. the aerodynamic loads created on the winglet.

All three of these phenomena create forces which add an increment in negative torque at the wing tip. Fig. 22 demonstrates, graphically, the aft shift in pressure at the wing tip for cruise condition 1. This effect is not seen inboard on the wing. In fact, the chordwise pressure distributions on the inboard wing sections are the same with or without winglets. Also in Fig. 22 there is a small spanwise movement of pressure implied along the aft chord section of the wing. Average pressures for each chord section were taken and plotted along spanwise locations of the wing in an attempt to show this over the whole wing. However, this effect is found to be very small and confined only to the most outboard section of wing panels. It should be pointed out that pressure plots of the outboard wing are somewhat degraded by neglecting the viscous interaction at the juncture of the wing and the winglet.

Perhaps the greatest contribution to the increase in "washout" at the tip comes from the aerodynamic forces on the winglet. Since the vortex diffusing effect of the winglet results in a more lift effective outboard wing,

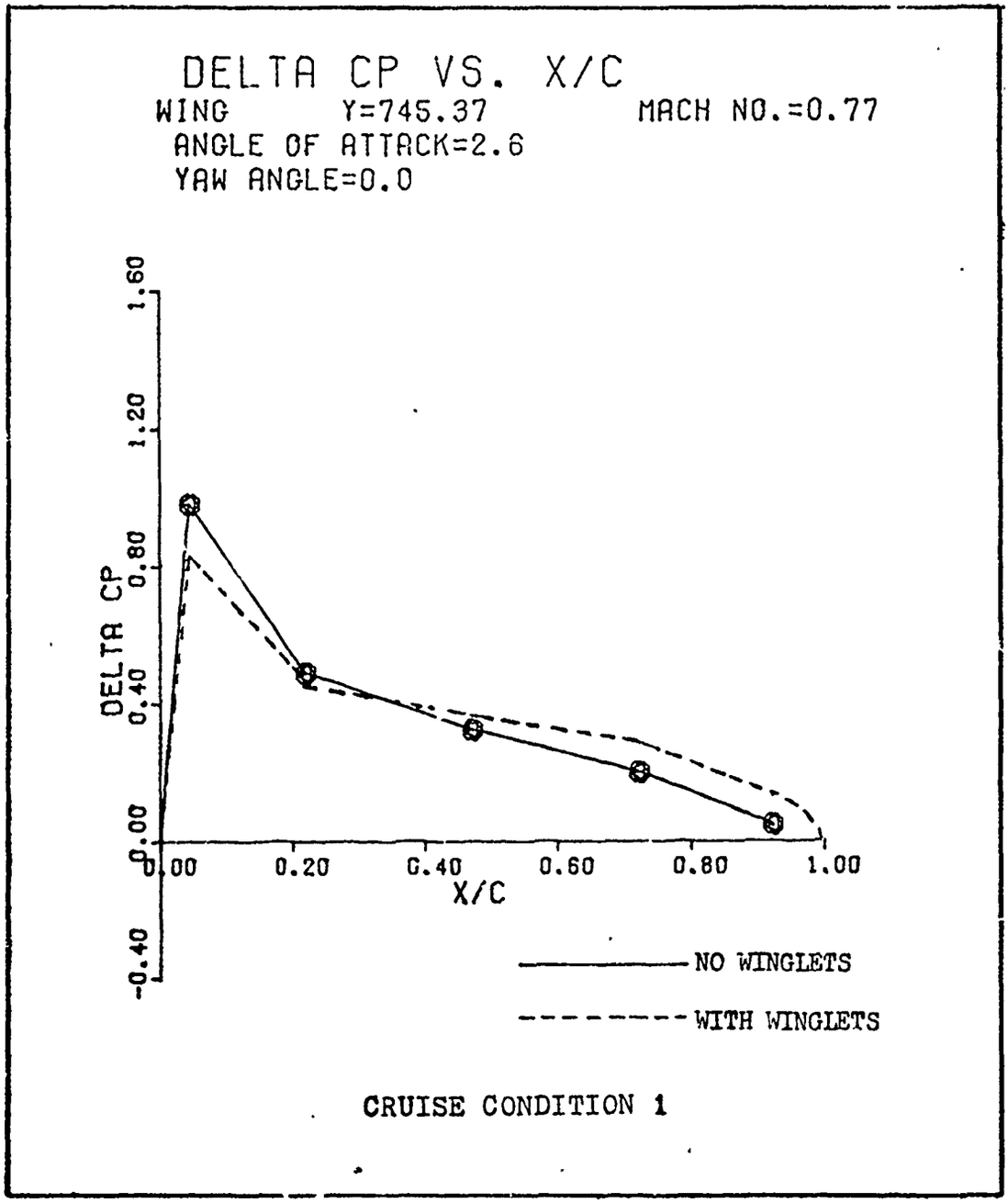

Fig. 22. Chordwise Pressure Distribution of Outboard Wing With and Without Winglets (elastic models)

the elastic winglet model experiences greater bending and consequently more washout due to the sweep of the wing. The sweep effect is shown in Fig. 23.

Referring to the designated chord sections on the FLEXSTAB winglet plot of Fig. 24, winglet chordwise pressure distributions for a rigid flight condition sample of the previous section are shown in Fig. 25. As expected, the pressure is generally higher at the leading edge then tapers off moving aft for each chord section shown. Looking at Fig. 26 for the winglet on the elastic model, however, the reverse is shown. There is a larger pressure rise indicated toward the trailing edge of the winglet. This effect, and the fact that for an airfoil the pressure differential is normally highest at the leading edge, make these results questionable. No explanation for these elastic winglet pressure distributions is available. The winglet pressure plots on the rigid model, however, seem credible.

Referring again to Table 26, observe the almost negligible winglet effect on angle of attack. This is a "washout" effect which was absent in the rigid analysis. Where an angle of attack reduction was consistently observed for the rigid winglet model because of a more lift effective outboard wing, the elastic winglet model's increased "washout" tendency reduces this effect. Nonetheless, the winglet still offers some vortex diffusing effects at the

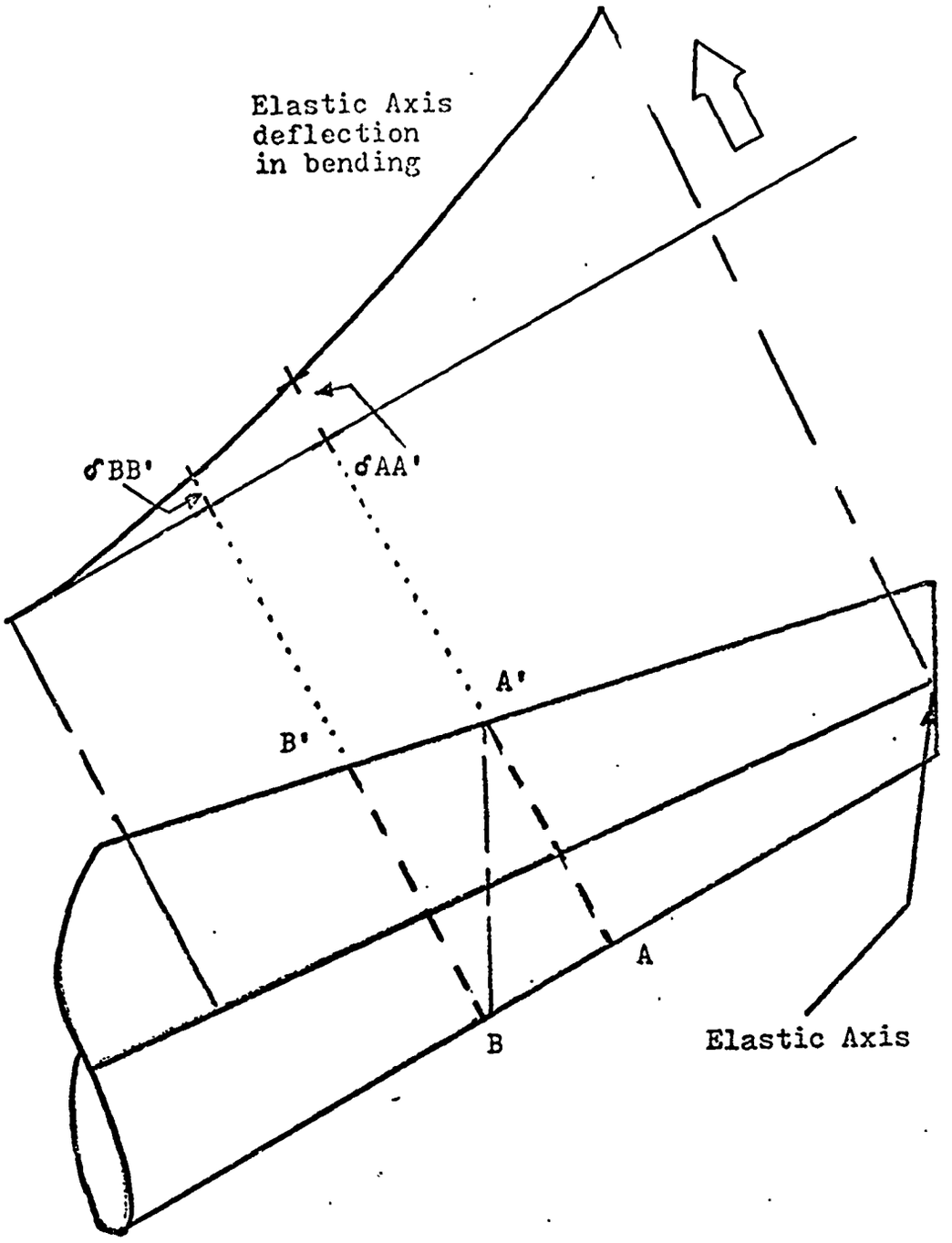

Moving outboard along the wing, the effective angle of attack decreases with the deflection of the elastic axis. This creates the outboard wing washout tendency as shown for the streamwise segment BA'.

Fig. 23. "Washout" of a Swept Wing Due to Bending

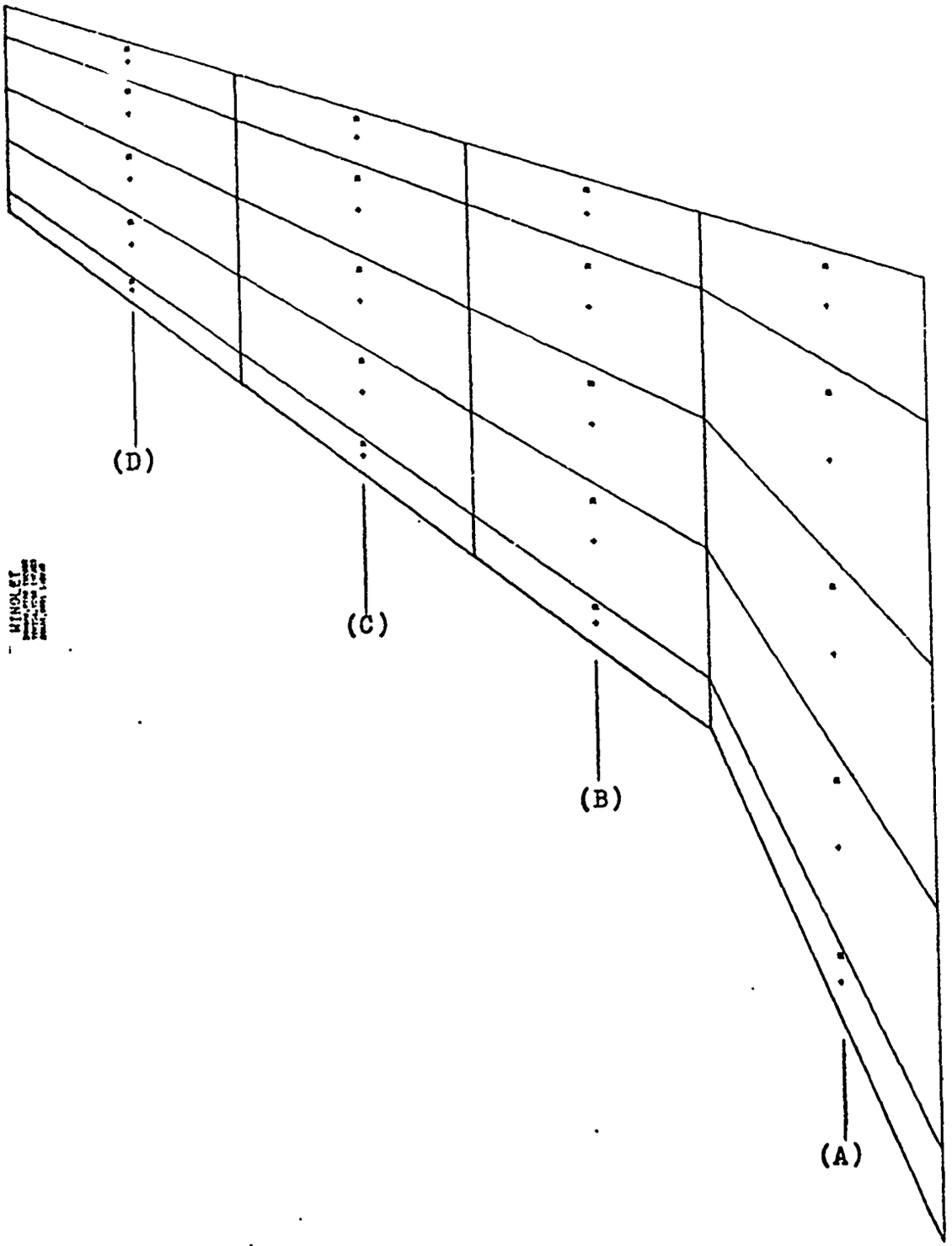

Fig. 24. Winglet Pressure Distribution Chord Sections

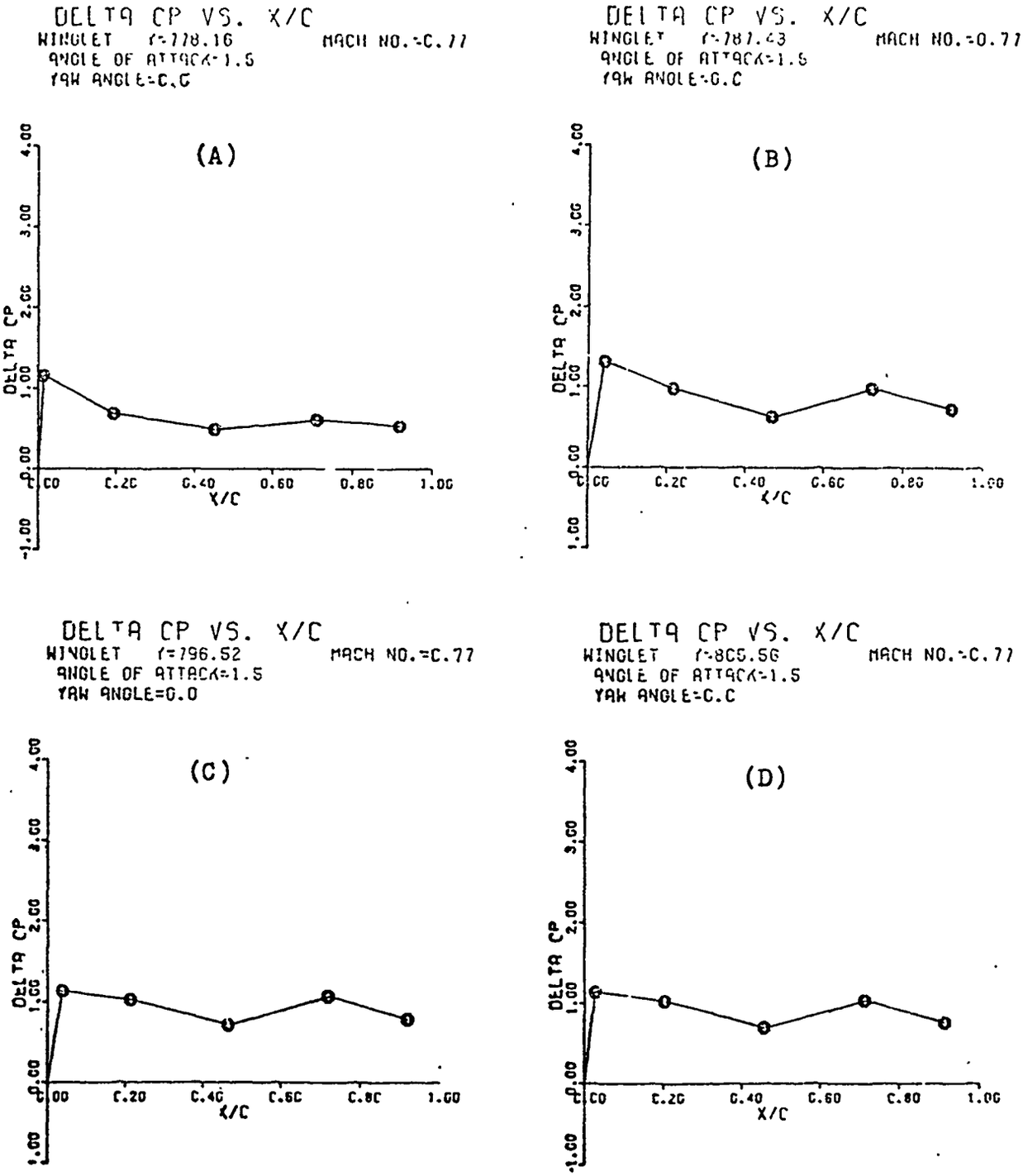

Fig. 25. Winglet Pressure Distribution Plots for Rigid Model

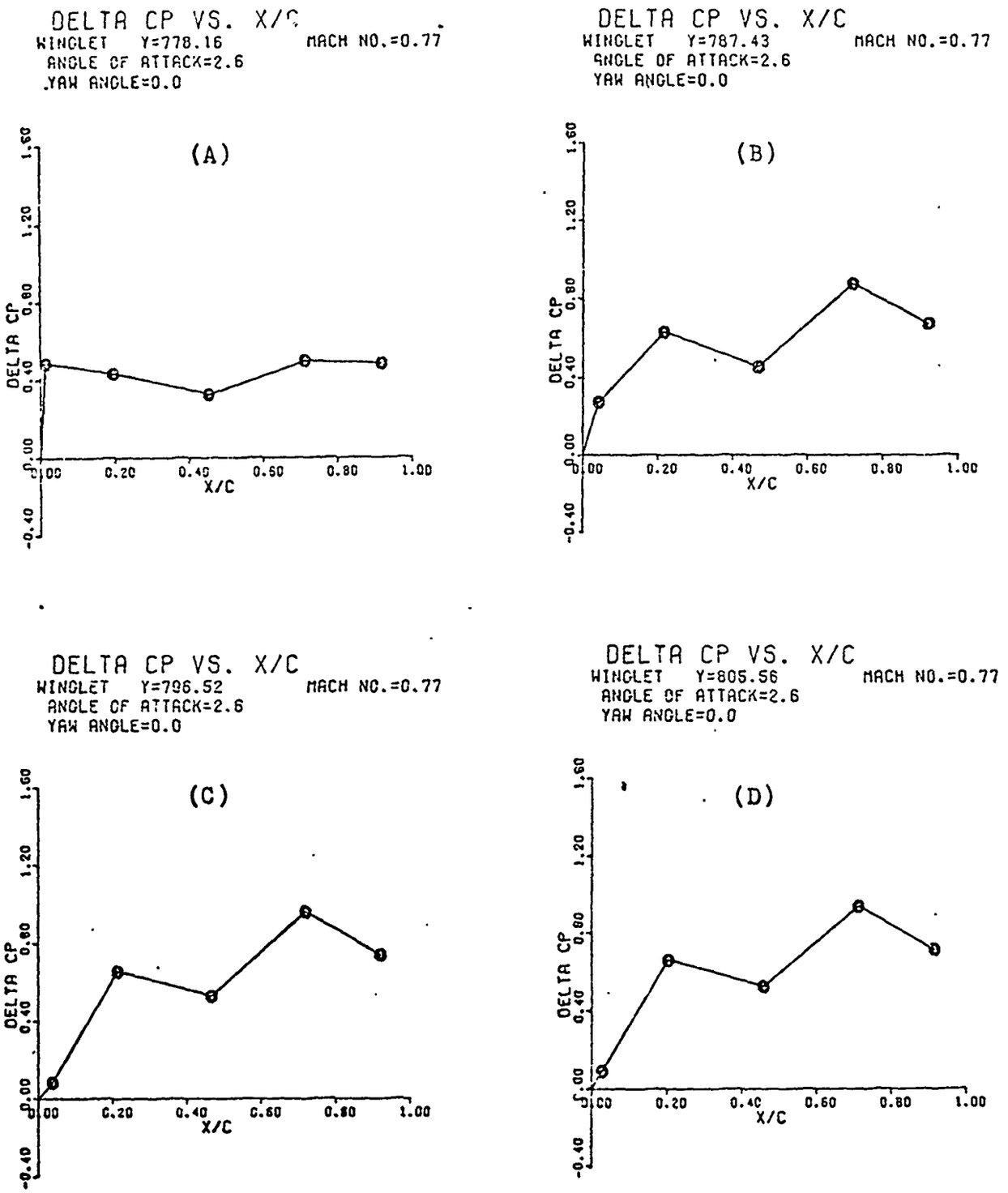

Fig. 26. Winglet Pressure Distribution Plots for Elastic Model

elastic wing tip, yielding the small performance improvements noted in Table 25.

Static Steady State Stability

Using the definitions and criteria for static steady state stability defined in the previous section, the elastic winglet model is evaluated longitudinally and laterally by comparison with the baseline model.

Longitudinal Static Stability. Referring to Table 27, all cruise conditions show an aft shift in aerodynamic center location due to winglets. These figures are roughly 3 to 4% less than those noted for the rigid model. Also, important to point out in Table 27, is that the static margin increased 7 to 11%. This has a positive stabilizing effect on C_{m_α} from equations previously related. Realize that this increase in static margin is little affected by the winglet induced aft shift in the overall center of gravity location of the model. This value is only $+.0022\bar{c}$ aft. Consequently, any weight penalty effect due to the winglet is negligible in this case.

From Table 28 there is a large difference between the rigid C_{L_α} increase with winglets and that noted using the elastic model. In fact, the elastic increases are almost negligible. This degradation in the elastic winglet effect on C_{L_α} is again due largely to the "washout" effect at the wing tip.

Having noted increases in both static margin and C_{L_α}, C_{m_α} becomes more negative by the amounts shown in Table 28.

Table 27
Winglet Effect on Aerodynamic Center Location

Cruise Condition (static elastic models)	1 ($\bar{q}$=261.67psf)	2 ($\bar{q}$=128.59psf)	3 ($\bar{q}$=181.69psf)
% Aft shift in Aerodynamic Center	*(7.92) 3.59	*(8.40) 5.98	*(7.05) 4.61
% Increase in Static Margin	*(15.08) 7.08	*(15.79) 11.60	*(13.39) 9.09

*rigid model changes

Table 28
Winglet Effect on C_{m_α} and C_{L_α} Derivatives

Cruise Condition (static elastic models)	1 ($\bar{q}$=261.67psf)	2 ($\bar{q}$=128.59psf)	3 ($\bar{q}$=181.69psf)
% Increase in C_{L_α} (more positive)	*(3.25) .68	*(3.41) 1.76	*(2.89) 1.30
% Decrease in C_{m_α} (more negative)	*(18.64) 8.00	*(19.56) 13.98	*(16.30) 10.42

*rigid model changes

Also comparing the elastic effect on C_{m_α} to the rigid winglet effect, the stabilizing improvement for the elastic model is significantly less.

In concluding this discussion of longitudinal static stability, it is interesting to observe the elastic effect

on selected longitudinal derivatives versus dynamic pressures shown in Fig. 27. Note that C_{m_α} is the most affected by aeroelastic effects. $C_{m_{\dot{\alpha}}}$ with winglets appears to remain the same as the rigid value over the interval of dynamic pressures shown. No explanation for this behavior is available.

Lateral Static Stability. Table 29 shows the winglet effect on selected lateral stability derivatives. Note that the winglets have a stabilizing effect on all these values. In comparing the winglet induced changes with the rigid changes that are observed, it is seen that the winglet effect on C_{y_β} and C_{n_r} is nearly the same. More changes are observed due to elastic effects on C_{n_β}, C_{ℓ_β} and C_{ℓ_p}.

Fig. 28 shows the elastic to rigid ratios calculated with and without winglets for the three cruise conditions observed. Note that for the model without winglets, C_{ℓ_β} ...rs to imp...ve its ratio with the rigid value with increasing dynamic pressure. The explanation for this is probably due to the additional dihedral of the wing due to bending. With winglets on the elastic model, however, the elastic to rigid value of C_{ℓ_β} decreases almost linearly with increasing dynamic pressure.

Summary. As far as static stability is concerned, the winglets contributed stabilizing effects to C_{L_α} and C_{m_α}. Laterally, the winglets were stabilizing to all the derivatives considered.

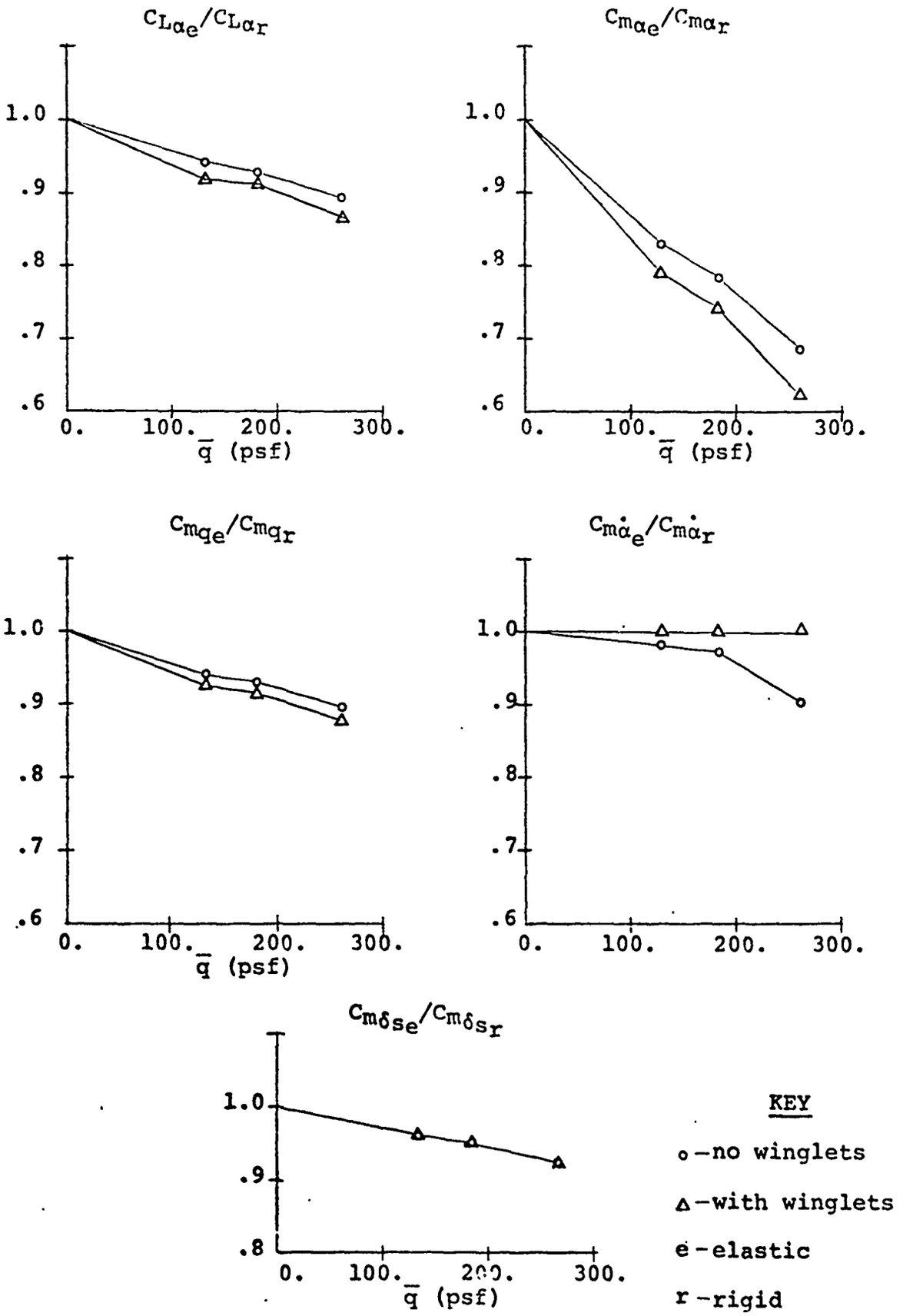

Fig. 27. Longitudinal Elastic to Rigid Ratios With and Without Winglets vs. Dynamic Pressure

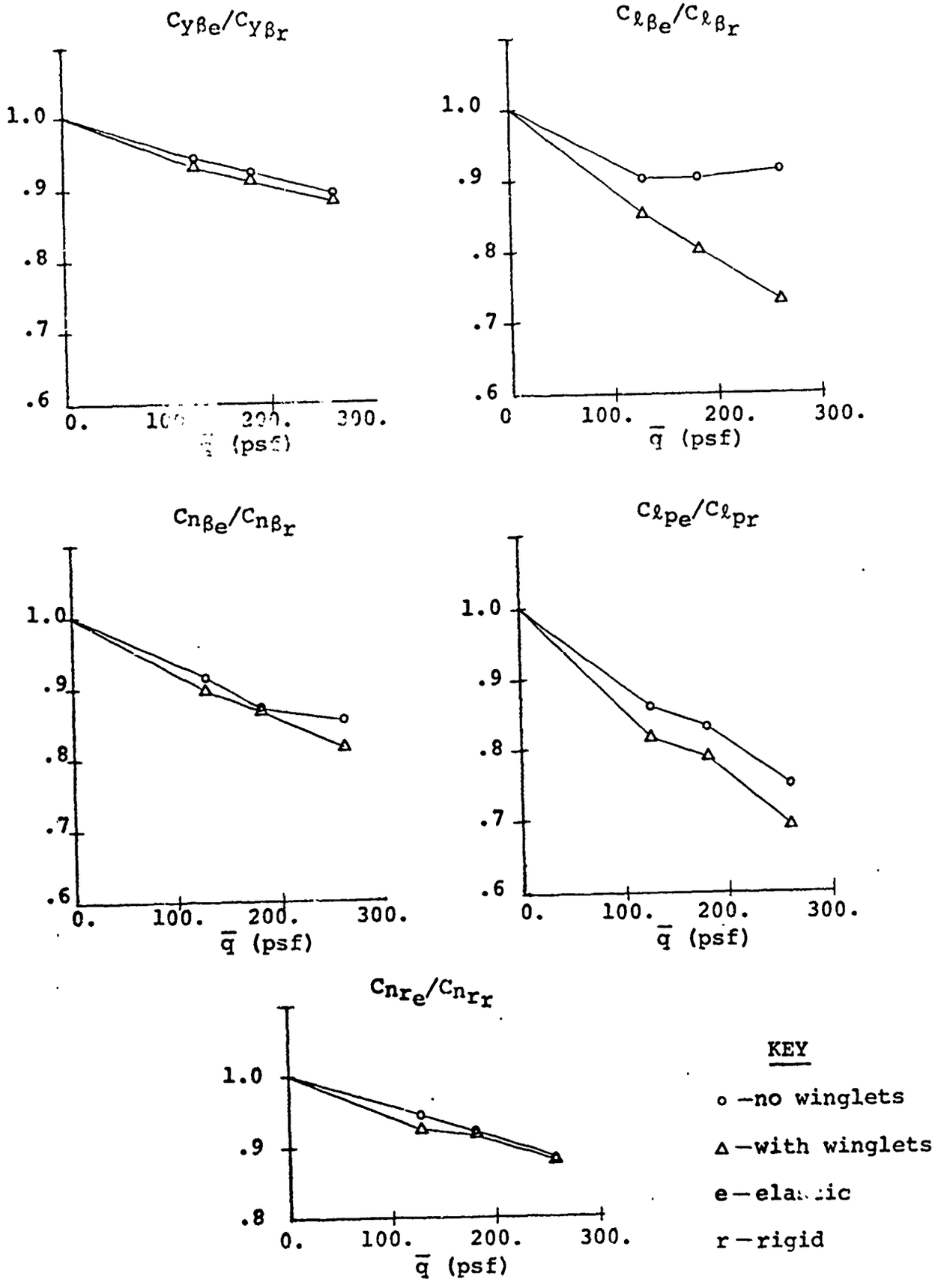

Fig. 28. Lateral Elastic to Rigid Ratios With and Without Winglets vs. Dynamic Pressure

Table 29
Winglet Effect on Lateral Stability Derivatives

Cruise Condition (static elastic models)	1 ($\bar{q}$=261.67psf)	2 ($\bar{q}$=128.59psf)	3 ($\bar{q}$=181.69psf)
% Decrease in C_{y_β} (more negative)	*(15.52) 14.56	*(15.52) 14.68	*(14.29) 13.4
% Increase in C_{n_β} (more positive)	*(11.76) 6.0	*(5.71) 3.13	*(6.67) 7.69
% Decrease in C_{ℓ_β} (more negative)	*(30.43) 4.76	*(28.57) 21.05	*(25.00) 11.11
% Decrease in C_{ℓ_p} (more negative)	*(11.96) 3.48	*(11.88) 6.67	*(10.75) 5.29
% Decrease in C_{n_r} (more negative)	*(7.34) 6.56	*(9.71) 8.19	*(6.54) 5.57

*rigid model values

Control Characteristics for Steady State Flight

Longitudinal. The winglets on the elastic model cause no effect on the longitudinal control derivatives $C_{L_{\delta_s}}$, $C_{D_{\delta_s}}$ and $C_{m_{\delta_s}}$ as Table III in Appendix E shows. However, since C_{m_α} is more negative, there is a requirement for more negative stabilizer trim. On the elastic model, the winglet effect on C_{m_α} is less. Consequently, the largest increase in stabilizer trim angle required is only 12%. This is a significant change from the 19 to 52% increase

in trim angle required by the rigid winglet model. Because the trim requirements are less for the elastic winglet model, there is assumed to be little or no noticeable decrease in the range of useful trim angles of attack and lift coefficients. The conclusion is that the elastic winglet model experiences almost no trim penalty. The winglet trim effect is shown in Table 30.

Using the same equations discussed in part III, the elastic model with winglets has a 9 to almost 12% increase in stick speed stability, $\frac{\partial \delta e}{\partial Vp}$, also shown in Table 30. Again, this comes about, directly, from the increase in static margin caused by the winglets.

Lateral Control. Consistent with the rigid analysis, the winglet had no effect on the rudder control derivatives $C_{y_{\delta R}}$, $C_{\ell_{\delta R}}$ and $C_{n_{\delta R}}$. This is shown in Table III of Appendix E.

However, unlike the rigid analysis where small reductions in inboard aileron control authority were observed, the elastic winglet model shows no change in $C_{y_{\delta A}}$, $C_{\ell_{\delta A}}$ or $C_{n_{\delta A}}$ compared to the baseline elastic model.

Steady State Maneuvering Flight. As with the rigid analysis, all the elastic flight conditions studied here are for symmetrical flight only. Consequently, the maneuvering characteristics are confined to pull-ups.

Table 31 shows the winglet effect in shifting the maneuver point aft. These figures are approximately 2 to

Table 30
Winglet Effect on Longitudinal Control Parameters

Cruise Condition (static elastic models)	1 ($\bar{q}$=261.67psf)	2 ($\bar{q}$=128.59psf)	3 ($\bar{q}$=181.69psf)
% Increase in δ_{strim} (more negative)	6.87	12.03	9.54
% Increase in Stick Speed Stability, $\frac{\partial \delta e}{\partial Vp}$	9.89	11.71	9.35

Table 31
Winglet Effect on Maneuvering Flight Parameters
(Steady State Pull-up Only)

Cruise Condition (static elastic models)	1 ($\bar{q}$=261.67psf)	2 ($\bar{q}$=128.59psf)	3 ($\bar{q}$=181.69psf)
% Aft Shift in Maneuver Point	*(7.66) 3.45	*(8.26) 5.88	*(6.68) 4.34
% Increase in Maneuver Margin	*(13.83) 6.43	*(15.14) 11.05	*(11.68) 7.79
% Decrease in C_{m_q} (more negative)	*(2.89) 1.48	*(3.10) 2.10	*(2.62) 1.64
% Decrease in $\frac{\partial \delta e}{\partial n}$ (steady pull-up) (more negative)	*(15.39) 6.64	*(16.82) 11.89	*(12.99) 8.30

*rigid model values

4% less than those observed for the rigid model. Using the development in reference 6, maneuver point for a symmetrical pull-up is defined as

$$M.P. = \bar{x}_{ac} - \frac{C_{m_q}\rho S\bar{c}g}{4W} \qquad \text{(From Ref 6:5.61)}$$

As indicated in Table 31, C_{m_q} becomes more negative with winglets and from Table 27 there is a winglet induced aft shift in aerodynamic center location, $\bar{x}_{ac}$. The result from the above equation verifies what is shown in Table 31.

The elastic winglet model has less elevator per g, however, which is also shown in Table 31. Equations showing how this value is determined are in reference 6, page 5.6.

Summary. The control effects of the winglets on the elastic model are less than the rigid model and in some cases negligible.

Longitudinally, no trim penalty effect due to winglets was assumed in view of the small changes in stabilizer trim angle required.

Laterally, control effectiveness in both rudder and aileron was unaffected by the addition of winglets to the model.

Consistent with what was found in the rigid study, the winglets resulted in increases in maneuver margin and in elevator required per g for a symmetrical steady state pull-up.

The Winglet Effect on Longitudinal and Lateral Dynamic Stability

Introduction. Due to time considerations, this dynamic analysis is confined to studying just the winglet effect on the primary dynamic aircraft modes. Responses to control inputs are not provided.

Longitudinal. The elastic winglet model, as shown in Table 32 proves to be less stable than the baseline model in the short period longitudinal mode for cruise conditions 1 and 2. Although cruise condition 3 is not strictly less stable in the short period mode, it is, nonetheless, more oscillatory and less damped than the baseline configured model. In general, the winglet effect on the short period mode is small. Unlike the rigid analysis where the winglet effect on the phugoid mode was found to be negligible, the elastic winglet model shows noticeable improvements in damping ratios and in times to half amplitude for all three cruise conditions.

Lateral. The winglet effect on all of the lateral dynamic modes is stabilizing. However, these improvements are less than those noted in the rigid analysis.

The spiral and rolling modes are only slightly improved with winglets. But, like the rigid dynamic analysis, the dutch roll mode characteristics are considered the most important. These are shown in Table 33. This winglet effect on dutch roll stability comes primarily from winglet

Table 32
Winglet Effect on Longitudinal Dynamic Modes

Cruise Condition (static elastic models)	1 M = .77 30,000 ft	2 M = .77 45,000 ft	3 M = .422 10,000 ft
Short Period			
% Increase in Undamped Natural Frequency, ω_n	3.47	6.3	4.45
% Decrease in Damping Ratio, $\zeta_{s.p.}$	3.89	6.25	4.11
% Increase in Time to Half Amplitude, T 1/2	.49	.45	0.0
% Decrease in Period, T	4.34	6.57	5.79
Phugoid			
% Increase in Undamped Natural Frequency, ω_n	4.33	1.45	3.00
% Increase in Damping Ratio, ζ_p	6.60	1.69	4.08
% Decrease in Time to Half Amplitude, T 1/2	10.07	3.15	6.35
% Decrease in Period, T	4.10	1.57	2.68

Table 33
Winglet Effect on Lateral Dynamic Modes

Cruise Condition (static elastic models) Dutch Roll	1 M = .77 30,000 ft	2 M = .77 45,000 ft	3 M = .422 10,000 ft
% Increase in Undamped Natural Frequency, ω_n	3.75	2.02	2.58
% Increase in Damping Ratio, $\zeta_{D.R.}$	11.46	5.48	6.15
% Decrease in Time to Half Amplitude, T 1/2	13.05	7.51	7.95
% Decrease in Period, T	3.5	1.90	2.42

induced improvements in Cn_r and Cn_β noted earlier. Both of these derivatives have a strong effect on the damping and natural frequency of this lateral mode (Ref 8:135).

Summary. The elastic winglet model is slightly less stable in the short period mode but consistently more stable in the phugoid. Laterally, the winglet effect on the spiral and rolling modes was small. Also, only small improvements were noted in the dutch roll dynamics.

V. Conclusion and Recommendations

Using geometry and aerodynamic data on the KC-135 and the Boeing winglet, a mathematical rigid and elastic FLEX-STAB model was successfully constructed. The correlation between the baseline model and available flight test data was considered close enough to regard the model as a good approximation of the actual aircraft. This flight test comparison was made for both the elastic and rigid models where the elastic structural definition consisted of a modified 707-320B model. The winglet geometry was modeled in detail with both thickness and twist definitions, however, maintained as a rigid structural body.

In the rigid study of the winglet effect, the baseline model was compared to the winglet configured version for five flight conditions which represent the KC-135 mission profile. The winglet effect on performance for the rigid model showed a 2.32 to 7.89% decrease in total airplane drag with an accompanying 2.47 to 8.58% increase in lift over drag ratios. However, an increase in negative stabilizer trim angle was consistently noted with winglets. Also, the range of useful trim lift coefficients and trim angles of attack was reduced. This result was directly due to increases in C_{L_α} and to the winglet induced aft shift in the aerodynamic center of the wing, which resulted in a 15.85 to 28% increase in static margin. Laterally, the

winglets were stabilizing to C_{n_β}. In aircraft control, the winglets had no effect on elevator authority, but some small reductions in inboard aileron effectiveness were noted. The rudder was unaffected by adding winglets to the model.

Dynamically, the rigid winglet model displayed a 6 to almost 12% reduction in the damping ratio of the short period mode along with 8 to 13% increases in undamped natural frequencies. No effect due to winglets was seen on the phugoid. Laterally, the rolling, spiral and dutch roll modes were all more stable with winglets. In particular, decreases in spiral divergence were noted along with a 10% reduction in the rolling mode time to half amplitude. The dutch roll winglet effect was regarded as the most significant, however, with 3 to 12% increases in damping ratios and 5 to 14% decreases in times to half amplitude.

Also included in the rigid analysis was an investigation of the lateral stability characteristics of the winglet model with a truncated vertical stabilizer. This resulted in less stable side force and yawing moment derivatives than for the baseline model. Reductions in rudder authority below the baseline configuration were also noted. Dynamically, the short tail model was less stable in dutch roll over the full tail model without winglets. No effect on the rolling mode was seen. The most remarkable result was the large increase in spiral stability seen with the winglet

short tail model over both of the full tail configurations compared.

Elastically, winglet performance improvements were degraded primarily by the increase in "washout" at the wing tip. Here, winglet drag reductions for the three cruise flight conditions studied amounted to only 1.3%, with only a 1.3 to 1.54% increase in L/D. Trim requirements, however, were much less than those found in the rigid analysis. Consequently, the elastic winglet model showed no noticeable trim penalty. The winglets were stabilizing longitudinally with 7 to 11.6% increases noted in static margin. Laterally, the elastic winglet model revealed the same general trend in improving stability.

Dynamically, the winglets had less of an effect in reducing the short period damping ratio on the elastic model. Winglets also had a stabilizing effect on the phugoid mode with small increases in damping ratios and 3 to 10% decreases in times to half amplitude. Lateral dynamic improvements due to winglets were not seen in the spiral or rolling modes. However, as with the rigid analysis, the dynamic characteristics of the dutch roll mode improved with winglets. Here, 5.48 to 11.46% increases in damping ratios along with 7 to 13% decreases in times to half amplitude were seen.

Generally, the overall winglet effect on performance for the models used in this study was not as great as that achieved in wind tunnel tests. Nevertheless, stability

improvements both longitudinally and laterally were consistently observed with winglets on the model. No significant detrimental effects due to the winglets were observed within the scope of this report. Due to the elastic model limitations, more research into winglet induced aeroelastic effects, particularly for asymmetrical flight conditions, is needed. A final assessment of the benefits derived from the application of winglets to the KC-135 versus the time and cost of eventual modification can only be made from the results born out of future flight tests.

Bibliography

1. Povinelli, F. P., J. M. Klineberg and J. J. Kramer. "Improving Aircraft Energy Efficiency." Astronautics & Aeronautics, 14:18-27 (February 1976).

2. "Design and Analysis of Winglets for Military Aircraft." Seattle, Washington: The Boeing Commercial Airplane Company, February 1976.

3. Jacobs, Peter F. and Stuart G. Flechner. The Effect of Winglets on the Static Aerodynamic Stability Characteristics of a Representative Second Generation Jet Transport Model. NASA Technical Note D-8267. Washington: National Aeronautics and Space Administration, July 1976.

4. AFFDL-TR-74-91. A Method for Predicting the Stability Characteristics of Control Configured Vehicles. Vol. II: FLEXSTAB 2.01.00 User's Manual. Seattle, Washington: The Boeing Commercial Airplane Company, November 1974.

5. Woodward, F. A.; Tinoco, E. N.; and Larsen, J. W.: Analysis and Design of Supersonic Wing-Body Combinations, Including Flow Properties in the Near Field. Part I: Theory and Application. NASA CR-73106, August 1967.

6. Roskam, Jan. Flight Dynamics of Rigid and Elastic Airplanes. Part I and Part II. Lawrence, Kansas: Roskam Aviation and Engineering Corporation, 1975.

7. "Summary of the Stability, Control and Flying Qualities Information for All the -135 Series." Seattle, Washington: The Boeing Commercial Airplane Company, October 1973.

8. MIL-F-8785B (ASG). Military Specification-Flying Qualities of Piloted Airplanes. August 1969.

9. T. O. 1C-135A-1. Flight Manual USAF Series C-135A and B Aircraft. Washington: Secretary of the Air Force, September 1974.

10. T. O. 1C-135B-1-1. Flight Manual USAF Series C-135B Aircraft Performance Data SAC Procedures. Washington: Secretary of the Air Force, October 1974.

11. Blakelock, John H. Automatic Control of Aircraft and Missiles. New York: John Wiley & Sons, Inc., 1965.

Appendix A

Airplane Small Perturbation Equations Used in Dynamic Time History Analysis

The dynamics of this report are concerned only with small perturbations relative to a steady state flight condition in which

a. no initial bank angle exists ($\phi_1 = 0$),

b. no initial side velocity exists ($V_1 = 0$), and

c. no initial angular velocities exist:

$$P_1 = Q_1 = R_1 = \dot{\psi}_1 = \dot{\theta}_1 = \dot{\phi}_1 = 0$$

(From Ref 6:2.36)

Therefore the equations of motion become longitudinally,

$$\begin{aligned} m(\dot{u} + W_1 q) &= - mg\theta\cos\theta_1 + f_{A_x} + f_{T_x} \\ m(\dot{w} - U_{1_q}) &= - mg\theta\sin\theta_1 + f_{A_z} + f_{T_z} \\ I_{yy}\dot{q} &= m_A + m_T \\ q &= \dot{\theta} \end{aligned} \tag{1}$$

(From Ref 6:2.36)

and laterally,

$$\begin{aligned} m(\dot{v} + U_1 r - W_1 p) &= mg\phi\cos\theta_1 + f_{A_y} + f_{T_y} \\ I_{xx}\dot{p} - I_{xz}\dot{p} &= \ell_A + \ell_T \\ I_{zz}\dot{r} - I_{xz}\dot{p} &= n_A + n_T \\ p &= \dot{\phi} - r\tan\theta_1 \end{aligned} \tag{2}$$

(From Ref 6:2.36)

These equations are then written in the stability axes system. Therefore, $W_1 = 0$ in both equation sets (1) and (2).

The inertial transformation from an arbitrary body fixed reference axis system to the stability axes system is accomplished using this matrix equation:

$$\begin{bmatrix} I_{xx_S} \\ I_{zz_S} \\ I_{xz_S} \end{bmatrix} = \begin{bmatrix} \cos^2\alpha_1 & \sin^2\alpha_1 & -\sin 2\alpha_1 \\ \sin^2\alpha_1 & \cos^2\alpha_1 & \sin 2\alpha_1 \\ 1/2\sin 2\alpha_1 & -1/2\sin 2\alpha_1 & \cos 2\alpha_1 \end{bmatrix} \begin{bmatrix} I_{xx_B} \\ I_{zz_B} \\ I_{xz_B} \end{bmatrix} \qquad (3)$$

Note that I_{yy} is invariant when a coordinate transformation consists of just a rotation about the airplane y-axis (Ref 6:3.43).

From the derivation of the perturbed state forces and moments given in section 4.2 of chapter 4 in part one of Reference 6, the complete small perturbation equations of motion for steady state flight become those given in Table I. Note that these equations assume that $C_{D_{\dot{\alpha}}}$, C_{D_q} and $(C_{T_{z_u}} + 2C_{T_{z_1}})$ are approximately equal to zero for the longitudinal set and that $C_{y_{\dot{\beta}}}$, $C_{\ell_{\dot{\beta}}}$ and $C_{n_{\dot{\beta}}}$ are approximately zero for the lateral set (Ref 6:4.113). In the FLEXSTAB characteristic equation rooting analysis, however, these derivatives are not assumed to be zero. This accounts for the small differences noted between the eigenvalues of FLEXSTAB and those calculated using CALMAT.

In Roskam's discussion of dynamic stability and response, he develops what he calls "dimensional stability derivatives." These allow simpler forms of the equations in Table I. The longitudinal equations are divided by m or I_{yy} where applicable and the lateral equations are divided by m, I_{xx} and I_{zz}, respectively. This results in the following forms of the perturbation equations in terms of "dimensional stability derivatives":

Longitudinal--

$$\begin{aligned}
\dot{u} &= -g\theta\cos\theta_1 + X_u U + X_{Tu} U + X_\alpha \alpha + X_{\delta e}\delta_e \\
\dot{w} - U_1 q &= -g\theta\sin\theta_1 + Z_u u + Z_\alpha \alpha + Z_{\dot{\alpha}}\dot{\alpha} + Z_q q + Z_{\delta_e}\delta_e \\
\dot{q} &= M_u u + M_{Tu} u + M_\alpha \alpha + M_{T\alpha}\alpha + M_{\dot{\alpha}}\dot{\alpha} + M_q q + M_{\delta_e}\delta_e \\
\dot{\theta} &= q
\end{aligned} \tag{4}$$

(From Ref 6:6.19)

Lateral--

$$\begin{aligned}
\dot{v} + U_1 r &= g\phi\cos\theta_1 + Y_\beta \beta + Y_p p + Y_r r + Y_{\delta A}\delta_A + Y_{\delta R}\delta_R \\
\dot{p} - A_1 \dot{r} &= L_\beta \beta + L_p p + L_r r + L_{\delta A}\delta_A + L_{\delta R}\delta_R \\
\dot{r} - B_1 \dot{p} &= N_\beta \beta + N_{T_\beta}\beta + N_p p + N_r r + N_{\delta A}\delta_A + N_{\delta R}\delta_R \\
\dot{\phi} &= p + r\tan\theta_1
\end{aligned} \tag{5}$$

where $A_1 = I_{xz} \div I_{xx}$, $B_1 = I_{xz} \div I_{zz}$

(From Ref 6:6.47)

The dimensional stability derivatives of equations (4) and (5) are defined in Tables II and III of this appendix.

Equation sets (4) and (5) can now be arranged in first order matrix form as shown in Table IV. In this state space form

$$\dot{\bar{X}} = \bar{A}\bar{X} + \bar{B}\bar{U} \qquad (6)$$

where $\bar{A}$ and $\bar{B}$ are, respectively, the matrices of stability and control derivatives. $\bar{X}$ is the column vector of the state variables and $\bar{U}$ is the column vector of the control variables.

The equations of Table IV represent the steady state uncoupled equations of motion in first order form as written in the stability axis system. This matrix equation is used in all of the dynamic analyses presented in this report. It is not necessarily the same form used in the FLEXSTAB computer program system.

Table I
Small Perturbation Equations
of Motion

Longitudinal Small Perturbation Equations (Stability Axes) $W_1 = 0$

$$m\dot{u} = -mg\theta\cos\theta_1 + \bar{q}_1 S\{-(C_{D_u} + 2C_{D_1})\frac{u}{U_1} + (C_{T_{x_u}} + 2C_{T_{x_1}})\frac{u}{U_1} - (C_{D_\alpha} - C_{L_1})\alpha - C_{D_{\delta e}}\delta e\}$$

$$m(\dot{w} - U_1 q) = -mg\theta\sin\theta_1 + \bar{q}_1 S\{-(C_{L_u} + 2C_{L_1})\frac{u}{U_1} - (C_{L_\alpha} + C_{D_1})\alpha - C_{L_{\dot{\alpha}}}\frac{\dot{\alpha}\bar{c}}{2U_1} - C_{L_q}\frac{q\bar{c}}{2U_1} - C_{L_{\delta_e}}\delta_e\}$$

$$I_{yy}\dot{q} = \bar{q}_1 Sc\{(C_{m_u} + 2C_{m_1})\frac{u}{U_1} + (C_{m_{T_u}} + 2C_{m_{T_1}})\frac{u}{U_1} + C_{m_\alpha}\alpha + C_{m_{T_\alpha}}\alpha + C_{m_{\dot{\alpha}}}\frac{\dot{\alpha}\bar{c}}{2U_1} + C_{m_q}\frac{q\bar{c}}{2U_1} + C_{m_{\delta e}}\delta e\}$$

$$\dot{\theta} = q$$

Lateral Small Perturbation Equations (Stability Axes)

$$m(\dot{v} + U_1 r) = mg\phi\cos\theta_1 + \bar{q}_1 S(C_{y_\beta}\beta + C_{y_p}\frac{pb}{2U_1} + C_{y_r}\frac{rb}{2U_1} + C_{y_{\delta_A}}\delta_A + C_{y_{\delta_R}}\delta_R)$$

$$I_{xx}\dot{p} - I_{xz}\dot{r} = \bar{q}_1 Sb(C_{\ell_\beta}\beta + C_{\ell_p}\frac{pb}{2U_1} + C_{\ell_r}\frac{rb}{2U_1} + C_{\ell_{\delta_A}}\delta_A + C_{\ell_{\delta_R}}\delta_R)$$

$$I_{zz}\dot{r} - I_{xz}\dot{p} = \bar{q}_1 Sb(C_{n_\beta}\beta + C_{n_{T_\beta}}\beta + C_{n_p}\frac{pb}{2U_1} + C_{n_r}\frac{rb}{2U_1} + C_{n_{\delta_A}}\delta_A + C_{n_{\delta_R}}\delta_R)$$

$$\dot{\phi} = p + r\tan\theta_1$$

(From Ref 6:6.5)

Table II
Longitudinal Dimensional Stability
Derivatives

$$X_u = \frac{-\bar{q}_1 S(C_{D_u} + 2C_{D_1})}{mU_1} (sec^{-1}) \qquad X_{T_u} = \frac{\bar{q}_1 S(C_{T_{x_u}} + 2C_{T_{x_1}})}{mU_1} (sec^{-1})$$

$$X_\alpha = \frac{-\bar{q}_1 S(C_{D_\alpha} - C_{L_1})}{m} (ft\ sec^{-2}) \qquad X_{\delta_e} = \frac{-\bar{q}_1 S C_{D_{\delta_e}}}{m} (ft\ sec^{-2}\ or\ ft\ sec^{-2} deg^{-1})$$

$$Z_u = \frac{-\bar{q}_1 S(C_{L_u} + 2C_{L_1})}{mU_1} (sec^{-1}) \qquad Z_\alpha = \frac{-\bar{q}_1 S(C_{L_\alpha} + C_{D_1})}{m} (ft\ sec^{-2})$$

$$Z_{\dot{\alpha}} = \frac{-\bar{q}_1 S C_{L_{\dot{\alpha}}} \bar{c}}{2mU_1} (ft\ sec^{-1}) \qquad Z_q = \frac{-\bar{q}_1 S C_{L_q} \bar{c}}{2mU_1} (ft\ sec^{-1})$$

$$Z_{\delta_e} = \frac{-\bar{q}_1 S C_{L_{\delta_e}}}{m} (ft\ sec^{-2}\ or\ ft\ sec^{-2} deg^{-1}) \qquad M_u = \frac{\bar{q}_1 S \bar{c}(C_{m_u} + 2C_{m_1})}{I_{yy} U_1} (ft^{-1} sec^{-1})$$

$$M_{T_u} = \frac{\bar{q}_1 S \bar{c}(C_{m_{T_u}} + 2C_{m_{T_1}})}{I_{yy} U_1} (ft^{-1}\ sec^{-1}) \qquad M_\alpha = \frac{\bar{q}_1 S \bar{c} C_{m_\alpha}}{I_{yy}} (sec^{-2})$$

$$M_{T_\alpha} = \frac{\bar{q}_1 S \bar{c} C_{m_{T_\alpha}}}{I_{yy}} (sec^{-2}) \qquad M_{\dot{\alpha}} = \frac{\bar{q}_1 S \bar{c}^2 C_{m_{\dot{\alpha}}}}{2I_{yy} U_1} (sec^{-1})$$

$$M_q = \frac{\bar{q}_1 S \bar{c}^2 C_{m_q}}{2I_{yy} U_1} (sec^{-1}) \qquad M_{\delta_e} = \frac{\bar{q}_1 S \bar{c} C_{m_{\delta_e}}}{I_{yy}} (sec^{-2}\ or\ sec^{-2} deg^{-1})$$

(From Ref 6:6.17)

Table III
Lateral-Directional Dimensional
Stability Derivatives

$$Y_\beta = \frac{\bar{q}_1 S C_{y_\beta}}{m} \quad (\text{ft sec}^{-2}) \qquad Y_p = \frac{\bar{q}_1 S b C_{y_p}}{2mU_1} \quad (\text{ft sec}^{-1})$$

$$Y_r = \frac{\bar{q}_1 S b C_{y_r}}{2mU_1} \quad (\text{ft sec}^{-1}) \qquad Y_{\delta_A} = \frac{\bar{q}_1 S C_{y_{\delta_A}}}{m} \quad (\text{ft sec}^{-2} \text{ or ft sec}^{-2} \text{ deg}^{-1})$$

$$Y_{\delta R} = \frac{\bar{q}_1 S C_{y_{\delta_R}}}{m} \quad (\text{ft sec}^{-2} \text{ or ft sec}^{-2} \text{ deg}^{-1}) \qquad L_\beta = \frac{\bar{q}_1 S b C_{\ell_\beta}}{I_{xx}} \quad (\text{sec}^{-2})$$

$$L_p = \frac{\bar{q}_1 S b^2 C_{\ell_p}}{2 I_{xx} U_1} \quad (\text{sec}^{-1}) \qquad L_r = \frac{\bar{q}_1 S b^2 C_{\ell_r}}{2 I_{xx} U_1} \quad (\text{sec}^{-1})$$

$$L_{\delta_A} = \frac{\bar{q}_1 S b C_{\ell_{\delta_A}}}{I_{xx}} \quad (\text{sec}^{-2} \text{ or } \text{sec}^{-2} \text{ deg}^{-1}) \qquad L_{\delta_R} = \frac{\bar{q}_1 S b C_{\ell_{\delta_R}}}{I_{xx}} \quad (\text{sec}^{-2} \text{ or } \text{sec}^{-2} \text{ deg}^{-1})$$

$$N_\beta = \frac{\bar{q}_1 S b C_{n_\beta}}{I_{zz}} \quad (\text{sec}^{-2}) \qquad N_{T_\beta} = \frac{\bar{q}_1 S b C_{n_{T_\beta}}}{I_{zz}} \quad (\text{sec}^{-2})$$

$$N_p = \frac{\bar{q}_1 S b^2 C_{n_p}}{2 I_{zz} U_1} \quad (\text{sec}^{-1}), \qquad N_r = \frac{\bar{q}_1 S b^2 C_{n_r}}{2 I_{zz} U_1} \quad (\text{sec}^{-1})$$

$$N_{\delta_A} = \frac{\bar{q}_1 S b C_{n_{\delta_A}}}{I_{zz}} \quad (\text{sec}^{-2} \text{ or } \text{sec}^{-2} \text{ deg}^{-1})$$

$$N_{\delta_R} = \frac{\bar{q}_1 S b C_{n_{\delta_R}}}{I_{zz}} \quad (\text{sec}^{-2} \text{ or } \text{sec}^{-2} \text{ deg}^{-1})$$

(From Ref 6:6.46)

Table IV
Aircraft Equations of Motion in First Order Matrix Form

Longitudinal--

$$\begin{bmatrix} \dot{u} \\ \dot{\alpha} \\ \dot{q} \\ \dot{\theta} \end{bmatrix} = \begin{bmatrix} X_u' & X_\alpha & 0 & -g\cos\theta_1 \\ \frac{Z_u}{U_1 - Z_{\dot{\alpha}}} & \frac{Z_\alpha}{U_1 - Z_{\dot{\alpha}}} & \frac{U_1 + Z_q}{U_1 - Z_{\dot{\alpha}}} & -\frac{g\sin\theta_1}{U_1 - Z_{\dot{\alpha}}} \\ M_u' + \frac{M_{\dot{\alpha}} Z_u}{U_1 - Z_{\dot{\alpha}}} & M_\alpha' + \frac{M_{\dot{\alpha}} Z_\alpha}{U_1 - Z_{\dot{\alpha}}} & M_q + \frac{M_{\dot{\alpha}}(Z_q + U_1)}{U_1 - Z_{\dot{\alpha}}} & -\frac{M_{\dot{\alpha}} g\sin\theta}{U_1 - Z_{\dot{\alpha}}} \\ 0 & 0 & 1 & 0 \end{bmatrix} \begin{bmatrix} u \\ \alpha \\ q \\ \theta \end{bmatrix}$$

$$+ \begin{bmatrix} X_{\delta E} & X_{\delta T} \\ \frac{Z_{\delta E}}{U_1 - Z_{\dot{\alpha}}} & \frac{Z_{\delta T}}{U_1 - Z_{\dot{\alpha}}} \\ M_{\delta E} + \frac{M_{\dot{\alpha}} Z_{\delta E}}{U_1 - Z_{\dot{\alpha}}} & M_{\delta T} + \frac{M_{\dot{\alpha}} Z_{\delta T}}{U_1 - Z_{\dot{\alpha}}} \\ 0 & 0 \end{bmatrix} \begin{bmatrix} \delta E \\ \delta T \end{bmatrix}$$

Lateral--

$$\begin{bmatrix} \dot{\beta} \\ \dot{p} \\ \dot{r} \\ \dot{\phi} \end{bmatrix} = \begin{bmatrix} \frac{Y_\beta}{U_1} & \frac{Y_p}{U_1} & \frac{Y_r}{U_1} - 1 & \frac{g\cos\theta_1}{U_1} \\ \frac{A_1 N_\beta + L_\beta}{1 - A_1 B_1} & \frac{A_1 N_p + L_p}{1 - A_1 B_1} & \frac{A_1 N_r + L_r}{1 - A_1 B_1} & 0 \\ \frac{B_1 L_\beta + N_\beta}{1 - A_1 B_1} & \frac{B_1 L_p + N_p}{1 - A_1 B_1} & \frac{B_1 L_r + N_r}{1 - A_1 B_1} & 0 \\ 0 & 1 & \tan\theta_1 & 0 \end{bmatrix} \begin{bmatrix} \beta \\ p \\ r \\ \phi \end{bmatrix}$$

$$+ \begin{bmatrix} Y_{\delta A} & Y_{\delta R} \\ L_{\delta A}' & L_{\delta R}' \\ N_{\delta A}' & N_{\delta R}' \\ 0 & 0 \end{bmatrix} \begin{bmatrix} \delta A \\ \delta R \end{bmatrix}$$

where

$$A_1 = \frac{I_{xz}}{I_{xx}} \quad \text{and} \quad B_1 = \frac{I_{xz}}{I_{zz}}$$

Appendix B

Program CALMAT

CALMAT is a digital computer program that computes and prints the stability and control derivatives matrices for the longitudinal and lateral matrix equations of Table IV in Appendix A. The program also uses A.F. Flight Dynamics Laboratory EISPACK subroutines to calculate the longitudinal and lateral eigenvalues and respective eigenvectors of the stability derivatives matrices. This function of EISPACK, used by CALMAT, is in effect a characteristic equation rooting analysis. After the roots are calculated by EISPACK, CALMAT then computes and prints the undamped natural frequency, damping ratio, period and time to one half amplitude of each mode. Any unstable roots are also noted and the time to twice amplitude is computed and printed for these.

The program can be used to calculate either body axes data matrices or stability axes matrices. As used in this report, all data input to CALMAT are in the stability axes system.

Data required for program execution makes up eleven cards specified in Table I of this Appendix.

The matrices, eigenvalues and eigenvectors computed by CALMAT are used in computing the modal time history and time history due to controller inputs of each of

the longitudinal and lateral state variables.

The program listing is shown in Table II and the program flow chart in Table III.

Table I
CALMAT Data Card Format

Card nu.	Data	Dimensions
1	θ, α_B, T_1	radians, pounds
2	$\bar{q}$, U_1, W_1	psf, fps
3	m, S, $\bar{c}$, b, d_T	slugs, ft^2, feet
*4	I_{xx}, I_{yy}, I_{zz}	slugs-ft^2
5	C_{L_1}, C_{L_α}, $C_{L_{\dot{\alpha}}}$, C_{L_q}, $C_{L_{\delta e}}$, C_{L_u}	rad^{-1}, $sec\text{-}rad^{-1}$
6	C_{D_1}, C_{D_α}, C_{D_u}, $C_{D_{\delta e}}$	rad^{-1}, $sec\text{-}rad^{-1}$
7	C_{m_1}, C_{m_α}, $C_{m_{\dot{\alpha}}}$, C_{m_q}, C_{m_u}, $C_{m_{\delta e}}$	rad^{-1}, $sec\text{-}rad^{-1}$
8	C_{mT_α}	rad^{-1}
9	C_{y_α}, C_{y_p}, C_{y_r}, $C_{y_{\delta A}}$, $C_{y_{\delta R}}$	rad^{-1}, $sec\text{-}rad^{-1}$
10	C_{ℓ_β}, C_{ℓ_p}, C_{ℓ_r}, $C_{\ell_{\delta A}}$, $C_{\ell_{\delta R}}$	rad^{-1}, $sec\text{-}rad^{-1}$
11	C_{n_β}, C_{nT_β}, C_{n_p}, C_{n_r}, $C_{n_{\delta A}}$, $C_{n_{\delta R}}$	rad^{-1}, $sec\text{-}rad^{-1}$

*Mass moments of inertia must be input in the principal axes system of the aircraft. The program uses the transformation of equation (3) in Appendix A to compute inertia terms in appropriate axes system.

Table II
CALMAT Program Listing

```
      PROGRAM CALMAT(INPUT=/80,OUTPUT,TAPE5=INPUT,TAPE6=OUTPUT)
      DIMENSION B(4,2), CASE(6)
      REAL M,IXX,IYY,IZZ,IXZ,MU,MTU,MA,MTA,MAD,MQ,MDE,MDT,LB,LP,
     1LDA,LDR,NB,NTB,NP,NR,NDA,NDR,A(4,4),OMEGN(4),ZETA(4),THALF(4),
     1REIG1,REIG2,PERIOD(4),PDD,T2(4)
      COMPLEX EIGVAL(4),EIGVEC(4,4),WORK(4),EIG,CEIGVAL
    1 READ 4, (CASE(I),I=1,6)
      IF (EOF(5LINPUT).NE.0) STOP "COMPUTATIONS COMPLETE"
    4 FORMAT (6A10)
      ICOUNT=0
      READ*, THETA,ALPHA,T1
      READ*,Q,U,M
      READ*,M,S,CMAC,B2,DT
      READ*, IXX, IYY, IZZ
      ANGLE=.0349+ALPHA
      SIXX=COS(ANGLE)**2*IXX+SIN(ANGLE)**2*IZZ
      SIZZ=SIN(ANGLE)**2*IXX+COS(ANGLE)**2*IZZ
      IXZ=.5*SIN(2.*(ANGLE))*(IXX-IZZ)
      IXX=SIXX
      IZZ=SIZZ
C*********LONGITUDINAL CALCULATIONS
      C1=Q*S/(M*U)
      C2=(0.,-1.)*C1
      C3=C2*U
      C4=C2*CMAC/2.
      C5=C1*M*CMAC/IYY
      C6=C5*U
      C7=C5*CMAC/2.
      READ*,CL1,CLA,CLAD,CLQ,CLDE,CLU
      READ*,CD1,CDA,CDU,CDDE
      READ*,CM1,CMA,CMAD,CMQ,CMU,CMDE
      READ*,CMTA
      CTX1=CD1-(M*32.174)*SIN(THETA)/(Q*S)
      CTXU=(0.,-2.)*CTX1
      CMT1=(0.,-1.)*CM1
      CMTU=(0.,-1.)*CTXU*DT/CMAC
      CDU=C2*(CDU+2.*CD1)
      XTU=C1*(CTXU+2.*CTX1)
      XA=C3*(CDA-CL1)
      XDE=C3*CDDE
      ZU=C2*(CLU+2.*CL1)
      ZA=C3*(CLA+CD1)
      ZAD=C4*CLAD
      ZQ=C4*CLQ
      ZDE=C3*CLDE
      MU=C5*(CMU+2.*CM1)
      MTU=C5*(CMTU+2.*CMT1)
      MA=C5*CMA
      MTA=C6*CMTA
      MAD=C7*CMAD
      MQ=C7*CMQ
      MDE=C6*CMDE
      DT1=T1/1000.
      CDDT=(0.,-1.)*CD1/DT1
      XDT=C3*CDDT
      CMDT=CMT1/DT1
      MDT=C6*CMDT
```

Table II (cont.)

```
      A(1,1)=XU+XTU
      A(1,2)=XA
      A(1,3)=(0.-1.)*W
      A(1,4)=(0.-1.)*32.174*COS(THETA)
      DEN=U-ZAD
      A(2,1)=ZU/DEN
      A(2,2)=ZA/DEN
      A(2,3)=(U+ZQ)/DEN
      A(2,4)=(0.-1.)*32.174*SIN(THETA)/DEN
      A(3,1)=MU+MTU+MAD*ZU/DEN
      A(3,2)=MTA+MA+MAD*ZA/DEN
      A(3,3)=MQ+MAD*(ZQ+U)/DEN
      A(3,4)=(0.-1.)*MAD*32.174*SIN(THETA)/DEN
      A(4,1)=0.0
      A(4,2)=0.0
      A(4,3)=1.0
      A(4,4)=0.0
      B(1,1)=XDE
      B(1,2)=XDT
      B(2,1)=ZDE/DEN
      B(2,2)=0.0
      B(3,1)=MDE+MAD*ZDE/DEN
      B(3,2)=MDT
      B(4,1)=0.0
      B(4,2)=0.0
      PRINT*
      PRINT*
      PRINT*
      PRINT*,"          ****************************************
     1************"
      PRINT 7, (CASE(I), I=1,6)
    7 FORMAT (11X,6A10)
      PRINT*,"          ****************************************
     1************"
      PRINT*
      PRINT*
      PRINT*, "MASS MOMENTS OF INERTIA IN STABILITY AXIS SYSTEM"
      PRINT*
      PRINT*, "IXX=",IXX,"     IZZ=",IZZ,"     IXZ=",IXZ
      PRINT*
      PRINT*
      PRINT*,"LONGITUDINAL A MATRIX"
      PRINT*
      DO 20 I=1,4
      PRINT 6, (A(I,J), J=1,4)
    6 FORMAT (5X,4F10.4)
      PRINT*
   20 CONTINUE
      PRINT*
      PRINT*, "LONGITUDINAL B MATRIX"
      PRINT*
      DO 30 I=1,4
      PRINT 9, (B(I,J), J=1,2)
    9 FORMAT (5X, 2F10.4)
      PRINT*
   30 CONTINUE
      GO TO 103
```

Table II (cont.)

```
C*********LATERAL CALCULATIONS
  2    C8=Q*S/M
       C9=C8*BB/(2.*U)
       C10=Q*S*BB/IXX
       C11=C10*BB/(2.*U)
       C12=Q*S*BB/IZZ
       C13=C12*BB/(2.*U)
       E=IXZ/IXX
       F=IXZ/IZZ
       READ*, CYB, CYP, CYR, CYDA, CYDR
       READ*, CLB, CLP, CLR, CLDA, CLDR
       READ*, CNB, CNTB, CNP, CNR, CNDA, CNDR
       YB=C8*CYB
       YP=C9*CYP
       YR=C9*CYR
       YDA=C8*CYDA
       YDR=C8*CYDR
       LB=C10*CLB
       LP=C11*CLP
       LR=C11*CLR
       LDA=C10*CLDA
       LDR=C10*CLDR
       NB=C12*CNB
       NTB=C12*CNTB
       NP=C13*CNP
       NR=C13*CNR
       NDA=C12*CNDA
       NDR=C12*CNDR
       H=1.-E*F
       A(1,1)=YB/U
       A(1,2)=(YP+W)/U
       A(1,3)=YR/U-1.0
       A(1,4)=32.174*COS(THETA)/U
       A(2,1)=(E*(NB+NTB)+LB)/H
       A(2,2)=(E*NP+LP)/H
       A(2,3)=(E*NR+LR)/H
       A(2,4)=0.0
       A(3,1)=NB+NTB+F*(E*(NB+NTB)+LB)/H
       A(3,2)=NP+F*(E*NP+LP)/H
       A(3,3)=NR+F*(E*NR+LR)/H
       A(3,4)=0.0
       A(4,1)=0.0
       A(4,2)=1.0
       A(4,3)=SIN(THETA)/COS(THETA)
       A(4,4)=0.0
       B(1,1)=YDA/U
       B(1,2)=YDR/U
       B(2,1)=(E*NDA+LDA)/H
       B(2,2)=(E*NDR+LDR)/H
       B(3,1)=NDA+F*B(2,1)
       B(3,2)=NDR+F*B(2,2)
       B(4,1)=0.0
       B(4,2)=0.0
       PRINT*
       PRINT*
       PRINT*, "LATERAL A MATRIX"
       PRINT*
```

Table II (cont.)

```
      DO 40 I=1,4
      PRINT 10, (A(I,J), J=1,4)
10    FORMAT (5X, 4F10.4)
      PRINT*
40    CONTINUE
      PRINT*
      PRINT*, "LATERAL B MATRIX"
      PRINT*
      DO 45 I=1,4
      PRINT 11, (B(I,J), J=1,2)
11    FORMAT (5X, 2F10.4)
      PRINT*
45    CONTINUE
C*********EIGENVALUE COMPUTATIONS
103   ICOUNT=ICOUNT+1
      N=4
      IND=1
      PRINT*
      PRINT*, "CHARACTERISTIC EQUATION ROOTING ANALYSIS"
      PRINT 160
160   FORMAT(//,1X,"MATRIX A",/)
      DO 300 I=1,N
      WRITE(6,301) (A(I,J),J=1,N)
301   FORMAT(1X,6(1PG16.8))
300   CONTINUE
      CALL RGEIG(4,4,A,IND,EIGVAL,EIGVEC,WORK)
      PRINT 170,(I,I=1,N)
170   FORMAT(//,T13,4("EIGVAL(",I1,")",23X),/)
      WRITE(6,3) (EIGVAL(I),I=1,N)
3     FORMAT(1X,8(1PG16.8))
      PRINT 180,(I,I=1,N)
180   FORMAT(//,T13,4("EIGVEC(",I1,")",23X),/)
      DO 5 I=1,N
      WRITE(6,5) (EIGVEC(I,J),J=1,N)
6     FORMAT(1X,8(1PG16.8))
5     CONTINUE
      DO 400 K=1,N
      EIG=EIGVAL(K)
      REIG1=EIG
      IF (REIG1.GT.0.0) GO TO 398
      REIG2=(0.,-1.)*REIG1
      EIG=(0.,-1.)*(EIG+REIG2)
      CEIGVAL=REIG1+EIG
      IF (EIGVAL(K).EQ.CEIGVAL) GO TO 393
      EIG=EIGVAL(K)*CEIGVAL
      PROD=EIG
      OMEGN(K)=SQRT(PROD)
      ZETA(K)=REIG2/OMEGN(K)
      PERIOD(K)=2.*3.141593/(OMEGN(K)*SQRT(1.-ZETA(K)**2))
      THALF(K)= .693/(OMEGN(K)*ZETA(K))
      PRINT*
      PRINT*,"OMEGN(",K,")=",OMEGN(K),"RAD/SEC","          ZETA(",K,")=
     1,ZETA(K)
      PRINT*
      PRINT*,"T(",K,")=",PERIOD(K),"SECS","          T1/2(",K,")=",THAL
     1(K),"SECS"
      PRINT*
```

Table II (cont.)

```
      GO TO 400
398   PRINT*
      T2(K)=.693/REIG1
      PRINT*,"****EIGVAL(",K,") IS DIVERGENT          T2(",K,")=",T2(K)
     1"SECS"
      PRINT*
      GO TO 400
399   PERIOD(K)=1./REIG2
      THALF(K)=.693/REIG2
      PRINT*
      PRINT*,"T(",K,")=",PERIOD(K),"SECS","          T1/2(",K,")=",THAL
     1(K),"SECS"
      PRINT*
400   CONTINUE
      IF (ICOUNT.EQ.2) GO TO 1
      GO TO 2
      END
```

Table III
CALMAT Flow Chart

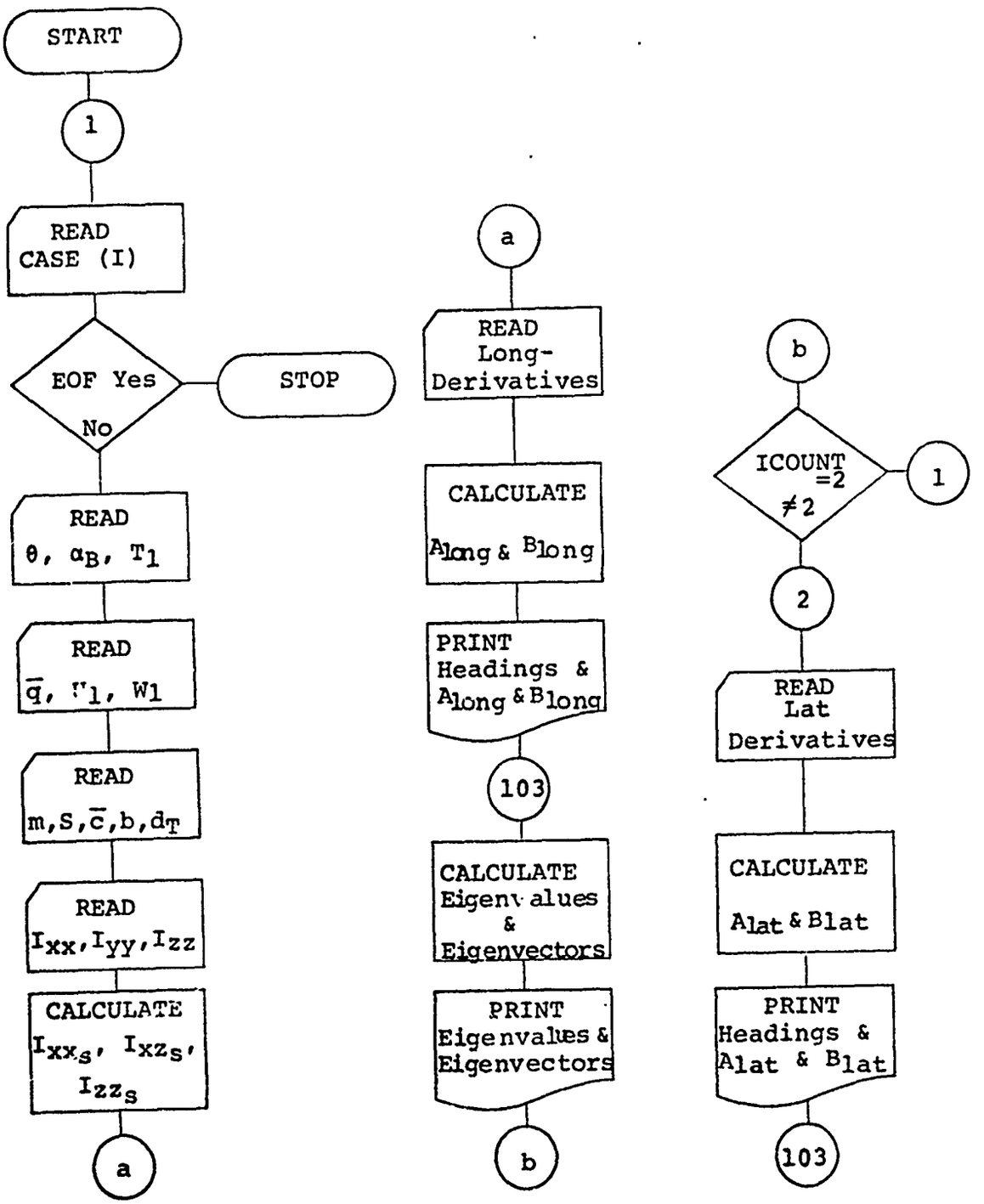

Appendix C

Program STATVAR

STATVAR is a digital program that numerically integrates the longitudinal and lateral equations of motion (first order form, Appendix A) of an arbitrary aircraft, producing the values of the state variables as a function of time. Inputs required are the integration time step, the maximum time value desired, the dimensional stability derivatives matrix, the control derivatives matrix and the initial values of the state variables. Different schedules and values of control inputs may be inserted by means of two control function subprograms. Output consists of a time listing of the state variables as well as CALCOMP plots of the longitudinal and lateral time response. The value of the time step T may be varied within a limited range without seriously deteriorating the accuracy of calculation, by adjusting the number of terms taken in the expansion of $e^{\bar{A}t}$.

Using the first order form of the equations of motion as developed in Appendix A, they can be written as

$$\dot{\bar{x}} = \bar{A}\,\bar{x} + \bar{B}\,\bar{u} \qquad (1)$$

where $\bar{A}$ and $\bar{B}$ are the matrices of stability derivatives and control derivatives respectively. $\bar{x}$ is the column vector of the state variables and $\bar{u}$ is the column vector of the control variables.

Taking the Laplace transform of equation (1) with zero initial conditions and rearranging:

$$s\bar{X}(s) - \bar{A}\bar{X}(s) = \bar{B}\bar{U}(s)$$

$$\bar{X}(s) = (s\bar{I} - \bar{A})^{-1}\bar{B}\bar{U}(s) \qquad (2)$$

Finding the homogeneous solution of equation (2)

$$\bar{X}(s) = (s\bar{I} - \bar{A})^{-1}\bar{X}_0$$

and taking the inverse Laplace transform yields equation (3):

$$\bar{x}(t) = L^{-1}[(s\bar{I} - \bar{A})^{-1}]\bar{x}_0 = e^{\bar{A}t}\bar{x}_0 \qquad (3)$$

where $e^{\bar{A}t} = L^{-1}(s\bar{I} - \bar{A})^{-1}$. Finding the particular solution of equation (2) for an impulse

$$\bar{X}(s)_{imp} = (s\bar{I} - \bar{A})^{-1}\bar{B}\begin{Bmatrix}1\\1\end{Bmatrix}$$

Let $\bar{X}(s)_{imp} = \bar{H}(s)^*$, where $\bar{H}(s)^*$ is a matrix of transfer functions between each of the state variables and control variables:

$$\text{e.g.} \qquad \bar{H}(s)^* = (s\bar{I} - \bar{A})^{-1}\bar{B} = \begin{bmatrix} G_{u\delta_e} & & G_{u\delta_t} \\ \vdots & \ddots & \vdots \\ G_{\theta\delta_e} & & G_{\theta\delta_t} \end{bmatrix}$$

Taking the inverse Laplace transform of $\bar{H}(s)^*$ yields equation (4):

$$\bar{x}(t)_{imp} = L^{-1}[(s\bar{I} - \bar{A})^{-1}]\bar{B} = e^{\bar{A}t}\bar{B} \qquad (4)$$

It can be shown that an arbitrary control function can be represented by a summation of impulse functions over the time interval in question. Therefore, the particular solution for an arbitrary control input can be written as

$$\bar{x}(t)_p = \int_0^t e^{\bar{A}(t - \tau)} \bar{B}\, \bar{u}(\tau) d\tau$$

Summing the homogeneous and the particular solution gives the complete solution:

$$\bar{x}(t) = e^{\bar{A}t}\bar{x}_0 + \int_0^t e^{\bar{A}(t - \tau)} \bar{B}\, \bar{u}(\tau) d\tau \qquad (5)$$

It is this equation that is numerically integrated by STATVAR.

Selecting a time step T, the homogeneous solutions at times $t_0 = 0$, $t_1 = T$ and $t_2 = t_1 + T$ are

$$\bar{x}(t_0) = \bar{x}_0,$$

$$\bar{x}(t_1) = e^{\bar{A}T}\bar{x}_0, \text{ and}$$

$$\bar{x}(t_2) = e^{\bar{A}(t_1 + T)}\bar{x}_0 = e^{\bar{A}T}\bar{x}(t_1)$$

This implies that $\bar{x}(t_n) = e^{\bar{A}T}\bar{x}(t_{n-1})$

or

$$\bar{x}[(k + 1)T] = e^{\bar{A}T}\bar{x}(kT).$$

For the particular solution

$$\bar{x}(T)_p = \int_0^T e^{\bar{A}(T - \tau)} \bar{B}\, \bar{u}(\tau) d\tau = e^{\bar{A}T} \int_0^T e^{-\bar{A}\tau} \bar{B}\, \bar{u}(\tau) d\tau \qquad (6)$$

For small values of T, $\bar{u}(\tau)$ can be approximated by a constant $\bar{u}(0)$. Therefore

$$\bar{x}(T)_p = (e^{\bar{A}T}\int_0^T e^{-\bar{A}T}d\tau)\bar{B}\,\bar{u}(0)$$

The complete solution is now

$$\bar{x}(T) = e^{\bar{A}T}\bar{x}(0) + (e^{\bar{A}T}\int_0^T e^{-\bar{A}\tau}d\tau)\bar{B}\,\bar{u}(0) \quad \text{and}$$

$$\bar{x}(2T) = e^{2\bar{A}T}\bar{x}(0) + e^{2\bar{A}T}\left\{\int_0^T e^{-\bar{A}\tau}d\tau\bar{B}\,\bar{u}(0)\right.$$

$$\left. + \int_T^{2T} e^{-\bar{A}\tau}d\tau\bar{B}\,\bar{u}(T)\right\}$$

This can be written more simply as

$$\bar{x}(2T) = e^{\bar{A}T}\bar{x}(T) + \left\{e^{\bar{A}T}\int_0^T e^{-\bar{A}\tau}d\tau\right\}\bar{B}\,\bar{u}(T)$$

or, in general

$$\bar{x}[(k+1)T] = e^{\bar{A}T}\bar{x}(kT) + (e^{\bar{A}T}\int_0^T e^{-\bar{A}\tau}d\tau)\bar{B}\,\bar{u}(kT)$$

$$\bar{x}[(k+1)T] = e^{\bar{A}T}\bar{x}(kT) + \bar{A}^{-1}(e^{\bar{A}T} - \bar{I})\bar{B}\,\bar{u}(kT) \qquad (7)$$

where $e^{\bar{A}T}$ can be calculated by a Taylor series expansion:

$$e^{\bar{A}T} = \bar{I} + \bar{A}T + A^{-2}\frac{T^2}{2!} + \bar{A}^3\frac{T^3}{3!} + \ldots\ldots\ldots$$

Program STATVAR carries out the integration of the time domain equation (5) by iterating solutions of equation (7).

The accuracy of the integrated solution of the state variable equations is affected by the integration time step T, the number of terms calculated in determining $e^{\bar{A}T}$ from the Taylor series expansion and by the type of control function used.

The error in the calculation of $e^{\bar{A}T}$ is determined by the size of the time step and the number of terms which are taken. In general, to maintain a desired maximum error as the size of the time step is increased, more terms must be taken in the expansion. For example, for a T = .1 seconds, a four term expansion will yield an error on the order of $\bar{A}^4 \frac{T^4}{4!} \approx \bar{A}^4 \times 10^{-6}$. If the time step is increased to T = .5 seconds, then a four term expansion will yield an error on the order of $\bar{A}^4 \times 10^{-3}$. Therefore, more terms must be taken in order to maintain the desired error margin.

Also, in developing the iteration of equation (7), it was assumed that $\bar{u}(t)$ was essentially constant over the time step T. Consequently, a rapidly varying control function, such as a sinusoidal input, will require a smaller time step than would an essentially constant control function, such as a step input or zero input.

See Tables I, II and III for input requirements, flow chart and program listing.

Table I.
STATVAR INPUT REQUIREMENTS

IFLAG:	0 < indicates longitudinal case only
	0 > indicates lateral case only
	= 0 indicates both longitudinal and lateral case
0:	indicates number of terms to be calculated for e^{AT}
T:	time step (seconds)
TMAX:	maximum time (seconds)
IUNITS:	= 0 indicates input angles in degrees
	= 1 indicates input angles in radians
M:	number of rows of A matrix
N:	number of columns of A matrix
MB:	number of rows of B matrix
NB:	number of columns of B matrix
AMAT(I,J):	elements of A matrix
BMAT(I,J):	elements of B matrix
*Note:	The units of the A & B matrices must be compatible with the units of X(I), FU1 and FU2, e.g., radians with radians & degrees with degrees.
X(I):	initial conditions of state variables

Control Function Subroutines

Various control functions may be inserted into the program by inserting different control function subroutines.

FU1:	elevator and aileron control functions
FU2:	throttle and rudder control functions

Some example control subroutines are included with the program listing.

Table II
STATVAR Flow Chart

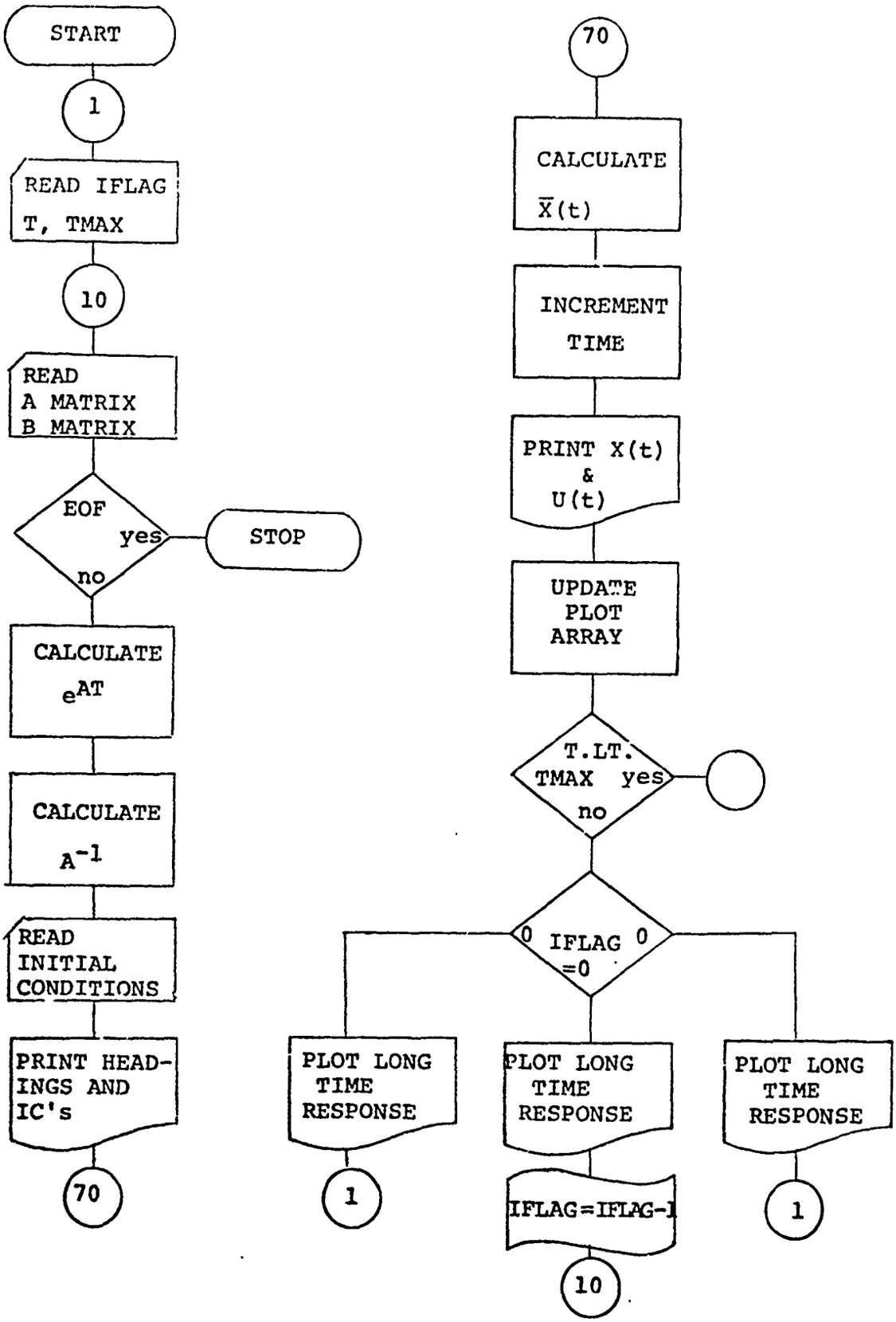

Table III
STATVAR Program Listing

```
      PROGRAM STATVAR(INPUT=/80,OUTPUT=/120,PLOT)
      DIMENSION AMAT(4,4),BMAT(4,2),X(4),UI(2),AI(4,4),LA(4),WA(4),
     1          FAT(4,4),AFAT(4,4),GX(4,1),AH(4,4),H(4,2),HU(4,1),XP(4)
     1          UP(2)
      COMMON/UFUNC/T,IFLAG
      COMMON/LONG/T1(305),U(305),Q(305),AL(305),TH(305),QE(305),QT(305)
     1            LON(2)
      COMMON/LAT /T2(305),P(305),R(305),BE(305),PH(305),QW(305),QR(305)
     1            LAT(2)
      INTEGER O
      NP1 = 0
      NP2 = 0
    1 READ*,IFLAG,O,T,TMAX,IUNITS
      IF(EOF(5LINPUT)) 150,10
   10 IF(IFLAG.LE.0) READ 5,(LON(I),I=1,2)
      IF(IFLAG.GT.0) READ 5,(LAT(I),I=1,2)
    5 FORMAT(2A10)
      READ*,M,N,MB,NB
      IF(EOF(5LINPUT)) 140,20
   20 READ*,((AMAT(I,J),J=1,N),I=1,M)
      READ*,((BMAT(I,J),J=1,NB),I=1,MB)
      NPLOT = TMAX/T/300.
      NPTS = TMAX/T/NPLOT
      IF(NPTS.GT.302) NPLOT=NPLOT+1
      CALL CATMAT(AMAT,FAT,AFAT,M,N,O,T)
      DO 30 I=1,M
      DO 30 J=1,N
   30 AI(I,J)=AMAT(I,J)
      CALL MTIN(AI,N,O,LA,WA)
      IF(O.EQ.0.) GO TO 150
      READ*,(X(I),I=1,M)
      TTOT=0.
      IPLOT = 0
      UI(1) = FU1(TTOT)
      UI(2) = FU2(TTOT)
      IF(IFLAG) 40,40,50
   40 PRINT 41,LON(1),LON(2)
   41 FORMAT(1X/1PX,"LONGITUDINAL TIME RESPONSE"/20X,2A10//5X,"TIME",7X
     1"U",8X,"ALPHA",8X,"Q",8X,"THETA",7X,"QE",8X,"QT")
      GO TO 60
   50 PRINT 51,LAT(1),LAT(2)
   51 FORMAT(1X/20X,"LATERAL TIME RESPONSE"/21X,2A10//5X,"TIME",5X,


     1"BETA",7X,"P",9X,"R",8X,"PHI",8X,"QW",8X,"QR")
      GO TO 60
   60 PRINT 61,"INIT COND",(X(I),I=1,M),UI(1),UI(2)
   61 FORMAT(1X,A9,2X,F9.5,1X,F9.5,2X,F9.5,1X,F10.5,2(2X,F9.5))
      CALL MATMULT(AI,AFAT,AH,M,N,N)
      CALL MATMULT(AH,BMAT,H,M,N,2)
   70 UI(1) = FU1(TTOT)
      UI(2) = FU2(TTOT)
      CALL MATMULT(FAT,X,GX,M,N,1)
      CALL MATMULT(H,UI,HU,M,2,1)
      CALL MATADD(GX,HU,X,M,1)
      TTOT=TTOT+T
      IF(IUNITS.EQ.0) GO TO 75
      DO 75 I=1,M
   75 XP(I) = X(I)*57.295
```

Table III (cont.)

```
      UP(1) = UI(1)*57.295
      UP(2) = UI(2)*57.295
      IF(IFLAG.LE.0) XP(1)=X(1)
      IF(IFLAG.LE.0) UP(2)=UI(2)
      GO TO 80
 76   DO 77 I=1,M
 77   XP(I) = X(I)
      UP(1) = UI(1)
      UP(2) = UI(2)
 80   PRINT 81,TTOT,(XP(I),I=1,M),UP(1),UP(2)
 81   FORMAT(1X,F10.5,1X,F9.5,1X,F9.5,1X,F9.5,2X,F9.5,1X,F10.5,2(2X,F9.5))
      IF(IFLAG) 90,90,100
C
C******* UPDATE LONGITUDINAL PLOT ARRAY
C
 90   IPLOT=IPLOT+1
      IF(IPLOT.LT.NPLOT) GO TO 95
      IPLOT = 0
      NP1 = NP1+1
      T1(NP1) = TTOT
      U(NP1) =  XP(1)
      AL(NP1) = XP(2)
      Q(NP1) =  XP(3)
      TH(NP1) = XP(4)
      DE(NP1) =UP(1)
      DT(NP1) =UP(2)
 95   IF(TTOT.LT.TMAX) GO TO 70
      GO TO 110
C
C******* UPDATE LATERAL PLOT ARRAY
C
100   IPLOT = IPLOT+1
      IF(IPLOT.LT.NPLOT) GO TO 105
      IPLOT = 0
      NP2 = NP2+1
      T2(NP2) = TTOT
      BE(NP2) = XP(1)
      P(NP2) =  XP(2)
      R(NP2) =  XP(3)
      PH(NP2) = XP(4)
      DW(NP2) =UP(1)
      DR(NP2) =UP(2)
105   IF(TTOT.LT.TMAX) GO TO 70
      GO TO 110
110   IF(IFLAG) 130,120,130
120   IFLAG = 1
      GO TO 10


C
C******* PLOT STATE VARIABLES
C
130   CALL OUTPLOT(NP1,NP2)
      GO TO 1
140   STOP "INSUFFICIENT DATA CARDS"
150   STOP "A MATRIX IS SINGULAR"
160   STOP
      END
```

Table III (cont.)

```
      SUBROUTINE EATMAT(AMAT,EAT,AEAT,M,N,O,T)
      DIMENSION AMAT(4,N),AINT(4,4),APOW(4,4),G(4,4)
      DIMENSION ID(4,4),ASUM(4,4),EAT(M,N),AEAT(M,N)
      INTEGER M,N,O
      DO 2 I=1,M
      DO 2 J=1,M
      ID(I,J)=0
    2 AINT(I,J)=AMAT(I,J)*T
      DO 3 I=1,M
    3 ID(I,I)=ID(I,I)+1
      DO 6 K=2,O
      CALL MATPOW(AMAT,APOW,M,N,K)
      DO 4 I=1,M
      DO 4 J=1,N
    4 G(I,J)=(APOW(I,J)*(T**K))/FACT(K)
      CALL MATADD(G,AINT,ASUM,M,N)
      DO 5 I=1,M
      DO 5 J=1,N
    5 AINT(I,J)=ASUM(I,J)
      DO 6 I=1,M
      DO 6 J=1,N
      AEAT(I,J)=AINT(I,J)
    6 EAT(I,J)=AEAT(I,J)+ID(I,J)
      RETURN
      END
```

```
INE MATADD     74/74   OPT=1                                    FTN 4.5+414

      SUBROUTINE MATADD(A,B,C,M,N)
      DIMENSION A(M,N),B(M,N),C(M,N)
      DO 1 I=1,M
      DO 1 J=1,N
    1 C(I,J)=A(I,J)+B(I,J)
      RETURN
      END
```

```
INE MATPOW     74/74   OPT=1                                    FTN 4.5+414

      SUBROUTINE MATPOW(A,C,M,N,O)
      DIMENSION A(M,N),B(4,4),C(M,N),D(4,4)
      INTEGER O
      ICOUNT=1
      DO 1 I=1,M
      DO 1 J=1,N
      D(I,J)=A(I,J)
    1 B(I,J)=A(I,J)
    3 DO 2 I=1,M
      DO 2 J=1,N
      C(I,J)=0
      DO 2 K=1,N
    2 C(I,J)=C(I,J)+D(I,K)*B(K,J)
      ICOUNT=ICOUNT+1
      IF(ICOUNT.GE.O)GO TO 100
      DO 4 I=1,M
      DO 4 J=1,N

    4 D(I,J)=C(I,J)
      GO TO 3
  100 CONTINUE
      RETURN
      END
```

Table III (cont.)

```
      FUNCTION FACT(N)
      INTEGER N,A
      A=1
      DO 1 K=1,N
    1 A=A*K
      FACT=A
      RETURN
      END
:NE MATMULT    74/74   OPT=1                              FTN 4.5+441+

      SUBROUTINE MATMULT(A,B,C,M,N,O)
      DIMENSION A(M,N),B(N,O),C(M,O),D(4,4)
      INTEGER M,N,O
      DO 1 I=1,M
      DO 1 J=1,N
    1 D(I,J)=A(I,J)
      DO 2 I=1,M
      DO 2 J=1,O
      C(I,J)=0
      DO 2 K=1,N
    2 C(I,J)=C(I,J)+D(I,K)*B(K,J)
      RETURN
      END
:NE OUTPLOT    74/74   OPT=1                              FTN 4.5+441+

      SUBROUTINE OUTPLOT (N1,N2)
      COMMON/LONG/T1(305),U(305),D(305),AL(305),TH(305),DE(305),DT(305),
     1            LON(2)
      COMMON/LAT /T2(305),P(305),R(305),BE(305),PH(305),DW(305),DR(305),
     1            LAT(2)
      CALL PLOTS(30)
      CALL PLOT(1.,-5.,-3)
      IF(N1.EQ.0) GO TO 30
C
C******* LONGITUDINAL VARIABLES
C
      CALL SCALE(T1,4.,N1,1)
      M=0
C
C******* PLOT DE, DT
C
      CALL PLOT(1.,1.,-3)
   10 CALL AXIS(0.,0.,11HT (SECONDS),-11,4.,0.,T1(N1+1),T1(N1+2))
      CALL AXIS(0.,0.,12HDE (DEGREES),+12,2.,90.,-20.,20.)
      CALL AXIS(4.,0.,10HDT (UNITS),-10,2.,90.,-10.,10.)
      DE(N1+1)=-20.
      DE(N1+2)=20.
      DT(N1+1)=-10.
      DT(N1+2)=10.
      J1 = N1/10
      CALL FLINE(T1,DE,-N1,1,J1,1)
      CALL FLINE(T1,DT,-N1,1,J1,2)
      CALL SYMBOL(1.53,2.,.24,128,0.,-1)
      CALL SYMBOL(1.80,2.,.07, 32,0.,-1)
      CALL SYMBOL(2.00,2.,.21, 73,0.,-1)
      CALL SYMBOL(2.21,2.,.24,128,0.,-1)
      CALL SYMBOL(2.42,2.,.07, 47,0.,-1)


      IF(M.EQ.1) GO TO 20
      M=1
      CALL PLOT(6.,0.,-3)
      GO TO 10
```

Table III (cont.)

```
C
C******* PLOT ALPHA
C
20      CALL PLOT(-5.,3.0,-3)
        CALL SCALE(AL,2.,N1,1)
        CALL AXIS(0.,0.,14 ,-1,4.,0.,T1(N1+1),T1(N1+2))
        CALL AXIS(0.,0.,94(DEGREES),+9,2.,90.,AL(N1+1),AL(N1+2))
        CALL FLINE(T1,AL,-N1,1, 0,1)
        CALL SYMBOL(2.,2.,.28, 91,0.,-1)
C
C******* PLOT THETA
C
        CALL PLOT(6.,0.,-3)
        CALL SCALE(TH,2.,N1,1)
        CALL AXIS(0.,0.,14 ,-1,4.,0.,T1(N1+1),T1(N1+2))
        CALL AXIS(0.,0.,94(DEGREES),+9,2.,90.,TH(N1+1),TH(N1+2))
        CALL FLINE(T1,TH,-N1,1, 0,1)
        CALL SYMBOL(2.,2.,.21,144,0.,-1)
C
C******* PLOT U
C
INE OUTPLOT    74/74   OPT=1                                FTN 4.5+414

        CALL PLOT(-5.,3.0,-3)
        CALL SCALE( U,2.,N1,1)
        CALL AXIS(0.,0.,14 ,-1,4.,0.,T1(N1+1),T1(N1+2))
        CALL AXIS(0.,0.,94 (FT/SEC),+9,2 .90., U(N1+1), U(N1+2))
        CALL FLINE(T1, U,-N1,1, 0,1)
        CALL SYMBOL(2.,2.,.21, 48,0.,-1)
C
C******* PLOT Q
C
        CALL PLOT(6.,0.,-3)
        CALL SCALE( Q,2.,N1,1)
        CALL AXIS(0.,0.,14 ,-1,4.,0.,T1(N1+1),T1(N1+2))
        CALL AXIS(0.,0.,94(DEG/SEC),+9,2.,90., Q(N1+1), Q(N1+2))
        CALL FLINE(T1, Q,-N1,1, 0,1)
        CALL SYMBOL(2.,2.,.21, 44,0.,-1)
        CALL SYMBOL(-3.35,2.8,.18,26HLONGITUDINAL TIME RESPONSE,0.,26)
        CALL SYMBOL(-2.5,2.5,.15,LON(1),0.,10)
        CALL SYMBOL(-1.0,2.5,.15,LON(2),0.,10)
C
C******* LATERAL VARIABLES
C
30      IF(N1.EQ.0) CALL PLOT(0.,5.,-3)
        IF(N2.EQ.0) GO TO 60
        CALL SCALE(T2,4.,N2,1)
        M=0
```

Table III (cont.)

```
C
C******* PLOT DR, DW
C
      CALL PLOT(7.,-6.,-3)
40    CALL AXIS(0.,0.,11HT (SECONDS),-11,4.,0.,T2(N2+1),T2(N2+2))
      CALL AXIS(0.,7.,94(DEGREES),+9,2.,90.,-20.,20.)
      DR(N2+1)=-20.
      DR(N2+2)=20.
      DW(N2+1)=-20.
      DW(N2+2)=20.
      J2 = N2/10
      CALL FLINE(T2,DR,-N2,1,J2,1)


      CALL FLINE(T2,DW,-N2,1,J2,2)
      CALL SYMBOL(1.59,2.,.24,128,0.,-1)
      CALL SYMBOL(1.80,2.,.07, 45,0.,-1)
      CALL SYMBOL(2.00,2.,.21, 73,0.,-1)
      CALL SYMBOL(2.21,2.,.24,128,0.,-1)
      CALL SYMBOL(2.42,2.,.07, 50,0.,-1)
      IF(M.EQ.1) GO TO 50
      M=1
      CALL PLOT(6.,0.,-3)
      GO TO 40
```

```
) C******* PLOT BETA
  C                          Table III (cont.)
  50     CALL PLOT(-6.,3.0,-3)
         CALL SCALE(BE,2.,N2,1)
         CALL AXIS(0.,0.,1H ,-1,4.,0.,T2(N2+1),T2(N2+2))
         CALL AXIS(0.,0.,9H(DEGREES),+9,2.,90.,BE(N2+1),BE(N2+2))
         CALL FLINE(T2,BE,-N2,1, 0,1)
         CALL SYMBOL(2.,2.,.28, 92,0.,-1)
  C
NE OUTPLOT     74/74   OPT=1                                  FTN 4.5+414

  C******* PLOT PHI
  C
         CALL PLOT(6.,0.,-3)
         CALL SCALE(PH,2.,N2,1)
         CALL AXIS(0.,0.,1H ,-1,4.,0.,T2(N2+1),T2(N2+2))
         CALL AXIS(0.,0.,9H(DEGREES),+9,2.,90.,PH(N2+1),PH(N2+2))
         CALL FLINE(T2,PH,-N2,1, 0,1)
         CALL SYMBOL(2.,2.,.28,140,0.,-1)
  C
  C******* PLOT P
  C
         CALL PLOT(-6.,3.0,-3)
         CALL SCALE( P,2.,N2,1)
         CALL AXIS(0.,0.,1H ,-1,4.,0.,T2(N2+1),T2(N2+2))
         CALL AXIS(0.,0.,9H(DEG/SEC),+9,2.,90., P(N2+1), P(N2+2))
         CALL FLINE(T2, P,-N2,1, 0,1)
         CALL SYMBOL(2.,2.,.21, 43,0.,-1)
  C
  C******* PLOT R
  C
         CALL PLOT(6.,0.,-3)
         CALL SCALE( R,2.,N2,1)
         CALL AXIS(0.,0.,1H ,-1,4.,0.,T2(N2+1),T2(N2+2))
         CALL AXIS(0.,0.,9H(DEG/SEC),+9,2.,90., R(N2+1), R(N2+2))
         CALL FLINE(T2, R,-N2,1, 0,1)
         CALL SYMBOL(2.,2.,.21, 45,0.,-1)
         CALL SYMBOL(-2.30,2.8,.18,21HLATERAL TIME RESPONSE,0.,21)
         CALL SYMBOL(-2.3,2.5,.15,LAT(1),0.,10)
         CALL SYMBOL(-1.7,2.5,.15,LAT(2),0.,10)
  60     CALL PLOTE(IDUMMY)
  C
         RETURN
  C
         END
ON FU1         74/74   OPT=1                                  FTN 4.5+414

         FUNCTION FU1(TTOT)
  C      ELEVATOR/AILERON ZERO INPUT
         FU1 = 0.
         RETURN
         END
ON FU2         74/74   OPT=1                                  FTN 4.5+414


         FUNCTION FU2(TTOT)
  C      THROTTLE/RUDDER IMPULSE INPUT
         COMMON/UFUNC/T,IFLAG
         TIMP = 0.
         FU2 = 0.
         IF(IFLAG.LE.0.AND.TTOT.GE.TIMP ) FU2 = 5.
         IF(IFLAG.GT.0.AND.TTOT.GE.TIMPP) FU2 = .175
         IF(TTOT.GE.TIMP+T) FU2=0.
         RETURN
```

Appendix D

FLEXSTAB Evaluation, Flow Charts and Input Listings

This Appendix evaluates the FLEXSTAB programs used in this report by discussing their overall effectiveness in meeting the requirements of the previous sections. Flow charts and input listings are also provided.

Generally, the use of the programs needed in this analysis is simplified by a well written user's manual. Many of the programs can be executed successfully only after one or two trial and error attempts.

The Geometry Definition (GD) program of FLEXSTAB is the easiest to understand and to use. However, some minor improvements in the plotting of the model would be very helpful. For instance, the fuselage camber definition needs to be plotted in order to give the user a better physical picture of his results. Also, as a minor change, the slender body fuselage definition plot should be shown closed at both ends. There is some possibility, in preparing the data for the fuselage definition, in which the user may in error leave the nose and tail open. If not desired, this creates erroneous calculations of the model's stability and control characteristics. These problems are avoided by using the program listing, but a more detailed plot of the airplane is by far more efficient in spotting errors.

The Aerodynamic Influence Coefficient (AIC) program of FLEXSTAB is, internally, the most complicated. This program uses the GD data to define the model aerodynamically. However, this is done for only one Mach number each time the program is executed. Due to the high time and cost of executing AIC, convenience in changing the Mach number for the model is not available. This is a possible improvement area needed in this program.

The Internal Structural Influence Coefficient (ISIC) program is far more complex than the GD program in defining the physical characteristics of the model. It is also the most difficult to use, particularly in troubleshooting errors in input data. For example, even though all the structural information input into ISIC must be defined for all slender and thin bodies defining the model, the program will execute successfully even when this requirement is not satisfied. Needless to say, this could have serious effects on subsequent programs where the results of ISIC are used.

The Stability Derivatives and Static Stability (SDSS) program uses the results of both GD and ISIC in its calculations. This program does not create significant problems in preparing input data but some improvement is needed in clarifying the program's output.

The static and dynamic stability derivatives that are listed by SDSS are in the stability axes system of

the model. However, no where on the listing does it indicate this. This creates problems if the data is subsequently used for a dynamic analysis, as it was in this report, and the incorrect body axes system is used. However, this is only a problem when a dynamic analysis uses programs external to FLEXSTAB.

The stability derivatives on the SDSS listing are generally quite clear and are shown in a standard format. The one exception, however, is in the speed stability derivatives. As listed by SDSS, CL(U), CD(U) and CM(U) are not the same as C_{L_u}, C_{D_u} and C_{m_u}. The FLEXSTAB values are:

$$CL(U) = C_{L_{\hat{u}}} + 2C_{L_1}$$

$$CD(U) = C_{D_{\hat{u}}} + 2C_{D_1}$$

$$CM(U) = C_{m_{\hat{u}}} + 2C_{m_1}$$

This is not clear on the output listing and some improvement here is also needed.

In tabulating the rigid and elastic model FLEXSTAB data with flight test values in section II, there is good correlation seen in those values compared. However, referring to Appendix E, there are a number of other FLEXSTAB derivatives that are shown but not used in this report. Generally, these values are unsteady derivatives and are not easy to interpret physically. They are assumed to have little or no impact on the research objectives and results of this study. Also lacking flight test or wind

tunnel data for making comparisons precludes any attempts to validate them. Note that the derivatives used in this report are those included in the aircraft equations of motion discussed in Appendix A.

FLEXSTAB, with only a few exceptions, is seen to be an accurate and effective analytical tool. It appears to do well in predicting rigid and elastic aircraft characteristics within the limitations of nonviscous linear potential flow theory.

Figures 1 and 2 of this Appendix display the two general program sections of FLEXSTAB. The cross hatched sections shown were not used. Sample input listings for GD, ISIC and SDSS are shown in Tables I, II and III, respectively.

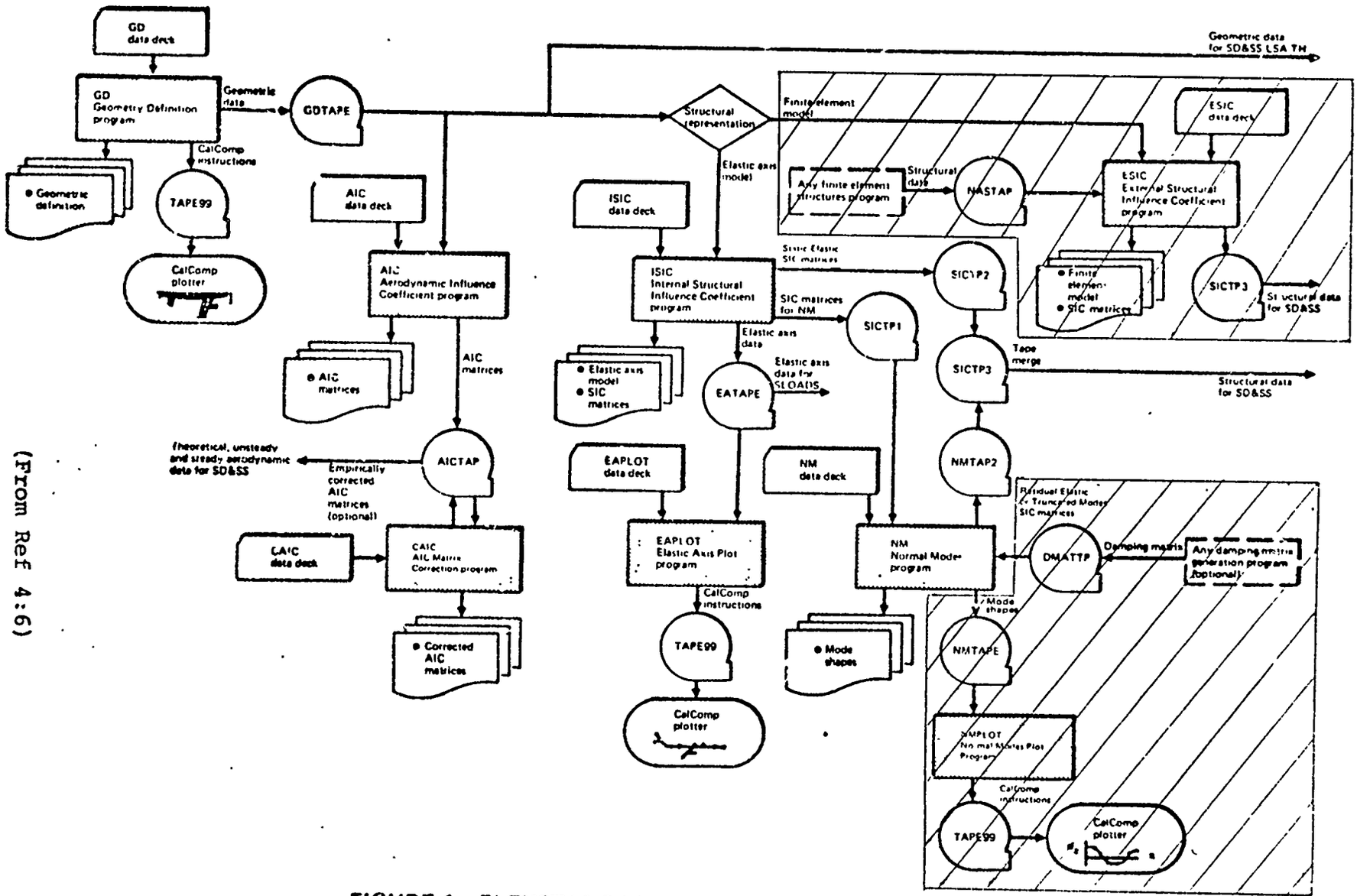

FIGURE 1 –FLEXSTAB 2.01.00: AIRPLANE DEFINITION SECTION

(From Ref 4:6)

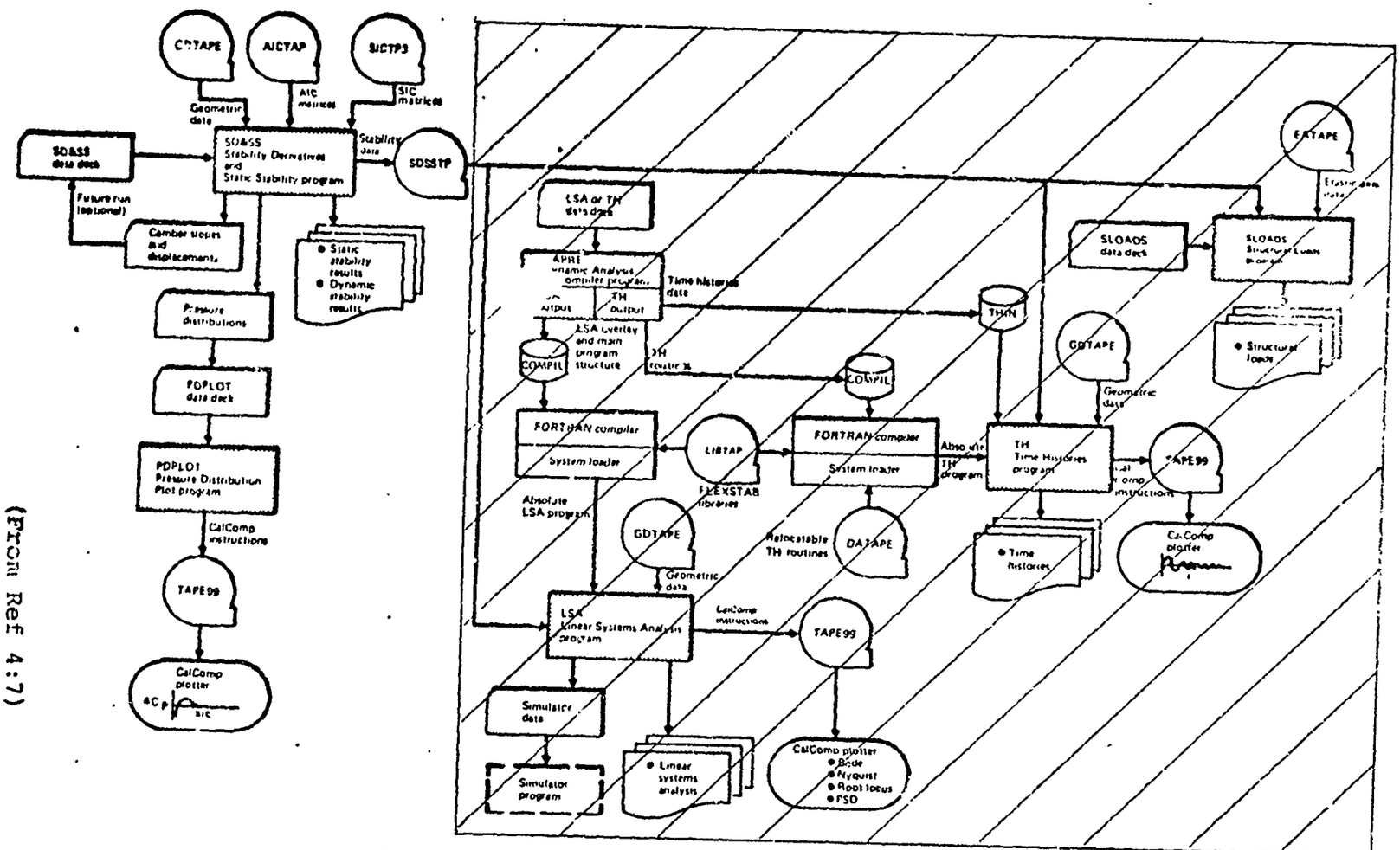

FIGURE 2.—FLEXSTAB 2.01.00: AIRPLANE ANALYSIS SECTION

(From Ref 4:7)

LIST OF INPUT DATA CARDS

```
NO.   CARD IMAGES
    1 $CASE FOR BOEING KC-135A PROBLEM 2
    2 GEOMETRY OF KC-135A WITH WINGLETS AND NO NACELLES
    3 CAPT. KENT R. CRENSHAW, AFIT/ENA, GAE76D
    4 $GENERAL SPECIFICATIONS
    5 .77                    INCHES
    6 $SLENDER BODY DATA
    7 FUSELAGE
    8 0.0        0.0         46.68
    9 1.0
   10 250.0      1546.0
   11 0.0        1546.0      15.0        0.0
   12 8.0        RADII       LINEAR
   13 0.0        100.0       200.0       945.6       1170.0      1300.0
   14 1500.0     1546.0
   15 0.0        53.32       83.0        83.0        65.0        40.0
   16 15.0       0.0
   17 XYZ        6.0                     LINEAR
   18 0.0        0.0         0.0         945.6       0.0         0.0
   19 1100.0     0.0         18.0        1300.0      0.0         43.0
   20 1500.0     0.0         68.0        1546.0      0.0         73.75
   21 $INTERFERENCE BODY DATA
   22 S.B.F.                 FUSELAGE
   23 0.0        0.0         46.68
   24 250.0      1546.0
   25            Y-Z         4.0         INPUT       11.0        3.0
   26 0.0        83.0        63.5        35.1487     63.5        -38.9413
   27 0.0        -83.0
   28 250.0      350.0       445.0       485.014     586.669     688.324
   29 790.0195   850.0       1000.0      1200.0      1400.0      1546.0
   30 WING       ROOT        63.5        -38.9413    7.0
   31 HOR TAIL   ROOT        63.5        35.1487     7.0
   32 VER TAIL   ROOT        0.0         83.0        90.0
   33 85.0
   34 $THIN BODY DATA
   35 VER TAIL               S.B.F.
   36 0.0        0.0         0.0         90.0
   37 3.0        2.0         4.0                                 NO PRINT
   38 1182.0     129.68      1317.0      210.0       1462.0      426.08
   39 1499.0     129.68      1567.0      426.08
   40 129.68     210.0       1.0         3.0         0.0         1.0
```

Table I
GD Input

NO.	CARD IMAGES					
41	36.0	73.0				
42	36.0	60.0				
43	210.0	300.0	1.0	3.0	0.0	0.0
44	36.0	60.0				
45	300.0	371.68	0.0			
46	371.68	426.08	0.0			
47	0.0					
48	0.0					
49	0.0					
50	$THIN BODY DATA					
51	FOR TAIL		S.S.F.			
52	0.0	0.0	74.09	7.0		
53	2.0	2.0	4.0			NC PRINT
54	1340.0	63.5	1515.0	265.0		
55	1525.0	63.5	1605.0	265.0		
56	63.5	100.0	1.0	3.0	0.0	0.0
57	36.0	72.0				
58	100.0	150.0	0.0			
59	150.0	207.5	0.0			
60	207.5	265.0	0.0			
61	0.0					
62	0.0					
63	0.0					
64	$THIN BODY DATA					
65	WING		S.S.F.			
66	0.0	0.0	0.0	7.0		
67	2.0	3.0	13.0			NC PRINT
68	445.0	63.5	995.0	780.0		
69	850.0	63.5	805.0	150.0	1105.0	780.0
70	63.5	100.0	1.0	5.0	0.0	0.0
71	9.88	34.98	60.08	85.19		
72	100.0	150.0	0.0			
73	150.0	207.5	0.0			
74	207.5	265.0	0.0			
75	265.0	326.0	0.0			
76	326.0	382.75	0.0			
77	382.75	439.5	0.0			
78	439.5	496.25	0.0			
79	496.25	553.0	0.0			
80	553.0	609.75	0.0			

Table I (cont'd)

GEOMETRY OF KC-135A WITH WINGLETS AND NO N...LES

NO.	CARD IMAGES					
81	609.75	666.5	0.0			
82	666.5	723.25	0.0			
83	723.25	780.0	0.0			
84	0.0					
85	5.0	LINEAR	NO PRINT			
86	63.5	11.0	0.0	100.0		
87	100.0	0.0	55.0	7.62	35.0	9.218
88	15.0	7.661	5.0	4.83	0.0	.74
89	5.0	-2.613	15.0	-4.51	35.0	-6.275
90	55.0	-5.185	100.0	0.0		
91	150.0	11.0	0.0	100.0		
92	100.0	0.0	60.0	6.284	35.0	7.92
93	15.0	6.436	5.0	3.998	0.0	.586
94	5.0	-1.915	15.0	-3.318	35.0	-4.98
95	60.0	-3.995	100.0	0.0		
96	242.0	11.0	0.0	100.0		
97	100.0	0.0	60.0	5.643	35.0	6.805
98	10.0	4.699	5.0	3.36	0.0	.374
99	5.0	-1.307	30.0	-3.425	45.0	-3.782
100	60.0	-3.174	100.0	0.0		
101	423.5	11.0	0.0	100.0		
102	100.0	0.0	70.0	4.267	50.0	6.078
103	35.0	6.43	10.0	4.423	5.0	3.13
104	0.0	.306	10.0	-1.187	35.0	-2.445
105	50.0	-2.501	100.0	0.0		
106	780.0	11.0	0.0	100.0		
107	100.0	0.0	70.0	4.267	50.0	6.078
108	35.0	6.43	10.0	4.423	5.0	3.13
109	0.0	.306	10.0	-1.187	35.0	-2.445
110	50.0	-2.501	100.0	0.0		
111	2.0	LINEAR				
112	63.5	2.0	780.0	-.8		
113	WITHIN BODY DATA					
114	WINGLET		WING			
115	995.0	774.186	95.0581	70.0		
116	3.0	2.0	4.0			
117	0.0	0.0	60.0	25.88	120.0	106.0
118	110.0	0.0	143.0	106.0		
119	0.0	25.88	1.0	5.0	0.0	0.0
120	9.88	34.98	60.08	85.19		

NO PRINT

Table I (cont'd)

NO.	CARD IMAGES					
121	25.88	52.59	0.0			
122	52.59	79.29	0.0			
123	79.29	106.0	0.0			
124	0.0					
125	4.0	LINEAR	NO PRINT			
126	0.0	10.0	0.0	100.0		
127	100.0	0.0	80.0	3.0	60.0	5.0
128	30.0	5.0	10.0	3.5	0.0	0.0
129	20.0	-2.0	70.0	-1.0	90.0	1.0
130	100.0	0.0				
131	21.2	10.0	0.0	100.0		
132	100.0	0.0	80.0	4.0	60.0	6.5
133	30.0	6.5	10.0	3.5	0.0	0.0
134	20.0	-1.5	70.0	1.5	90.0	1.5
135	100.0	0.0				
136	44.202	10.0	0.0	100.0		
137	100.0	0.0	80.0	4.0	60.0	7.0
138	30.0	7.0	10.0	4.0	0.0	0.0
139	20.0	-1.0	70.0	2.0	90.0	2.0
140	100.0	0.0				
141	106.0	10.0	0.0	100.0		
142	100.0	0.0	80.0	4.0	60.0	7.0
143	30.0	7.0	10.0	4.0	0.0	0.0
144	20.0	-1.0	70.0	2.0	90.0	2.0
145	100.0	0.0				
146	4.0	LINEAR				
147	0.0	-3.1	31.8	-2.1	42.4	-2.5
148	106.0	-2.5				
149	$PLOT DATA					
150	PLOT	AUTO	OTHER	.333		
151	COMPLETE					
152	END OF LIST					
153	$END OF CASE					

Table I (cont'd)

LIST OF INPUT DATA CARDS

NO.	CARD IMAGES
1	$CASE FOR ISIC PROGRAM BOEING KC-135A WITHOUT NACELLES
2	KC-135A NO WINGLETS
3	CAPT. KENT R. CRENSHAW, AFIT/ENA, GAE76D
4	$GEOMETRY TAPE DATA
5	1. 0.
6	$OPTION
7	RESIDUAL-ELASTIC RESIDUAL-ELASTIC
8	$STRUCTURAL DATA
9	$JUNCTION POINT DATA
10	4.0
11	0.0 1.0
12	610.0 1.0
13	1360.0 1.0
14	1428.0 1.0
15	3.0
16	2.0
17	1.0 2.0
18	3.0
19	1.0 2.0 3.0
20	4.0
21	1.0 2.0 3.0 4.0
22	$SLENDER BODY DATA
23	$PART 1
24	15.0 1.0 2.0
25	$COORDINATES OF SEGMENTS
26	38.0 97.5 174.1 199.4 272.2 283.0
27	300.0 360.0 369.0 397.8755 426.751 444.151
28	480.551 561.151
29	$STIFFNESS DATA
30	0.0 0.6E11 1.3E11 0.95E11
31	0.0 2.05E11 3.6E11 2.6E11
32	0.0 4.05E11 4.90E11 3.85E11
33	0.0 5.55E11 6.40E11 4.50E11
34	0.0 6.70E11 6.90E11 4.80E11
35	0.0 7.60E11 7.30E11 5.00E11
36	0.0 7.80E11 7.40E11 5.05E11
37	0.0 8.30E11 7.40E11 5.20E11
38	0.0 8.30E11 7.40E11 5.20E11
39	0.0 9.10E11 7.15E11 5.20E11
40	0.0 1.04E12 8.00E11 6.35E11

Table II
ISIC

Table II (cont'd)

NO.	CARD IMAGES					
41	0.0	1.10E12	8.80E11	7.10E11		
42	0.0	1.00E13	1.00E13	1.00E13		
43	0.0	1.00E13	1.00E13	1.00E13		
44	0.0	1.00E13	1.00E13	1.00E13		
45	$LUMPED MASSES					
46	14.0					
47	2.329	42.981	85.047156	13.9865	68.24	30.0
48	30.5565	49.08	37.9527	98.5044	55.6275	0.0
49	69.1825	47.76				
50	$PART 2					
51	12.0	2.0	3.0			
52	$COORDINATES OF SEGMENTS					
53	646.551	717.551	793.851	821.151	841.751	1004.3935
54	1167.036	1178.036	1202.936	1278.536	1351.736	
55	$STIFFNESS DATA					
56	0.0	1.00E13	1.00E13	1.00E13		
57	0.0	2.50E12	1.64E12	4.50E11		
58	0.0	2.59E12	1.48E12	3.20E11		
59	0.0	2.64E12	1.34E12	9.60E11		
60	0.0	2.66E12	1.30E12	9.10E11		
61	0.0	1.71E12	1.17E12	7.20E11		
62	0.0	8.40E11	7.80E11	4.80E11		
63	0.0	7.40E11	6.80E11	4.30E11		
64	0.0	6.70E11	6.20E11	3.90E11		
65	0.0	5.20E11	4.50E11	2.80E11		
66	0.0	3.80E11	3.00E11	1.90E11		
67	0.0	2.70E11	1.80E11	1.35E11		
68	$LUMPED MASSES					
69	11.0					
70	210.9612	179.0624	86.595	10.5675	65.282	130.328
71	6.216	7.9255	77.371444	13.789	13.19722	
72	$PART 3					
73	2.0	3.0	4.0			
74	$COORDINATES OF SEGMENTS					
75	1404.854					
76	$STIFFNESS DATA					
77	0.0	1.00E11	0.40E11	0.70E11		
78	0.0	0.50E11	0.20E11	0.35E11		
79	$LUMPED MASSES					
80	1.0					

```
NO.    CARD IMAGES
  81   10.465
  82   $PART 4
  83   1.0        4.0        0.0
  84   $COORDINATES OF SEGMENTS
  85   1466.154
  86   $STIFFNESS DATA
  87   0.0              0.50E11    0.20E11    0.35E11
  88   $LUMPED MASSES
  89   1.0
  90   2.39
  91   $THIN BODY DATA  VERTICAL TAIL
  92   3.0        0.0
  93   $PART
  94   12.
  95   $COORDINATES OF SEGMENTS
  96   0.         45.        0.         64.        7.         87.
  97   20.        104.       27.5       127.       35.5       144.
  98   45.3       164.       54.5       183.       74.        219.
  99   93.        263.       113.       304.       146.       362.
 100   $STIFFNESS DATA
 101   0.              1.0E12     1.0E12
 102   0.0            22.0E09    22.0E09
 103   0.0            20.0E09    20.0E09
 104   0.0            17.4E09    18.4E09
 105   0.0            13.7E09    12.8E09
 106   0.0            10.8E09    9.55E09
 107   0.0             8.60E09    7.60E09
 108   0.0             6.85E09    6.20E09
 109   0.0             5.10E09    5.15E09
 110   0.0             3.25E09    3.80E09
 111   0.0             2.00E09    2.00E09
 112   0.0             1.00E09    1.00E09
 113   $LUMPED MASSES
 114   12.
 115   0.0
 116   0.0
 117   2.0
 118   168.77     -59.0      34.10      74.0
 119   0.0
 120   2.0
```

Table II (cont'd)

NO.	CARD IMAGES					
121	289.64	-53.0	266.54	68.0		
122	0.0					
123	0.0					
124	2.0					
125	150.59	-44.0	378.94	58.0		
126	2.0					
127	161.80	-40.0	191.76	51.0		
128	2.0					
129	94.06	-32.5	139.41	44.		
130	2.0					
131	98.25	-29.0	203.37	35.0		
132	2.0					
133	92.52	-23.5	137.03	20.0		
134	$SCALE					
135	0.031081	0.031081	0.031081	0.031081	0.031081	0.031081
136	0.031081	0.031081	0.031081	0.031081	0.031081	0.031081
137	0.031081	0.031081				
138	$THIN BODY DATA HORIZONTAL TAIL					
139	4.0	0.0				
140	$PART					
141	8.0					
142.	$COORDINATES OF SEGMENTS					
143	0.0	12.0	0.0	36.0	11.0	56.0
144	32.0	95.0	54.0	134.0	76.0	174.0
145	97.0	213.0	119.0	254.0		
146	$STIFFNESS DATA					
147	0.0	11.0E09	7.15E09			
148	0.0	15.0E09	18.0E09			
149	0.0	13.3E09	16.5E09			
150	0.0	10.1E09	12.6E09			
151	0.0	6.30E09	7.30E09			
152	0.0	3.40E09	3.90E09			
153	0.0	1.80E09	2.40E09			
154	0.0	1.00E09	1.15E09			
155	$LUMPED MASSES					
156	8.0					
157	2.0					
158	207.01	-33.0	80.22	27.0		
159	3.0					
160	72.23	-76.0	90.23	6.0	75.85	59.0

Table II (cont'd)

NO.	CARD IMAGES					
161	3.0					
162	107.37	-57.0	180.31	6.0	123.86	52.0
163	3.0					
164	103.87	-51.0	151.82	7.0	99.94	49.0
165	3.0					
166	66.64	-44.0	142.30	8.0	87.14	45.0
167	3.0					
168	68.74	-38.0	10.59	9.0	66.27	41.0
169	3.0					
170	25.94	-31.0	115.52	10.0	50.57	38.0
171	3.0					
172	10.46	-24.0	143.48	12.0	39.63	34.0
173	$SCALE					
174	0.031081	0.031081	0.031081	0.031081	0.031081	0.031081
175	0.031081	0.031081	0.031081	0.031081	0.031081	0.031081
176	0.031081	0.031081	0.031081	0.031081	0.031081	0.031081
177	0.031081	0.031081	0.031081	0.031081	0.031081	
178	$THIN BODY DATA WINS					
179	2.0	0.0				
180	$PART					
181	13.0					
182	$COORDINATES OF SEGMENTS					
183	0.0	50.0	11.78	88.0	33.78	138.0
184	58.7799	188.0	84.7799	238.0	140.7799	318.0
185	140.7799	326.0	179.2799	381.0	240.2756	481.0
186	282.2756	541.0	282.2756	553.0	366.6505	661.0
187	430.6829	753.847				
188	$STIFFNESS DATA					
189	0.	4.62E11	1.[illegible]			
190	0.0	4.47E11	4.7[illegible]			
191	0.0	2.80E11	1.94E11			
192	0.0	1.92E11	1.29E11			
193	0.0	1.31E11	0.94E11			
194	0.0	0.85E11	0.68E11			
195	0.0	6.00E10	4.31E10			
196	0.0	6.00E10	3.29E10			
197	0.0	3.30E10	2.21E10			
198	0.0	2.22E10	1.55E10			
199	0.0	1.59E10	1.11E10			
200	0.0	0.83E10	0.62E10			

Table II (cont'd)

NO.	CARD IMAGES					
201	0.0	0.40E10	0.30E10			
202	$LUMPED MASSES					
203	13.0					
204	2.0					
205	4989.8367	-124.0	11620.9850	95.0		
206	4.0					
207	1658.0	-80.0	4183.0	-36.0	2370.0	52.0
208	2538.0	92.0				
209	2.0					
210	6211.0	-32.0	3664.0	50.0		
211	2.0					
212	965.0	-66.0	1591.0	82.0		
213	4.0					
214	1087.0	-63.0	2199.0	-30.0	2507.0	42.0
215	1555.0	73.0				
216	4.0					
217	477.0	-70.0	3322.7345	-42.0	2874.0	22.0
218	1497.0	46.0				
219	3.0					
220	6935.1057	-156.6	1.0	-71.6	560.0	-29.0
221	4.0					
222	464.0	-37.0	1433.0	-19.0	1886.7155	24.0
223	652.0	50.0				
224	4.0					
225	1005.0	-30.0	723.0	-15.0	559.345	18.0
226	1336.0	38.0				
227	2.0					
228	8.185	10.0	64.2386	28.0		
229	5.0					
230	6695.0877	-99.0	437.9139	-19.0	293.0	-2.0
231	475.0	26.0	402.0	43.0		
232	4.0					
233	477.0	-20.0	735.6553	-9.0	1007.0	10.0
234	351.0	23.0				
235	4.0					
236	422.0	-18.0	48.0	-11.0	313.0	7.0
237	341.7361	17.0				
238	$SCALE					
239	0.031801	0.031081	0.031081	0.031081	0.031081	0.031081
240	0.031801	0.031081	0.031081	0.031081	0.031081	0.031081

Table II (cont'd)

NO.	CARD IMAGES					
241	0.031081	0.031081	0.031081	0.031081	0.031081	0.031081
242	0.031081	0.031081	0.031081	0.031081	0.031081	0.031081
243	0.031081	0.031081	0.031081	0.031081	0.031081	0.031081
244	0.031081	0.031081	0.031081	0.031081	0.031081	0.031081
245	0.031081	0.031081	0.031081	0.031081	0.031081	0.031081
246	0.031801	0.031081	0.			
247	$MATRIX PRINT LIST					
248	0.	0.	0.	0.	0.	1.
249	$END OF CASE					

Table II (cont'd)

BOEING KC-135A WITH WINGLETS AND NO NACEL

LIST OF INPUT DATA CARDS

NO.	CARD IMAGES				
1	$CASE FOR STABILITY DERIVATIVES AND STATIC STABILITY PROGRAM				
2	BOEING KC-135A WITH WINGLETS AND NO NACELLES				
3	CAPT. KENT R. GREENSHAW, AFIT/ENA, GAE76D, BOX 4218				
4	$GENERAL SPECIFICATIONS				
5	COUPLED REFERENCE MOTION			RIGID MODEL	
6		THICKNESS L	THRUST	SPEED	MACH
7	GDTAPE	2.0		AICTAP	
8	IN/FT	ALTITUDE			
9				.77	
10	21500.0	0.0	0.0		
11	0.0	0.0	0.0		
12	350362.0	241.8804	1569.96		
13	$THRUST DATA				
14	1.0				
15	FUSELAGE	1.0	15.0		
16	1.0	1546.0	-1.0	0.0	0.0
17	$TRIM CONTROL DATA				
18	LONGITUDINAL				
19	1.0	SWEEP	1462.0	63.5	1574.3514 265.0
20	HOR TAIL	12.0			
21	1.0	1.0			
22	2.0	1.0			
23	3.0	1.0			
24	4.0	1.0			
25	5.0	1.0			
26	6.0	1.0			
27	7.0	1.0			
28	8.0	1.0			
29	9.0	1.0			
30	10.0	1.0			
31	11.0	1.0			
32	12.0	1.0			
33	AILERON				
34	1.0	SWEEP	821.2431	265.0	852.9235 326.0
35	WING	1.0			
36	25.0	1.0			
37	RUDDER				
38	1.0	SWEEP	1472.9	129.68	1515.9097 371.68
39	VER TAIL	3.0			
40	3.0	1.0			

Table III
SDSS

```
NO.   CARD IMAGES

41    6.0         1.0
42    9.0         1.0
43    END OF TRIM CONTROL DATA
44    $STABILITY PROBLEM DATA
45    CONSTANT
46    REFERENCE SOLVE       0.0         646.5003  PRINT
47    1.0         0.0       1.0         0.0       1.0         0.0
48    10.0        -10.0     100000.0    0.0       30.0        -30.0
49    20.0        -20.0     30.0        -30.0     40.0        -40.0
50    $PERTURBATION DATA
51    BOTH        UNSTEADY                                    PRINT
52
53
54    $DYNAMIC ANALYSIS OPTIONS
55    END OF OPTIONS
56    $STRUCTURAL DATA
57    735.1391                20.28
58    2935500.0 4660000.0 7474500.0 -158700.0
59    8328.1007
60    $END OF CAS
```

Table III (cont'd)

Appendix E

FLEXSTAB Model Data Tables

Table I

FLEXSTAB Rigid Model Data

	FLT COND 1		FLT COND 2		FLT COND 2A		FLT COND 3		FLT COND 4	
	NW	WW	NW	WW	NW	WW	NW	WW	NW	WW
Mach	.77	.77	.77	.77	.77	.77	.422	.422	.211	.211
h (ft)	28.5M	28.5M	45.6M	45.6M	28.5M	28.5M	S.L.	S.L.	S.L.	S.L.
V_T(fps)	771.47	771.47	745.89	745.89	771.47	771.47	471.44	471.44	235.72	235.72
$\bar{q}$(psf)	279.98	279.98	124.96	124.96	279.98	279.98	264.14	264.14	66.04	66.04
γ(deg)	0.0	0.0	0.0	0.0	0.0	0.0	4.01	4.01	-2.5	-2.5
θ_B(deg)	2.52	2.42	1.63	1.52	-.89	-.941	7.07	6.951	.066	-.074
α_w(deg)	4.5176	4.4218	3.63	3.52	1.11	1.059	9.07	8.951	2.066	1.926
c.g. $\bar{\bar{c}}$	.242	.242	.321	.321	.321	.321	.247	.247	.321	.321
* I_{xx}(sl-ft^2) x 10^6	2.93	2.93	2.05	2.05	2.05	2.05	3.17	3.17	2.05	2.05
* I_{yy}(sl-ft^2) x 10^6	4.66	4.66	2.46	2.46	2.46	2.46	4.72	4.72	2.46	2.46
* I_{zz}(sl-ft^2) x 10^6	7.48	7.48	4.36	4.36	4.36	4.36	7.7	7.7	4.36	4.36
Weight (lb)	284.M	284.M	130.M	130.M	130.M	130.M	297.M	297.M	130.M	130.M
T_1(lb_f)	16.32M	15.47M	7.51M	7.12M	2.6M	2.36M	45.91M	44.9M	13.08M	12.65M
δ_{STRIM} (deg)	-2.28	-2.93	-1.87	-2.59	-.83	-1.26	-3.843	-4.597	-1.825	-2.672

Longitudinal Data

** L/D	17.38	18.35	17.29	18.26	50.26	54.57	11.75	12.26	6.89	7.06
C_{Lo}	.193	.202	.2869	.3008	.287	.3008	.2401	.251	.6181	.6321
C_{Do}	.0017	.0015	.0048	.0041	.0048	.0041	.0049	.0044	.0545	.0530
C_{Mo}	-.0205	-.0334	-.0376	-.0560	-.0376	-.056	-.0503	-.065	-.0201	-.0380

Table I
FLEXSTAB Rigid Model Data (cont'd)

	FLT COND 1		FLT COND 2		FLT COND 2A		FLT COND 3		FLT COND 4	
	NW	WW	NW	WW	NW	WW	NW	WW	NW	WW
$\bar{C}_{L\hat{u}}$(1/rad)	1.1413	1.1477	1.1675	1.1744	.5361	.5387	.9836	.9859	1.6375	1.6389
$\bar{C}_{D\hat{u}}$(1/rad)	.0634	,0602	.0658	.0626	.0077	.0069	.0826	.0794	.2376	.2322
$\bar{C}_{M\hat{u}}$(1/rad)	-.0063	-.0196	-.0048	-.0186	.00096	-.0055	.0160	.0126	.0100	.0086
$C_{L\alpha}$(1/deg)	.0986	.1017	.0986	.1017	.0989	.102	.0837	.0861	.0791	.0813
$C_{D\alpha}$(1/deg)	.0077	.0069	.0071	.0062	.0017	.0012	.0081	.0072	.0106	.0097
$C_{M\alpha}$(1/deg)	-.0212	-.0257	-.0133	-.0175	-.0129	-.0169	-.0173	-.0206	-.0106	-.0135
C_{Lq}(1/rad)	11.2739	11.6808	10.385	10.762	10.386	10.758	9.6091	9.9271	8.5395	8.8184
C_{Dq}(1/rad)	.3060	.1957	.2080	.0877	-.1459	-.2168	.3149	.2018	.2826	.1625
C_{Mq}(1/rad)	-18.2668	-18 8457	-17.251	-17.761	-17.243	-17.73	-15.636	-16.081	-14.252	-14.625
$C_{L\delta s}$(1/deg)	.0109	.0110	.0109	.0110	.0110	.0110	.0097	.0097	.0094	.0094
$C_{D\delta s}$ (1/deg)	.0004	.0003	.0002	.00014	-.0004	-.0005	.0005	.0004	.0007	.0006
$C_{M\delta s}$ (1/deg)	-.0325	-.0326	-.0317	-.0317	-.0317	-.0317	-.028	-.028	-.0262	-.0265
C_{L1}	.4163	.4164	.4271	.4272	.191	.191	.4596	.4598	.8041	.8044
C_{D1}	.0239	.0227	.0247	.0234	.0038	.0035	.0391	.0375	.1166	.1139
C_{M1}	.00262	.00248	.0019	.0018	.00029	.00027	.0082	.0081	.0063	.00605

Table I
FLEXSTAB Rigid Model Data (cont'd)

	FLT COND 1		FLT COND 2		FLT COND 2A		FLT COND 3		FLT COND 4	
	NW	WW	NW	WW	NW	WW	NW	WW	NW	WW
$C_{L\dot{\alpha}}$(1/rad)	-5.1742	-6.1515	-5.1871	-6.164	-5.198	-6.174	-1.022	-1.5126	-.3655	-.7778
$C_{D\dot{\alpha}}$(1/rad)	-.3324	-.3336	-.3534	-.3543	-.126	-.0891	.1536	-.1653	-.0724	-.0796
$C_{M\dot{\alpha}}$(1/rad)	-10.219	-9.1875	-10.634	-9.684	-10.634	-9.684	-6.791	-6.257	-6.2301	-5.806
C_{Lq}(1/rad)	-20.673	-22.536	-19.882	-21.591	-19.903	-21.610	-9.562	-10.471	-7.647	-8.345
$C_{D\dot{q}}$ (1/rad)	-1.0887	-1.0809	-.9182	-.9067	-.047	.0218	-.6897	-.6998	-.4788	-.4781
$C_{M\dot{q}}$(1/rad)	-4.252	-2.3773	-4.219	-2.6478	-4.219	-2.6478	-4.401	-3.459	-4.1069	-3.428
Static Margin	.2152	.2527	.1344	.1722	.1300	.1660	.2069	.2397	.1340	.1662
$\partial\delta e/\partial n$	-3.2609	-3.8287	-2.21	-2.7809	-1.1051	-1.3491	-4.441	-5.0835	-7.4059	-8.5566
$\bar{x}_{ac}$ N.P	.4576	.4951	.4554	.4932	.4510	.4870	.4539	.4867	.4550	.4872
Maneuver Pt.	.4819	.5202	.4793	.5178	.5017	.5392	.5048	.5391	.5645	.5998
Maneuver Margin	.2394	.2777	.1583	.1968	.1807	.2182	.2578	.2921	.2435	.2788
$\partial\delta e/\partial V$	.0105	.012	.0065	.008	.0034	.0041	.0168	.0194	.0370	.0464

Lateral Data

	FLT COND 1		FLT COND 2		FLT COND 2A		FLT COND 3		FLT COND 4	
	NW	WW	NW	WW	NW	WW	NW	WW	NW	WW
$C_{Y\beta}$(1/deg)	-.0116	-.0133	-.0116	-.0133	-.0116	-.0134	-.0105	-.012	-.0102	-.0116
$C_{\ell\beta}$(1/deg)	-.0025	-.0032	-.0025	-.0032	-.0026	-.0034	-.0022	-.0029	-.0022	-.0027
$C_{n\beta}$(1/deg)	.0034	.0036	.0032	.0034	.0032	.0034	.0029	.0031	.0026	.0027

Table I
FLEXSTAB Rigid Model Data (cont'd)

	FLT COND 1		FLT COND 2		FLT COND 2A		FLT COND 3		FLT COND 4	
	NW	WW	NW	WW	NW	WW	NW	WW	NW	WW
C_{Y_p}(1/rad)	-.1850	-.3295	-.1786	-.3218	-.1786	-.3218	-.1799	-.2989	-.1709	-.283
C_{ℓ_p}(1/rad)	-.4969	-.5590	-.4952	-.5565	-.4956	-.5577	-.4428	-.4932	-.4277	-.475
C_{N_p}(1/rad)	.0188	.0377	.0129	.02739	.0135	.0344	.0211	.0334	-.0052	.0024
C_{Y_r}(1/rad)	.7078	.8234	.696	.8154	.6615	.7532	.6258	.7183	.6250	.7149
C_{ℓ_r}(1/rad)	.2502	.2914	.2632	.3055	.1892	.2222	.2230	.2564	.2715	.3072
C_{N_r}(1/rad)	-.2926	-.3161	-.2815	-.3038	-.2677	-.2851	-.2648	-.2822	-.2580	-.2728
$C_{Y_{\delta A}}$(1/deg)	1.31×10^{-4}	$.93\times10^{-4}$	1.31×10^{-4}	$.94\times10^{-4}$	1.31×10^{-4}	$.94\times10^{-4}$	$.95\times10^{-4}$	$.71\times10^{-4}$	$.88\times10^{-4}$	$.67\times10^{-4}$
$C_{\ell_{\delta A}}$(1/deg)	-5.82×10^{-4}	-5.98×10^{-4}	-5.8×10^{-4}	-5.96×10^{-4}	-5.74×10^{-4}	-5.9×10^{-4}	-4.8×10^{-4}	-4.9×10^{-4}	-4.54×10^{-4}	-4.63×10^{-4}
$C_{N_{\delta A}}$(1/deg)	-1.24×10^{-4}	-1.2×10^{-4}	-1.22×10^{-4}	-1.19×10^{-4}	-1.32×10^{-4}	-1.27×10^{-4}	$-.95\times10^{-4}$	$-.93\times10^{-4}$	$-.98\times10^{-4}$	-97×10^{-4}
$C_{Y_{\delta R}}$(1/deg)	.0076	.0075	.0076	.0075	.0076	.0075	.0064	.0064	.0061	.0061
$C_{\ell_{\delta R}}$(1/deg)	.00067	.00067	.00069	.00069	.00084	.00084	.0006	.00055	.00052	.00052
$C_{N_{\delta R}}$(1/deg)	-.0036	-.0035	-.0035	-.0034	-.0034	-.0034	-.00297	-.00296	-.0028	-.0028
$C_{Y_{\dot{\beta}}}$(1/rad)	-.1784	-.1746	-.1784	-.1746	-.1784	-.1746	-.1748	-.1735	-.1741	-.1731
$C_{\ell_{\dot{\beta}}}$(1/rad)	-.0029	.0024	-.0021	.0031	-.0022	.0030	-.0036	-.0012	-.0029	-.0008
$C_{N_{\dot{\beta}}}$(1/rad)	.0058	.0056	.0037	.0034	.0036	.0036	.0029	.003	.00068	.00085

Table I
FLEXSTAB Rigid Model Data (cont'd)

	FLT COND 1		FLT COND 2		FLT COND 2A		FLT COND 3		FLT COND 4	
	NW	WW	NW	WW	NW	WW	NW	WW	NW	WW
C_{Y_p}(1/rad)	-.1568	-.1348	-.155	-.1331	-.155	-.133	-.125	-.1107	-.1162	-.1034
C_{ℓ_p}(1/rad)	-.0066	-.0085	-.0067	.0082	-.0097	.0055	-.0128	-.0041	-.0139	-.0064
C_{N_p}(1/rad)	.0689	.0649	.0672	.0634	.0669	.0637	.0538	.0510	.0485	.0473
C_{Y_r}(1/rad)	-.0128	-.0143	-.0171	-.0185	-.0171	-.0185	-.0010	-.0014	-.0022	-.0024
C_{ℓ_r}(1/rad)	.0010	-.0013	.0013	-.0009	.0022	-.0001	.0010	0.0	.0011	00034
C_{N_r}(1/rad)	-.0192	-.0192	-.0193	-.0193	-.0192	-.0193	-.0197	-.0198	-.0198	-.02

Dynamic Modes Comparison

	FLT COND 1		FLT COND 2		FLT COND 2A		FLT COND 3		FLT COND 4	
	NW	WW	NW	WW	NW	WW	NW	WW	NW	WW
					* Longitudinal*					
Short Period										
ω_n(rad/sec)	1.99	2.17	1.49	1.68	2.37	2.65	1.81	1.96	1.17	1.27
Peroid (sec)	3.49	3.13	4.91	4.18	3.67	3.03	4.17	3.75	9.24	7.605
$\zeta_{s.p.}$	.418	.383	.509	.450	.691	.621	.556	.519	.814	.76
$T_{\frac{1}{2}}$ (sec)	.835	.833	.918	.914	.423	.421	.687	.681	.726	.717

Table I
FLEXSTAB Rigid Model Data (cont'd)

	FLT COND 1		FLT COND 2		FLT COND 2A		FLT COND 3		FLT COND 4	
	NW	WW	NW	WW	NW	WW	NW	WW	NW	WW
Phugoid										
ω_n (rad/sec)	.065	.064	.065	.064	.061	.060	.094	.094	.151	.157
Period (sec)	96.59	97.82	96.49	97.92	103.74	104.53	67.13	67.06	41.66	40.18
ζ_p	.024	.023	.026	.026	.010	.011	.011	.010	.080	.077
$T\frac{1}{2}$ (sec)	439.19	478.52	411.26	420.06	1135.44	1044.8	663.96	733.60	57.08	57.32
				Lateral						
Dutch Roll										
ω_n (rad/sec)	1.57	1.62	1.33	1.37	1.93	1.98	1.39	1.43	.918	.94
Period (sec)	4.03	3.91	4.74	4.61	3.3	3.22	4.59	4.49	6.98	6.83
ζ_{DR}	.129	.145	.107	.118	.153	.168	.184	.197	.198	.204
$T\frac{1}{2}$ (sec)	3.414	2.949	4.88	4.27	2.36	2.09	2.71	2.46	3.82	3.62
Spiral										
T_s (sec)	T2 =	T2 =	T2 =	T2 =	293.44	204.3	T2 =	T2 =	T2 =	T2 =
$T\frac{1}{2}$ (sec)	156.35	268.42	146.7	261.75	203.4	141.61	66.55	98.37	43.78	88.21

Table I
FLEXSTAB Rigid Model Data (cont'd)

	FLT COND 1		FLT COND 2		FLT COND 2A		FLT COND 3		FLT COND 4	
	NW	WW	NW	WW	NW	WW	NW	WW	NW	WW
Roll										
T_R (sec)	.804	.726	1.167	1.05	.540	.483	.626	.563	.786	.705
$T_{\frac{1}{2}}$ (sec)	.558	.503	.809	.730	.374	.335	.34	.390	.545	.489

*Moments of inertia wrt principal axes, +2° about Y-axis from FRL.
Mass of winglets is neglected in all cases.
**L/D = C_{L1}/C_{D1} and includes induced drag only.

Table II .

FLEXSTAB Rigid Short Tail Model Data (Flight Condition 2A)

	No Winglets (Rigid)	With Winglets (Rigid)	*Short Tail* With Winglets (Rigid)
Mach	.77	.77	.77
h (ft)	28,500	28,500	28,500
V(fps)	771.47	771.47	771.47
$\bar{q}$(psf)	279.98	279.98	279.98
γ (deg)	0.0	0.0	0.0
θ_B (deg)	-.89	-.941	-.941
α_w (deg)	1.11	1.059	1.059
c.g.$\bar{c}$	.321	.321	.321
* $I_{xx} \times 10^6$ (sl-ft^2)	2.05	2.05	2.05
* $I_{yy} \times 10^6$ (sl-ft^2)	2.46	2.46	2.46
* $I_{zz} \times 10^6$ (sl-ft^2)	4.36	4.36	4.36
* $I_{xz} \times 10^6$ (sl-ft^2)	-	-	-
Weight (lbs)	130000.0	130000.0	130000.0
T_1 (lbs)	2600.0	2360.0	2360.0
δ_{STRIM} (deg)	-.83	-1.26	-1.26

*Mass moments of inertia wrt principal axis system.

Table II

FLEXSTAB Rigid Short Tail Model Data (Flight Condition 2A) - cont'd

Lateral

	No Winglets (Rigid)	With Winglets (Rigid)	*Short Tail* With Winglets (Rigid)
$C_{Y\beta}$(1/deg)	-.0116	-.0134	-.0111
$C_{\ell\beta}$ (1/deg)	-.0026	-.0034	-.0029
$C_{N\beta}$(1/deg)	.0032	.0034	.0024
C_{Yp}(1/rad)	-.1786	-.3218	-.2976
$C_{\ell p}$(1/rad)	-.4959	-.5577	-.5533
C_{Np}(1/rad)	.0135	.0344	.0233
C_{Yr}(1/rad)	.6615	.7532	.6192
$C_{\ell r}$(1/rad)	.1892	.2222	.1975
C_{Nr}(1/rad)	-.2677	-.2851	-.2237
$C_{Y\delta A}$(1/deg)	1.31×10^{-4}	$.94 \times 10^{-4}$	$.34 \times 10^{-4}$
$C_{\ell\delta A}$(1/deg)	-5.74×10^{-4}	-5.9×10^{-4}	-6.01×10^{-4}
$C_{N\delta A}$(1/deg)	-1.32×10^{-4}	-1.27×10^{-4}	$-.99 \times 10^{-4}$
$C_{Y\delta R}$(1/deg)	.0076	.0075	.0066
$C_{\ell\delta R}$(1/deg)	.00084	.00084	.00066
$C_{N\delta R}$(1/deg)	-.0034	-.0034	-.0030
$C_{Y\dot{\beta}}$(1/rad)	-.1784	.1746	-.1988
$C_{\ell\dot{\beta}}$(1/rad)	-.0022	.0030	.0016
$C_{N\dot{\beta}}$(1/rad)	.0036	.0036	.0104
$C_{Y\dot{p}}$(1/rad)	-.155	-.133	-.1108
$C_{\ell\dot{p}}$(1/rad)	-.0097	.0055	.0100
$C_{N\dot{p}}$(1/rad)	.0669	.0637	.0532

Table II
FLEXSTAB Rigid Short Tail Model Data (Flight Condition 2A) - cont'd

	No Winglets (Rigid)	With Winglets (Rigid)	*Short Tail* With Winglets (Rigid)
C_{Yr} (1/rad)	-.0171	-.0185	.0028
$C_{\ell r}$ (1/rad)	.0022	-.0001	.0019
C_{Nr} (1/rad)	-.0192	-.0193	-.0275

Dynamic Modes Comparison

Longitudinal

Short Period			
ω_n (rad/sec)	2.37	2.65	2.65
Period (sec)	3.67	3.03	3.03
$\zeta_{s.p.}$	.691	.621	.621
$T_{\frac{1}{2}}$ (sec)	.423	.421	.421
Phugoid			
ω_n (rad/sec)	.061	.060	.060
Period (sec)	103.74	104.53	104.53
ζ_p	.010	.011	.011
$T_{\frac{1}{2}}$ (sec)	1135.44	1044.84	1044.84

Lateral

Dutch Roll			
ω_n (rad/sec)	1.93	1.98	1.66
Period (sec)	3.3	3.22	3.83
ζ_{DR}	.153	.168	.158
$T_{\frac{1}{2}}$ (sec)	2.36	2.09	2.65

Table II

FLEXSTAB Rigid Short Tail Model Data (Flight Condition 2A) - cont'd

	No Winglets (Rigid)	With Winglets (Rigid)	*Short Tail* With Winglets (Rigid)
Spiral			
$T^1/_{10}$ (sec)	675.68	470.42	358.3
$T_{\frac{1}{2}}$ (sec)	203.4	141.61	107.86
Roll			
$T^1/_{10}$ (sec)	1.242	1.113	1.113
$T_{\frac{1}{2}}$ (sec)	.374	.335	.335

Table III

FLEXSTAB Elastic Model Data

Flight Condition Parameters

	CRUISE 1		CRUISE 2		CRUISE 3	
$\gamma = 0°$	NW	WW	NW	WW	NW	WW
Mach	.77	.77	.77	.77	.422	.422
h (ft)	30.000	30.000	45,000	45,000	10,000	10,000
V_{p_1} (-ps)	767.3	767.3	745.9	745.9	454.96	454.96
$\bar{q}$ (psf)	261.67	261.67	128.59	128.59	181.69	181.69
θ_B (deg)	2.573	2.583	7.262	7.212	5.716	5.687
c.g. $\bar{c}$	.2299	.2321	.2299	.2321	.2299	.2321
* $I_{xx} \times 10^6$ (sl-ft^2)	3.694	3.746	3.694	3.746	3.694	3.746
* $I_{yy} \times 10^6$ (sl-ft^2)	3.716	3.728	3.716	3.728	3.716	3.728
* $I_{zz} \times 10^6$ (sl-ft^2)	7.256	7.319	7.256	7.319	7.256	7.319
* $I_{xz} \times 10^6$ (sl-ft^2)	.252	.255	.252	.255	.252	.255
Weight (lbs)	268,500	269,900	268,500	268,900	268,500	268,900
T_1 (lbs)	19,502.0	19,261.0	41,242.6	40,691.2	34,354.19	33,915.14
δ_{STRIM} (deg)	-2.62	-2.80	-5.82	-6.52	-4.61	-5.05
L/D	13.75	13.95	6.46	6.55	7.77	7.89

*Mass moments of inertia are wrt the body axis system.

Table III
FLEXSTAB Elastic Model Data (cont'd)

Longitudinal Data

	CRUISE 1				CRUISE 2			
	No Winglets		With Winglets		No Winglets		With Winglets	
	Rigid	Elastic	Rigid	Elastic	Rigid	Elastic	Rigid	Elastic
$\bar{C}_{L\hat{u}}$ (1/rad)	1.1514	.9607	1.1602	.9426	2.2959	2.0982	2.3148	2.0698
$\bar{C}_{D\hat{u}}$ (1/rad)	.0821	.0670	.0815	.0655	.3562	.3241	.3533	.3153
$\bar{C}_{M\hat{u}}$ (1/rad)	-.0083	.0542	-.0196	.0806	-.0239	.0475	-.0500	.0756
$C_{L\alpha}$ (1/deg)	.0984	.0876	.1016	.0882	.0969	.0908	.1002	.0924
$C_{D\alpha}$ (1/deg)	.0091	.0082	.0088	.0079	.0188	.0178	.0179	.0167
$C_{M\alpha}$ (1/deg)	-.0220	-.0150	-.0261	-.0162	-.0225	-.0186	-.0269	-.0212
C_{Lq} (1/rad)	11.4102	10.2467	11.7926	10.3237	11.3689	10.7552	11.7684	10.9525
C_{Dq} (1/rad)	.4646	.4003	.4287	.3474	1.1220	1.0369	.9929	.8801
C_{Mq} (1/rad)	-18.4064	-16.4194	-18.9379	-16.6202	-18.4196	-17.3860	-18.9912	-17.7512
$C_{L\delta s}$ (1/deg)	.0109	.0121	.0110	.0121	.0108	.0116	.0109	.0116
$C_{D\delta s}$ (1/deg)	.0005	.0006	.0005	.0006	.0016	.0017	.0016	.0017
$C_{M\delta s}$ (1/deg)	-.0326	-.0300	-.0326	-.0301	-.0326	-.0313	-.0326	-.0314
C_{L1}	.5117	.4207	.5325	.4213	.9308	.8481	.9546	.8495
C_{D1}	.0378	.0306	.0384	.0302	.1305	.1313	.1458	.1296
C_{M1}	-.0338	.00086	-.0572	.00085	-.0305	.00329	-.0544	.0032

Table III
FLEXSTAB Elastic Model Data (cont'd)

	CRUISE 1				CRUISE 2			
	No Winglets		With Winglets		No Winglets		With Winglets	
	Rigid	Elastic	Rigid	Elastic	Rigid	Elastic	Rigid	Elastic
$C_{L\dot{\alpha}}$ (1/rad)	-5.1806	-5.3422	-6.1565	-4.4607	-5.1274	-4.4426	-6.0987	-5.0322
$C_{D\dot{\alpha}}$ (1/rad)	-.4388	-.4388	-.4684	-.3283	-.8608	-.7393	-.9637	-.7900
$C_{M\dot{\alpha}}$ (1/rad)	-10.1493	-9.1353	-9.1247	-9.3254	-10.1493	-9.9606	-9.1247	-9.3582
$C_{L\dot{q}}$ (1/rad)	-20.8081	-21.3292	-22.6651	-20.5068	-20.6301	-19.9160	-22.4790	-21.1328
$C_{D\dot{q}}$ (1/rad)	-1.3254	-1.3520	-1.3896	-1.2166	-3.0219	-2.8950	-3.2142	-2.9974
$C_{M\dot{q}}$ (1/rad)	-4.2358	-2.9027	-2.3308	-2.8947	-4.2358	-4.0141	-2.3308	-2.7418
C_{Lo}	.2869	.2266	.3008	.2271	.8869	.2524	.3008	.2568
C_{Do}	.0048	.0028	.0042	.0022	.0048	.0036	.0042	.0030
C_{Mo}	-.0640	-.0405	-.0829	-.0437	-.0640	-.0505	-.0830	-.0591

Table III
FLEXSTAB Elastic Model Data (cont'd)

Longitudinal Data for Cruise 3

	No Winglets		With Winglets	
	Rigid	Elastic	Rigid	Elastic
C_{Lo}	.2401	.2073	.2509	.2100
C_{Do}	.0049	.0038	.0044	.0033
C_{Mo}	-.0549	-.0419	-.0691	-.0474
$\bar{C}_{L\hat{u}}$ (1/rad)	1.2883	1.1666	1.2927	1.1503
$\bar{C}_{D\hat{u}}$ (1/rad)	.1648	.1486	.1629	.1449
$\bar{C}_{M\hat{u}}$ (1/rad)	.0013	.0517	-.0022	.0729
$C_{L\alpha}$ (1/deg)	.0831	.0772	.0855	0782
$C_{D\alpha}$ (1/deg)	.0129	.0122	.0125	.0116
$C_{M\alpha}$ (1/deg)	-.0184	-.0144	-.0214	-.0159
C_{Lq} (1/rad)	9.7516	9.1391	10.0542	9.2709
C_{Dq} (1/rad)	.7448	.6773	.6774	.5913
C_{Mq} (1/rad)	-15.8058	-14.7360	-16.2204	-14.9776
$C_{L\delta s}$ (1/deg)	.0096	.0103	.0096	.0104
$C_{D\delta s}$ (1/deg)	.0011	.0012	.0011	.0012
$C_{M\delta s}$ (1/deg)	-.0281	-.0267	-.0281	-.0268
C_{L1}	.6720	.6025	.6893	.6034
C_{D1}	.0868	.0775	.0874	.0765
C_{M1}	-.0270	.0070	-.0444	.0020
$C_{L\dot{\alpha}}$ (1/rad)	-1.0139	-.5056	-1.5030	-.7633
$C_{D\dot{\alpha}}$ (1/rad)	-.2007	-.1246	-.2376	-.1368
$C_{M\dot{\alpha}}$ (1/rad)	-6.7647	-6.5758	-6.2265	-6.2853
$C_{L\dot{q}}$ (1/rad)	-9.5543	-9.1060	-10.4705	-9.6547
$C_{D\dot{q}}$ (1/rad)	-1.1385	-1.0723	-1.2074	-1.0996
$C_{M\dot{q}}$ (1/rad)	-4.4516	-4.3491	-3.4729	-3.7398

Table III
FLEXSTAB Elastic Model Data (cont'd)

Static Stability Parameters

CRUISE 1		No Winglets	With Winglets
Static Margin	(Rigid)	.2235	.2572
	(Elastic)	.1709	.1830
Neutral Point	(Rigid)	.4534	.4893
	(Elastic)	.4008	.4152
Neutral Point Shift (Elastic-Rigid)		-.0526	-.0741
Maneuver Point	(Rigid)	.4779	.5145
	(Elastic)	.4226	.4372
Maneuver Margin	(Rigid)	.2480	.2923
	(Elastic)	.1927	.2051
Longitudinal Control Per G for Steady Pull-Up (Deg/unit load factor)			
	(Rigid)	-3.4111	-3.9361
	(Elastic)	-2.8686	-3.0590
Stick Speed Stability (Deg/ft/sec)		.0091	.0100

Table III
FLEXSTAB Elastic Model Data (cont'd)

Static Stability Parameters

CRUISE 2		No Winglets	With Winglets
Static Margin	(Rigid)	.2318	.2684
	(Elastic)	.2052	.2290
Neutral Point	(Rigid)	.4617	.5005
	(Elastic)	.4351	.4611
Neutral Point Shift (Elastic-Rigid)		-.0266	-.0394
Maneuver Point	(Rigid)	.4743	.5135
	(Elastic)	.4470	.4733
Maneuver Margin	(Rigid)	.2444	.2814
	(Elastic)	.2171	.2411
Longitudinal Control Per G for Steady Pull-up (Deg/unit load factor)	(Rigid)	-6.9187	-8.0827
	(Elastic)	-6.3949	-7.1555
Stick Speed Stability (Deg/ft/sec)		.0205	.0229

Table III
FLEXSTAB Elastic Model Data (cont'd)

Static Stability Parameters

CRUISE 3		No Winglets	With Winglets
Static Margin	(Rigid)	.2211	,2507
	(Elastic)	,1870	,2030
Neutral Point	(Rigid)	.4510	,4828
	(Elastic)	,4169	,4361
Neutral Point Shift (Elastic-Rigid)		-,0341	-,0467
Maneuver Point	(Rigid)	.4928	,5257
	(Elastic)	.4558	,4756
Maneuver Margin	(Rigid)	.2629	,2936
	(Elastic)	.2259	,2435
Longitudinal Control Per G for Steady Pull-up (Deg/unit/load factor)			
	(Rigid)	-5,9830	-6,7604
	(Elastic)	-5,3997	-5,8477
Stick Speed Stability (Deg/ft/sec)		.0214	,0234

Table III
FLEXSTAB Elastic Model Data (cont'd)

	CRUISE 1				CRUISE 2			
	No Winglets		With Winglets		No Winglets		With Winglets	
	Rigid	Elastic	Rigid	Elastic	Rigid	Elastic	Rigid	Elastic
$C_{Y\beta}$ (1/deg)	-.0116	-.0103	-.0134	-.0118	-.0116	-.0109	-.0134	-.0125
$C_{\ell\beta}$ (1/deg)	-.0023	-.0021	-.0030	-.0022	-.0021	-.0019	-.0027	-.0023
$C_{N\beta}$ (1/deg)	.0035	.0029	.0038	.0031	.0035	.0032	.0037	.0033
C_{Yp} (1/rad)	-.1673	-.1562	-.3087	-.2513	-.1673	-.1664	-.3087	-.2760
$C_{\ell p}$ (1/rad)	-.4907	-.3674	-.5494	-.3802	-.4924	-.4214	-.5509	-.4495
C_{Np} (1/rad)	.0254	.0246	.05108	.0407	.0232	.0176	.0369	.0234
C_{Yr} (1/rad)	.7090	.6285	.8105	.7082	.7741	.7319	.9287	.8638
$C_{\ell r}$ (1/rad)	.2349	.1848	.2646	.1859	.3712	.3209	.4162	.3364
C_{Nr} (1/rad)	-.2984	-.2639	-.3203	-.2812	-.3438	-.3225	-.3772	-.3489
$C_{Y\delta A}$(1/deg)	1.3×10^{-4}	$.77\times10^{-4}$	9.4×10^{-5}	7.3×10^{-5}	1.3×10^{-4}	1.02×10^{-4}	$.94\times10^{-4}$	$.84\times10^{-4}$
$C_{\ell\delta A}$ (1/deg)	-5.83×10^{-4}	-4.34×10^{-4}	$-5.98\cdot10^{-4}$	$-4\times38\times10^{-4}$	$-.59\times10^{-3}$	$-.51\times10^{-3}$	$-.61\times10^{-3}$	$-.52\times10^{-3}$
$C_{N\delta A}$ (1/deg)	-1.11×10^{-4}	$-.82\times10^{-4}$	-1.04×10^{-4}	$-.82\times10^{-4}$	$-.94\times10^{-4}$	$-.84\times10^{-4}$	$-.9\times10^{-4}$	$-.86\times10^{-4}$
$C_{Y\delta R}$ (1/deg)	.0076	.0052	.0075	.0052	.0076	.0063	.0075	.0063
$C_{\ell\delta R}$ (1/deg)	.0006	.0004	.0006	.0004	.0003	.0003	.0003	.0003
$C_{N\delta R}$(1/deg)	-.0036	-.0025	-.0036	-.0025	-.0036	-.0030	-.0036	-.0030

Table III
FLEXSTAB Elastic Model Data (cont'd)

	CRUISE 1				CRUISE 2			
	No Winglets		With Winglets		No Winglets		With Winglets	
	Rigid	Elastic	Rigid	Elastic	Rigid	Elastic	Rigid	Elastic
$C_{Y\dot{\beta}}$ (1/rad)	-.1784	-.1629	-.1746	-.1564	-.1784	-.1683	-.1746	-.1648
$C_{\ell\dot{\beta}}$ (1/rad)	-.0004	.0016	.0048	.0050	.0001	.0013	.0052	.0048
$C_{N\dot{\beta}}$ (1/rad)	.0062	-.0008	.0057	.0027	.0062	.0016	.0053	.0008
$C_{Y\dot{p}}$ (1/rad)	-.1519	-.1898	-.1301	-.1172	-.1519	-.1446	-.1301	-.1233
$C_{\ell\dot{p}}$ (1/rad)	-.0042	0024	.0106	.0070	.0015	.0042	.0158	.0131
$C_{N\dot{p}}$ ((1/rad)	.0693	.0868	.0650	.0586	.0694	.0659	.0639	.0607
$C_{Y\dot{r}}$ (1/rad)	-.0121	-.0265	-.0137	-.0277	-.0121	-.0198	-.0137	-.0213
$C_{\ell\dot{r}}$ (1/rad)	-.0012	-.0012	-.0012	-.0020	-.0004	-.0011	-.0028	-.0027
$C_{N\dot{r}}$ (1/rad)	-.0193	-.0128	-.0191	-.0127	-.0193	-.0158	-.0190	-.0155

Table III
FLEXSTAB Elastic Model Data (cont'd)

Lateral Data CRUISE 3

	No Winglets		With Winglets	
	Rigid	Elastic	Rigid	Elastic
$C_{Y\beta}$ (1/deg)	-.0105	-.0097	-.0120	-.0110
$C_{\ell\beta}$ (1/deg)	-.0020	-.0018	-.0025	-.0020
$C_{N\beta}$ (1/deg)	.0030	.0026	.0032	.0028
C_{Yp} (1/rad)	-.1626	-.1537	.2790	-.2433
$C_{\ell p}$ (1/rad)	-.4364	-.3612	-.4833	-.3803
C_{Np} (1/rad)	.0277	.0221	.0441	.0316
C_{Yr} (1/rad)	.6414	.5952	.7319	.6717
$C_{\ell r}$ (1/rad)	.2264	.1931	.2530	.2004
C_{Nr} (1/rad)	-.2798	-.2586	-.2981	-.2730
$C_{Y\delta A}$ (1/deg)	.000095	.000068	.000071	.000059
$C_{\ell\delta A}$ (1/deg)	-.000486	-.000412	-.000495	-.000416
$C_{N\delta A}$ (1/deg)	-.000080	-.000070	-.000077	-.000070
$C_{Y\delta R}$ (1/deg)	.0064	.0052	.0064	.0052
$C_{\ell\delta R}$ (1/deg)	.0003	.0003	.0003	.0003
$C_{N\delta R}$ (1/deg)	-.0030	-.0025	-.0030	-.0025
$C_{Y\dot{\beta}}$ (1/rad)	-.1748	-.1678	-.1735	-.1666
$C_{\ell\dot{\beta}}$ (1/rad)	-.0010	-.0001	.0015	.0014
$C_{N\dot{\beta}}$ (1/rad)	.0033	.0001	.0032	.0000
$C_{Y\dot{p}}$ (1/rad)	-.1200	-.1129	-.1057	-.0993
$C_{\ell\dot{p}}$ (1/rad)	-.0085	-.0068	-.0001	-.00[illegible]
$C_{N\dot{p}}$ (1/rad)	.0544	.0511	.0512	.0482

Table III
FLEXSTAB Elastic Model Data (cont'd)

	No Winglets		With Winglets	
	Rigid	Elastic	Rigid	Elastic
$C_{Y_{\dot{r}}}$ (1/rad)	-.0001	-.0046	-.0006	-.0051
$C_{\ell_{\dot{r}}}$ ((1/rad)	.0001	-.0003	-.0010	-.0011
$C_{N_{\dot{r}}}$ (1/rad)	-.0197	-.0177	-.0198	-.0177

Table III
FLEXSTAB Elastic Model Data (cont'd)

Dynamic Modes Comparison
Longitudinal

	CRUISE 1		CRUISE 2		CRUISE 3	
	No Winglets	With Winglets	No Winglets	With Winglets	No Winglets	With Winglets
Short Period						
ω_n (rad/sec)	1.818	1.881	1.382	1.469	1.528	1.596
Period (sec)	3.898	3.729	4.798	4.483	4.868	4.586
$\zeta_{s.p.}$	.463	.445	.320	.300	.535	.513
$T_{\frac{1}{2}}$ (sec)	.824	.828	1.567	1.574	.847	.847
Phugoid						
ω_n (rad/sec)	.0693	.0723	.069	.070	.100	.103
Period (sec)	90.746	87.024	90.896	89.473	62.655	60.978
ζ_p	.0409	.0405	.0830	.0844	.049	.051
$T_{\frac{1}{2}}$ (sec)	244.477	219.857	120.330	116.541	141.692	132.691
Dutch Roll						
ω_n (rad/sec)	1.36	1.411	1.041	1.062	1.122	1.151
Period (sec)	4.641	4.478	6.050	5.955	5.650	5.513
ζ_{DR}	.0942	.105	.075	.077	.130	.138
$T_{\frac{1}{2}}$ (sec)	5.401	4.696	9.180	8.491	4.741	4.364
Spiral	T2 =	T2 =	T2 =	T2 =		
$T_{\frac{1}{2}}$ (sec)	2008.92	1619.65	43.22	52.869	T2=75.917	T2=104.508
Roll						
$T_{\frac{1}{2}}$ (sec)	.9289	.931	1.601	1.526	.818	.792

Vita

Kent R. Crenshaw was born on January 21, 1947. He graduated from Littleton Senior High School, Colorado, in 1965 and then attended the United States Military Academy at West Point, New York. Upon graduation in 1969, he received a Bachelor of Science degree and a commission in the United States Air Force. From there he entered pilot training at Moody Air Force Base, Georgia and graduated in August of 1970. Following pilot training, he was assigned aircrew duties first in the C-7 aircraft, flying airlift missions in Southeast Asia, and then reassigned to the Strategic Air Command in the B-52 aircraft. Stateside assignments have included Westover A.F.B., Massachusetts, and Robins A.F.B., Georgia. In June of 1975, he entered the Air Force Institute of Technology.

UNCLASSIFIED

SECURITY CLASSIFICATION OF THIS PAGE (When Data Entered)

REPORT DOCUMENTATION PAGE		READ INSTRUCTIONS BEFORE COMPLETING FORM
1. REPORT NUMBER GAE/MC/76D-5	2 GOVT ACCESSION NO	3 RECIPIENT'S CATALOG NUMBER
4. TITLE (and Subtitle) Stability and Control Characteristics of the Winglet Configured KC-135A		5 TYPE OF REPORT & PERIOD COVERED 6. PERFORMING ORG. REPORT NUMBER
7. AUTHOR(s) Kent R. Crenshaw Captain USAF		8. CONTRACT OR GRANT NUMBER(s)
9. PERFORMING ORGANIZATION NAME AND ADDRESS Air Force Institute of Technology Wright-Patterson AFB, Ohio 45433		10. PROGRAM ELEMENT, PROJECT, TASK AREA & WORK UNIT NUMBERS
11. CONTROLLING OFFICE NAME AND ADDRESS Air Force Institute of Technology Wright-Patterson AFB, Ohio 45433		12. REPORT DATE December 1976 13. NUMBER OF PAGES 190
14. MONITORING AGENCY NAME & ADDRESS(if different from Controlling Office)		15. SECURITY CLASS. (of this report) UNCLASSIFIED 15a. DECLASSIFICATION/DOWNGRADING SCHEDULE

16. DISTRIBUTION STATEMENT (of this Report)

Approved for Public Release; Distribution Unlimited

17. DISTRIBUTION STATEMENT (of the abstract entered in Block 20, if different from Report)

18. SUPPLEMENTARY NOTES

Approved for Public Release; IAW AFR/190-17.
Jerral F. Guess, Captain, USAF
Director of Information

19. KEY WORDS (Continue on reverse side if necessary and identify by block number)

FLEXSTAB Computer System
Rigid Aircraft Model KC-135
Elastic Aircraft Model KC-135
Boeing Winglet Application

20. ABSTRACT (Continue on reverse side if necessary and identify by block number)

Using the Boeing FLEXSTAB digital computer system, rigid and elastic models of the winglet configured KC-135A are made. With a rigid analysis, the winglets reduce total drag from 2 to almost 8% with improvements both laterally and longitudinally in static stability. Dynamically, the rigid winglet model is more stable laterally but slightly more oscillatory longitudinally. The lateral dutch roll

DD FORM 1 JAN 73 1473 EDITION OF 1 NOV 65 IS OBSOLETE

UNCLASSIFIED

SECURITY CLASSIFICATION OF THIS PAGE (When Data Entered)

Block 20.

mode damping ratio increased with winglets from 3 to 12% with only a 3% increase in frequency. The effect of shortening the vertical stabilizer on the rigid winglet model reveals less stable values for $C_{y\beta}$, $C_{n\beta}$, and C_{n_r} and somewhat less lateral dynamic stability than the baseline model. For the elastic winglet model, the drag reductions noted are only 1.3% due to the "washout" effect at the wing tip. Elastic static stability is still improved both laterally and longitudinally with winglets; and dynamically, the winglets improve lateral stability with very little effect longitudinally. With aeroelastic effects, the overall benefit derived from winglet application to the model is less. However, no significant detrimental effects due to winglets are found.